



VCU

Virginia Commonwealth University
VCU Scholars Compass

Theses and Dissertations

Graduate School

2022

THE INFLUENCE OF SALINITY ON THE STRUCTURE AND FUNCTION OF SOIL PROKARYOTIC COMMUNITIES IN COASTAL FRESHWATER WETLANDS

Joseph C. Morina II
Virginia Commonwealth University

Follow this and additional works at: <https://scholarscompass.vcu.edu/etd>



Part of the [Environmental Microbiology and Microbial Ecology Commons](#)

© Joseph C. Morina II

Downloaded from

<https://scholarscompass.vcu.edu/etd/6977>

This Dissertation is brought to you for free and open access by the Graduate School at VCU Scholars Compass. It has been accepted for inclusion in Theses and Dissertations by an authorized administrator of VCU Scholars Compass. For more information, please contact libcompass@vcu.edu.

THE INFLUENCE OF SALINITY ON THE STRUCTURE AND FUNCTION OF SOIL PROKARYOTIC COMMUNITIES IN COASTAL FRESHWATER WETLANDS

A dissertation submitted in partial fulfillment of the requirements for the degree
of Doctor of Philosophy at Virginia Commonwealth University.

By

Joseph C. Morina II
Bachelor of Science, Virginia Commonwealth University, 2013

Advisor: Rima B. Franklin
Associate Professor, Department of Biology

Virginia Commonwealth University
Richmond, Virginia
May 2022

ACKNOWLEDGEMENTS

There are many people I'd like to thank for their support, guidance, and tutelage during my time as a graduate student. First I want to thank Leslie Cohen-Gee, whose letter of recommendation sparked this whole journey. My advisor, Dr. Rima Franklin, always pushed me to produce my best work, while simultaneously providing me with unparalleled support. Her mentorship was an invaluable part of my development as a scientist, and as a critical thinker. Because of her, I have come to think of research as a story, and our discussions revolving around the lead characters and their plots were some of my most memorable conversations. Thank you for everything, Rima. My committee guided me through not only my dissertation, but the foundational knowledge I needed to perform this level of research. It was Dr. Crawford's class that inspired me to change my major to Biology during my undergraduate career; neither of us realized at the time I was destined to study the ecosystems near and dear to his heart, wetlands. Dr. Zinnert helped me frame my thinking of ecological community analysis, a core tenant of this dissertation. Both Dr. Neubauer and Dr. Bukaveckas helped me get my head out of the dirt, and to see how different components of ecosystems work in tandem and relate to one another. In addition, both of them always encouraged me to "do the math".

Without the support of my lab mates I would never have finished this dissertation. Chansotheary Dang and David Berrier helped me conceptualize, design, and implement my experiments, which ranged from late nights in the basement of Trani drawing on whiteboards, to hiking miles through the woods to collect soil bags. Dr. Battistelli, Aoife Mahaney, Mary Coughter, and Ella Balasa always were there to offer a helping hand, or words of encouragement during stressful times. I am forever grateful to Drashty Mody, who I had the honor to mentor during the course of my graduate studies. She quickly learned to perform a slew of assays that were complex and tedious, always with a smile and her characteristic chipper attitude. I also want to thank Joe Brown, Lisa Haber, and Melissa Davis for their advice and camaraderie during our graduate studies.

I would like to thank my parents, brother, and my whole family for their support and encouragement, there were many days I relied on them to recharge my batteries. My Dad would always tell me when I was younger, "if you're going to do something, do it right". Those words echoed in my head every time I had to create or optimize a new assay. Thanks Dad, you were right. I think about my Grandmother's advice often, despite not knowing anything about microbial ecology or graduate programs, her words were always exactly what I needed to hear. I also want to thank my partner, Jaime Barnett. She was there through the late nights and early mornings to support me during the final stages of this dissertation. She always believed in me, even when I questioned myself. She helped me to find balance and grounded me every day. After long hours in the lab I would come home to her smile and Rolo's bays which never failed to lift my spirits.

Lastly, I want to thank the funding sources that allowed me to perform my research. The National Science Foundation, Virginia Sea Grant, Virginia Water Resources Research Center, and VCU Rice Rivers Center which played a pivotal role in my college education. As an undergraduate I went to VCU RRC for multiple classes, and as a graduate student I used the field station to conduct research, lead outreach events, and present the results of my experiments.

TABLE OF CONTENTS

ACKNOWLEDGEMENTS	II
TABLE OF CONTENTS	III
ABSTRACT	V
CHAPTER 1: INTRODUCTION	1
1. Significance	2
2. Background and Objectives	3
3. Dissertation Format	8
4. Tables	10
CHAPTER 2: INTENSITY AND DURATION OF EXPOSURE DETERMINE PROKARYOTIC COMMUNITY RESPONSE TO SALINIZATION IN FRESHWATER WETLAND SOILS.....	12
1. Introduction	13
2. Methods.....	15
3. Results.....	23
4. Discussion.....	31
5. Conclusions	38
6. Tables and Figures	40
7. Supplemental Materials.....	49
CHAPTER 3: PROKARYOTIC COMMUNITY DYNAMICS DURING A THREE-YEAR <i>IN-SITU</i> SALINITY MANIPULATION IN A TIDAL FRESHWATER WETLAND	59
1. Introduction	60
2. Methods.....	62
3. Results.....	70
4. Discussion.....	74
5. Conclusions	81
6. Tables and Figures	82
CHAPTER 4: RECONSIDERING ASSAYS OF ENZYME ACTIVITIES IN WETLAND SOILS.....	93
1. Introduction	94
2. Methods.....	96
3. Results.....	100
4. Discussion.....	103
5. Conclusions	108
6. Tables and Figures	110
CHAPTER 5: SYNTHESIS.....	120

REFERENCES..... 127
VITA..... 144

ABSTRACT

INFLUENCE OF SALINITY ON THE STRUCTURE AND FUNCTION OF SOIL PROKARYOTIC COMMUNITIES IN COASTAL FRESHWATER WETLANDS

By Joseph C. Morina II

A dissertation submitted in partial fulfillment of the requirements for the degree of Doctor of Philosophy at Virginia Commonwealth University.

Advisor: Rima B. Franklin
Associate Professor, Department of Biology

Microbial communities are critical biological components of the world's ecosystems, and their respiratory pathways are directly involved in the biogeochemical cycling of essential nutrients. As genomic technologies advance, allowing for more detailed profiling of microbial communities, efforts have successfully linked microbial community composition to ecosystem-level functions and have shown microbial communities are susceptible and resistant to disturbance events. The goal of this dissertation is to address the temporal scales in which microbial communities respond to the disturbance of salinization, and the repercussions this has on microbially-mediated carbon and nitrogen cycling. Coastal freshwater wetlands are an excellent study system to investigate salinization effects, as their soils harbor functionally- and taxonomically-diverse communities that provide critical ecosystem services, which appear sensitive to changes in salinity.

For this dissertation, I performed three experiments to advance our understanding of how prokaryotic communities respond in both structure and function to salinization in coastal freshwater wetlands. I utilized *in-situ* salinity manipulations over relatively long temporal scales (2-3 years) as well as shorter-term laboratory incubations. I paired DNA-based assessments of the prokaryotic communities

with functional measurements (NO_3^- reduction, CH_4 production, and CO_2 production) for a more complete understanding of the temporal scales in which freshwater communities change due to salinization.

The response of prokaryotic communities to salinization was predicated on salinity level and exposure length. Mesohaline levels of salinity resulted in the rapid formation of transitional communities, which took approximately two years to match native mesohaline communities. However, freshwater prokaryotic communities appear structurally resistant to salinization when allowing for and excluding the immigration of more saline-adapted prokaryotic taxa. The differential response of freshwater prokaryotes to different salinity levels suggests that freshwater prokaryotes are somewhat capable of competing with oligohaline taxa for resources, but are less competitive under mesohaline conditions, a pattern that was also observed in the response of putative nitrate-reducing taxa.

The effects of salinization on nitrate reduction pathways agreed well with past efforts that found rates of dissimilatory nitrate reduction to ammonium (DNRA) are higher under increased salinities, which I observed under mesohaline levels of salinity. However, the effects of salinization on denitrification were more difficult to interpret, as no consistent response to salinization was observed, highlighting the importance of studying changes to this pathway over longer (years) time scales and multiple salinity levels.

I observed changes in the terminal end products of soil organic matter mineralization, wherein oligohaline levels of salinization consistently suppressed methane production, without decreasing the abundance of the archaea responsible for methanogenesis, suggesting these prokaryotes either switch to alternative respiratory pathways or, more likely, become dormant under moderate salinity levels. Unlike methane production, carbon dioxide production did not show a response to oligohaline levels of salinity. This could be a result of the freshwater

community structure being relatively resistant to oligohaline salinity levels, the exclusion of immigration of more saline-tolerant community members, or it could be due to functional redundancy as multiple respiratory pathways produce carbon dioxide as an end product. I observed that freshwater soil enzyme activities were not suppressed by salinization, but rather were unchanged or stimulated when exposed to salinization ranging from freshwater to mesohaline salinities. This suggests that the enzymes produced by freshwater prokaryotes are functional under more saline conditions, at least when considering short time scales.

This work underscores the importance of considering multiple disturbance levels and exposure lengths when profiling the prokaryotic community response, and that these two effects can interact to dictate changes to community structure. Novel communities that form during a salinity disturbance are transitional when viewed over multi-year temporal scales. Findings of this dissertation also suggest that the prokaryotes of coastal freshwater wetland soils can tolerate oligohaline levels of salinity without drastic changes to taxonomic profiles, but functional changes may manifest without observed treatment effects on metrics of prokaryotic community structure. The findings of this dissertation highlight the value of profiling the prokaryotic communities responsible for the biogeochemical cycling of carbon and nitrogen. Furthermore, my results suggest that coastal freshwater wetland soils, from both tidal and non-tidal wetlands, are relatively resistant to oligohaline levels of salinity, suggesting that mechanisms of salinization resulting in oligohaline levels of salinity will likely not result in the restructuring of these communities.

CHAPTER 1: INTRODUCTION

Joseph C. Morina

1. Significance

Microbial communities dictate the biogeochemical cycles of life's most essential nutrients (Falkowski et al., 2008). Yet, despite their critical importance, these microbes remain largely uncharacterized (Ramirez et al., 2014) due to the paucity of environmental microorganisms that have been cultured under laboratory conditions. With the increasingly widespread availability of nucleic acid-based analyses, our understanding of these communities has drastically improved. Significant recent advancements include the identification of environmental drivers of microbial community structure at the continental scale (Lauber et al., 2009, Fierer and Jackson 2006) and the incorporation of microbial community data into ecosystem functional models (Graham et al., 2016, Delgado-Baquerizo et al., 2020). Several researchers have successfully linked metrics of microbial community structure (composition, abundance, and diversity) and function (e.g., Orland et al., 2018, Handa et al., 2014), but the uncoupling of these parameters is also frequently observed. Efforts to synthesize the links between microbial community structure and function have highlighted our lack of understanding of the temporal scales over which structural changes impart functional shifts (as reviewed in Bier et al. (2015)). It also appears that metrics of microbial community structure are more explanatory for functions that are phylogenetically restricted or only performed by a small subset of the overall community, such as methanogenesis and, to a lesser extent, denitrification (Graham et al., 2016, Bier et al., 2015). Furthermore, metrics that quantify taxa belonging to functional guilds more often are linked to the respective function than broader metrics of the whole community. As our understanding deepens about when and how microbial community structure and function are related, many scientists are applying this knowledge to see how communities respond to disturbance events, with a particular interest in learning whether microbial community responses may be useful for predicting how critical ecosystem services will be altered (Bardgett and Caruso, 2020, Philippot et al., 2022, Shade et al., 2012).

2. Background and Objectives

2.1. Salinization Effects on Wetland Microbial Communities

Coastal freshwater wetlands provide a multitude of ecosystem services. However, at the global scale, these ecosystems are experiencing anthropogenically-driven disturbances, including the salinization of historically freshwater wetlands (Herbert et al., 2015). Salinization is occurring due to multiple global change stressors, and coastal freshwater wetlands are especially affected by changes in hydrological management (e.g., damming of rivers, water diversions for irrigation, and extraction of ground water), increased intensity and frequency of storm surges, and sea level rise (Herbert et al., 2015, Tully et al., 2019). Salinization of coastal freshwater wetlands will likely impart drastic restructuring of the associated microbial communities, since salinity one of, if not the most, dominant factor determining microbial community composition at the global scale (Lozupone and Knight 2007, Auguet et al., 2009). However, these reviews (Lozupone and Knight 2007, Auguet et al., 2009) were unable to identify specific mechanisms by which salinity alters microbial community composition, most likely due to the complexity of direct and indirect effects salinity can have on biological communities.

One of the simplest ways salinity can affect microbial communities is increased osmotic stress, which can select for microbes that have physiological adaptations to higher salt concentrations. Because osmoregulation is a major homeostatic mechanism across all domains of life, it is reasonable to hypothesize this effect might be the major cause of microbial community shifts associated with salinity increases. However, studies indicate the direct effects of osmotic stress alone are actually modest compared to effects of certain ions or indirect effects mediated through other environmental compartments (Podell et al., 2014, Hollister et al., 2010). For example, salinization increases the availability of sulfate (SO_4^{2-}), which can be utilized during microbial respiration as a terminal electron acceptor for sulfate-reducing bacteria (SRB). Increased concentrations of SO_4^{2-} can stimulate SRB in

wetland soils, thus altering competition for resources and potentially altering the terminal end products of soil organic matter (OM) mineralization. Indirectly, salinity can affect microbial communities via changes to multiple environmental parameters (e.g., organic matter availability, sorption, plant communities), which are known to vary with salinity. Previous efforts synthesizing how microbially-governed biogeochemical transformations are altered after salinization have indicated that salinization will likely alter the cycling of both carbon and nitrogen in coastal wetlands systems (Luo et al., 2019). Of particular concern are the impacts increased salinity has on microbially-mediated ecosystem services such as the ability of wetlands to sequester carbon for long-term storage in soils (Mitra et al., 2005) and remove nitrogen, specifically nitrate (NO_3^-), from surface waters (Hansen et al., 2018).

When predicting how microbial communities in freshwater soils will respond to salinization, it is useful to consider how microbial communities are structured across salinities gradients. It is well documented that microbial communities along estuarine and lacustrine salinity gradients are divergent and unique (e.g., see Francis et al., 2013, Song et al., 2014, Mosier and Francis 2008, Yang et al., 2016, Franklin et al., 2017). This year, the first meta-analysis synthesizing microbial community composition across salinity gradients was published (Chen et al., 2022), which characterized broad taxonomic patterns. While informative, salinity gradients are not necessarily representative of the salinization disturbance events as communities have had time to restructure in response to disturbance, thereby excluding short- to mid-term community responses from gradient studies. Recently, researchers have started to probe the response of wetland microbial communities by experimentally creating salinization events. For instance, Dang et al. (2019) utilized a soil transplant approach to salinize freshwater soils under mesohaline conditions while allowing for the mixing of the two microbial communities by using mesh bags. The results of this study were noteworthy, as the authors found a novel structure in transplant communities relative to freshwater and mesohaline control communities. These findings suggest that salinization either results in a novel community state or that the novel community structure

they observed was successional and required more time (> 1 year) to transition and stabilize before matching the mesohaline control community. Another recent study employed an *in-situ* watering approach using saltwater from an adjacent brackish marsh to salinize tidal freshwater wetland soils; they found that the NO_3^- reducing community responded to increased salinity and formed distinct community structure, relative to control communities, after three years of saltwater additions (Neubauer et al., 2019). Lastly, the importance of community coalescence (i.e., mixing of two discrete communities) during salinization events was recently highlighted by Rocca et al. (2020), who examined planktonic estuarine communities and found that the freshwater community response differed between treatments that permitted and excluded freshwater and marine community mixing. Furthermore, this study found that when freshwater and marine communities were mixed, a novel community formed that was composed of low abundance taxa from both sites. The results of these studies highlight the importance of considering longer temporal scales (i.e., multiple years) and community mixing when profiling the microbial response to salinization. Further, these studies allude to potentially different effects based on the level of salinity increase, but this has rarely been tested.

The overarching goal of this dissertation is to study how the ecological disturbance of salinization affects wetland microbial communities considering multiple salinity levels and time scales.

Concurrent with profiling multiple metrics of microbial community structure, I measured several microbial functions with ecosystem-level relevance. Chapter 2 focuses on potential functional changes to nitrogen biogeochemistry, specifically NO_3^- reduction pathways. Chapters 3 and 4 focus on potential functional changes associated with carbon biogeochemistry by assessing changes to the terminal products of organic matter mineralization (CO_2 and CH_4), and the activity of soil enzymes.

2.2. Salinization Impacts Carbon Cycling

Soil enzymes are critical to consider when investigating carbon availability in soils, as the activities of soil enzymes are generally viewed as the rate-limiting steps of soil organic matter mineralization. Mineralization occurs when the polymers of organic matter are first broken down by soil enzymes produced by the soil microbial communities. These monomers are then utilized as electron donors in the respiratory pathways of heterotrophic prokaryotes, with the final end products of these processes being carbon dioxide (CO₂) and methane (CH₄). Thus, alterations to soil enzyme activities due to salinization could restructure the mineralization pathways mediated by soil microbes. To learn more about the impacts salinization has on microbially-mediated C cycling, I studied the response of soil enzyme activities to increased salinity (Chapter 4).

Wetland soils account for around $\sim 1/3^{\text{rd}}$ of total global CH₄ emissions (Bridgman et al., 2013), and thus understanding how CH₄ dynamics will be altered in wetlands experiencing salinization is a globally relevant question. Methane production is a relatively well-studied response in wetland salinization studies, with results generally showing suppression of CH₄ production after salinization (as reviewed by Herbert et al. (2015) and Luo et al. (2019)). This is often attributed to the stimulation of SRB when SO₄²⁻ availability is increased. Once stimulated, SRB can directly outcompete methanogens (CH₄ producing archaea) for substrates, or indirectly via the disruption of methanogen-syntroph interactions (Berrier et al., 2022). If this paradigm is correct, then CH₄ production should decrease after salinization, with the potential of increased CO₂ production due to the stimulation of SRB activity (Chambers et al., 2011, Neubauer 2013). However, discrepancies in this trend (Weston et al., 2011, Ardón et al., 2018) suggest that we still do not fully understand the controls over these processes, and that probing the prokaryotic community responsible for these biogeochemical cycles would likely improve our understanding. Therefore, in Chapter 3, I determined the effect of salinization on the balance between

CO₂ and CH₄ production while profiling changes in the prokaryotic community throughout a three-year *in-situ* salinization experiment.

2.3. Partitioning of NO₃⁻ After Salinization

In addition to affecting carbon cycling, salinization can impact microbial nitrogen transformations, especially the pathways of NO₃⁻ reduction. The ability of wetland ecosystems to remove NO₃⁻ is largely attributed to denitrifying microbes (Seitzinger et al., 2006). This diverse group of facultative anaerobes, both autotrophic and heterotrophic, is capable of performing multiple respiratory pathways that all involve the stepwise reduction of NO₃⁻ to nitrogenous gasses. The second most common pathway for NO₃⁻ reduction is dissimilatory nitrate reduction to ammonium (DNRA). Similar to denitrification, DNRA is performed by facultative anaerobes, and the ability to perform DNRA is widespread across many phylogenetic groups. Unlike denitrification, DNRA is viewed as an N retention pathway, as NO₃⁻ is transformed to another biologically available form, NH₄⁺, which is more likely to be retained in the ecosystem compared to the gaseous products of denitrification. There exists a third NO₃⁻ reduction pathway called anaerobic ammonium oxidation (anammox). Although this pathway can be a major part of N cycling in estuarine sediments (Engström et al., 2005), it is typically not detected or is a tiny percentage (< 10%) of the total NO₃⁻ reduced in wetland ecosystems (Koop-Jakobsen and Giblin 2009). Due to the fact that our research occurs in marsh soils, and the fact we could not detect measurable rates of anammox in preliminary assays, we herein focus on denitrification and DNRA.

In recent years, several studies have examined how NO₃⁻ reduction pathways vary across salinity gradients (Table 1). Denitrification appears to be the dominant pathway in most freshwater soils and sediments, but no clear pattern emerges when considering oligohaline to polyhaline salinities. The increased concentration of SO₄²⁻ is thought to be one of the major factors influencing NO₃⁻ partitioning during salinization. Sulfate is the second most abundant anion in seawater, and its concentration

generally increases when moving from the head to the mouth of an estuary. Sulfate acts as a terminal electron acceptor for SRB, who reduce SO_4^{2-} to produce hydrogen sulfide (H_2S), effectively increasing the H_2S concentrations in estuarine wetland soils. Elevated H_2S (and its dissociation products: HS^- and S^{2-}) has been shown to affect many of the nitrogen cycling pathways common in wetlands, including denitrification and DNRA, but the effects are often nonlinear. For example, researchers have reported a stimulatory effect of H_2S on denitrification (Brettar and Rheinheimer 1991) at very low concentrations, whereas higher concentrations, such as those found in salt marshes, have been shown to suppress denitrification via the inhibition of denitrification enzymes (Senga et al., 2006). Regarding rates of DNRA, the role of H_2S is also not fully understood. The presence of H_2S may directly increase rates of DNRA as some members of this functional group can use H_2S as an electron donor (Brunet and Garcia-Gil 1996, Senga et al., 2006). Indirect effects, wherein H_2S impacts NO_3^- availability, rather than affecting DNRA *per se*, are also possible. For example, toxic effects of H_2S on nitrification would decrease NO_3^- availability thus creating a more favorable for DNRA as it is thought to be favored over denitrification under NO_3^- limiting conditions (Yoon et al., 2015). In Chapter 2 of my dissertation, I address how two different levels of salinization alter the rates of denitrification and DNRA over the course of two years, while simultaneously profiling changes to the prokaryotic community involved in both NO_3^- reduction pathways.

3. Dissertation Format

In the introduction to this dissertation, I used the term microbial communities to broadly discuss research efforts in the field of microbial ecology and biogeochemistry. However, due to the methods employed in Chapter 2 and Chapter 3, this dissertation only captures the structure of the prokaryotic community (bacteria and archaea) and does not include any assessment of the micro-eukaryotic

community members. Therefore, in those chapters, I use the term prokaryotic when discussing community and taxa responses.

For this dissertation, I performed three experiments to advance our understanding of how prokaryotic communities respond in both structure and function to salinization in coastal freshwater wetlands. My first two studies utilize *in-situ* salinity manipulations over relatively long temporal scales (2-3 years), which allowed for the incorporation of environmental and seasonal variation not achievable with laboratory-based manipulations. In these studies, I pair DNA-based assessments of the prokaryotic communities with functional measurements (NO_3^- reduction, CH_4 production, and CO_2 production) for a more complete understanding of the temporal scales in which freshwater communities change due to salinization. In Chapter 2, I allowed for the immigration and colonization of prokaryotes from more saline wetlands, whereas in Chapter 3, I exclude the possibility of community coalescence during salinization. By using these contrasting approaches, I can assess the relative importance of community coalescence in prokaryotic community response to salinization. In my final study (Chapter 4), I reconsider commonly used assays of soil enzyme activity to determine if novel methodological approaches could be more representative of wetland field conditions, and assess the feasibility of cross-study comparisons of soil enzymes along wetland salinity gradients using different methodological approaches. In addition, I profiled the sensitivity of soil enzyme activities from the same sites as Chapter 2 to salinization over short timescales (hours).

The chapters of my dissertation take the form of three independent manuscripts. A single reference list has been compiled and is included at the end. Given that each research paper was written to stand alone, some of the material in each chapter is recurrent, especially when different investigations used common methodologies.

4. Tables

Table 1. Rates of denitrification, anammox, and DNRA for select studies that measured rates for at least two of the three major NO₃⁻ reduction pathways found in wetland soils and aquatic sediments. Reduction pathways that were not measured in a study are represented by (-). Not all studies note the salinity measurements (ppt) for a given study site; instead, they use broad classifications (e.g., mesohaline). Studies that provide no indication of salinity are represented by (†).

Reference	Locations	Ecosystem	Salinity	Contribution to total NO ₃ ⁻ reduction (%)		
				Denitrification	Anammox	DNRA
Wang et al., 2012	Pearl River Estuary	Estuarine Sediment	Fresh	93-99.5	0.5-7	-
Scott et al., 2008	Lake Waco	Freshwater Wetland	Fresh	99	-	1
Scott et al., 2008	Lake Waco	Freshwater Wetland	Fresh	99	-	1
Koop-Jakobsen & Giblin 2009	Plum Island Sound	Marsh	Fresh	97	3	0
Naeher et al., 2015	Seine Estuary	Estuarine Sediment	Fresh	92-97	3-8	0
Scott et al., 2008	Lake Waco	Freshwater Wetland	Fresh	94	-	6
Scott et al., 2008	Lake Waco	Freshwater Wetland	Fresh	94	-	6
Sgouridis et al., 2011	River Cole	Floodplain Soil (HM)	Fresh	93	-	7
Sgouridis et al., 2011	River Cole	Floodplain Soil (BZ)	Fresh	93	-	7
Scott et al., 2008	Lake Waco	Freshwater Wetland	Fresh	91	-	9
Scott et al., 2008	Lake Waco	Freshwater Wetland	Fresh	91	-	9
Sgouridis et al., 2011	River Cole	Floodplain Soil (GG)	Fresh	91	-	9
Molnar et al., 2013	St. Vincent Bay	Mangrove	†	90	-	10
Sgouridis et al., 2011	River Cole	Floodplain Soil (FM)	Fresh	90	-	10
Wenk et al., 2014	Lake Lugano	Lake Sediment	Fresh	82	6	12
Zheng et al., 2016	Yangtze Estuary	Tidal Flat	10 ppt	33.7-78.1	6.5-24.1	12.7-56.8
Tobias et al., 2001	York River	Marsh	Mesohaline	74.2	-	25.8
Yang et al., 2015	Tomales Bay	Salt Marsh	10 ppt	73	-	27
Giblin et al., 2010	Plum Island Sound	Estuarine Sediment	2 ppt	69	-	31

Table 1 (continued). Rates of denitrification, anammox, and DNRA.

Reference	Locations	Ecosystem	Salinity	Contribution to total NO ₃ ⁻ reduction (%)		
				Denitrification	Anammox	DNRA
Molnar et al., 2013	St. Vincent Bay	Mangrove	†	66	-	34
Scott et al., 2008	Lake Waco	Freshwater Wetland	Fresh	63	-	38
Koop-Jakobsen & Giblin 2010	Plum Island Sound	Marsh Platform	28 ppt	57	-	43
Song et al., 2014	New River Estuary	Estuarine Sediment (JAX)	Mesohaline	55	-	45
Koop-Jakobsen & Giblin 2010	Plum Island Sound	Creek Sediment	25 ppt	49	-	51
Hou et al., 2012	Copnano Bay	Estuarine Sediment	30 ppt	25.2-46.5	0.3-1.45	1.8-3.6
Dong et al. 2009	Colne River	River Sediment	†	45	18	37
Song et al., 2014	New River Estuary	Estuarine Sediment (M47)	Mesohaline	44	-	56
Yang et al., 2015	Tomales Bay	Salt Marsh	10 ppt	42	-	58
Song et al., 2014	New River Estuary	Estuarine Sediment (AA2)	Oligohaline	41	-	59
Smith et al., 2015	Conle Estuary	Estuarine Sediment (EH)	2-17 ppt	38	-	62
Dong et al., 2011	Vunidawa-Rewa	Estuarine Sediment	†	33	-	67
Song et al., 2014	New River Estuary	Estuarine Sediment (M15)	Polyhaline	33	-	67
Song et al., 2014	New River Estuary	Estuarine Sediment (M31)	Polyhaline	31	-	69
Crowe et al., 2012	St. Lawrence	Estuarine Sediment	30 ppt	30	70	0
Giblin et al., 2010	Plum Island Sound	Estuarine Sediment	5 ppt	29	-	71
Dong et al., 2011	Mae Klong	Estuarine Sediment	†	26	-	74
Dong et al., 2011	Cisadane	Estuarine Sediment	†	25	-	75
Smith et al., 2015	Conle Estuary	Estuarine Sediment (EM)	28-32 ppt	10.4	-	89.6
Smith et al., 2015	Conle Estuary	Estuarine Sediment (ME)	20-32 ppt	9.3	-	90.7
Giblin et al., 2010	Plum Island Sound	Estuarine Sediment	14 ppt	8	-	92

**CHAPTER 2: INTENSITY AND DURATION OF EXPOSURE DETERMINE
PROKARYOTIC COMMUNITY RESPONSE TO SALINIZATION IN FRESHWATER
WETLAND SOILS**

Joseph C. Morina and Rima B. Franklin

Department of Biology, Virginia Commonwealth University, Richmond, VA 23284 USA

1. Introduction

Coastal wetlands provide a multitude of ecosystem services. Their ability to remove nitrate (NO_3^-) from surface waters is particularly important as it helps ameliorate coastal eutrophication (Hansen et al., 2018, Jordan et al., 2011). Research considering how coastal wetlands respond to climate change stressors has predominately focused on brackish and marine systems, with less attention focused on the response of coastal freshwater wetlands (Grieger et al., 2020). However, these ecosystems are vulnerable to salinization, which can have a significant impact on soil physicochemistry and wetland biota, in turn threatening ecosystem stability and functioning (Herbert et al., 2015), and ecosystem services such as NO_3^- removal (Ardón et al., 2013, Larsen et al., 2010). These sorts of functional changes can be driven, at least in part, by the response of the soil prokaryotic communities to elevated salinity. Previous research has found salinity can control both archaeal and bacterial community composition (Lozupone and Knight 2007, Auguet et al., 2010) and that increasing salinity in freshwater systems can induce shifts in community composition and function (e.g., Dang et al., 2019, Neubauer et al., 2019, Rocca et al., 2020).

Given the importance of coastal wetlands in NO_3^- removal, there is considerable interest in how salinization impacts microbial N cycling (Zhou et al., 2017, Osborne et al., 2015, Santoro 2010). Effects on denitrification and dissimilatory nitrate reduction to ammonium (DNRA) are of interest as the end products of these pathways have differential impacts on ecosystem N availability. Denitrification, the stepwise reduction of NO_3^- to N_2O or N_2 , acts as an N removal pathway, whereas DNRA ($\text{NO}_3^- \rightarrow \text{NH}_4^+$) acts as a conservation pathway. Increasing salinity generally suppresses denitrification (Neubauer et al., 2019, Wang et al., 2018, Weston et al., 2006, Craft et al., 2009) and stimulates DNRA (Giblin et al., 2010, Gardener and McCarthy 2009, Giblin et al., 2013); however, contradictory findings (Marks et al., 2016, Marton et al., 2012, Bernard et al., 2015) suggest this understanding is incomplete. One explanation for

these seemingly conflicting results may be the different time scales or intensities of salinization considered (as discussed in Steinmuller and Chambers (2018)). There are very few studies that explicitly consider both salinity intensity and exposure length (Marks et al., 2016, Wilson et al., 2018, van Dijk et al., 2019), and comparing them is challenging due to different confounding factors (e.g., prior exposure to elevated salinity). Moreover, many of the aforementioned studies view salinization from a biogeochemical perspective, typically measuring gas and dissolved nutrient fluxes without incorporating a microbial component, although soil enzyme activities are occasionally assayed (Servais et al., 2020). Thus, our understanding of how the NO_3^- reducing communities respond to salinization is largely based on salinity gradient studies (Franklin et al., 2017, Chi et al., 2021, Zhang et al., 2021, Song et al., 2014), with community transitions during actual salinization less studied.

To address this knowledge gap, we conducted a two-year *in situ* experiment to assess prokaryotic community responses to two levels of salinization. We utilized a soil transplant approach along a naturally-occurring salinity gradient, and exposed freshwater wetland soil to both oligohaline and mesohaline salinities. The community response was assessed using amplicon sequencing (*16s rRNA* gene) and predictive metagenome inference. To learn more about the specific functional implications of salinization on NO_3^- reduction, we supplemented that analysis by measuring denitrification and DNRA rates and quantifying the abundance of corresponding functional genes. Our results indicate that overall community responses and the response of NO_3^- reducers are temporally dynamic, so conclusions about salinization effects may vary depending on when in the successional process measurements are made. Further, we found responses varied depending on the level of salinization, which has important implications for efforts to synthesize and generalize prior research.

2. Methods

2.1. Site Description and Monitoring

This research utilized the naturally-occurring salinity gradient of Taskinas Creek, located within York River State Park and the Chesapeake Bay National Estuarine Research Reserve (CBNERR-VA) in Virginia (USA). Three sites were selected along the creek based on salinity: freshwater (37°23'56.999" N, 76°43' 16.801" W), oligohaline (37°24'27.313" N, 76°43'31.014" W), and mesohaline (37°24'52.255 N, 76°42'57.45" W). The plant community at the freshwater ("Fresh") site were dominated by *Typha angustifolia*, and the plant community at oligohaline ("Oligo") site was a mix of *Spartina cynosuroides* and *Typha latifolia*. The mesohaline ("Meso") site was dominated by *Spartina alterniflora*. In January 2017, a plot (10 m × 5 m each, subdivided into 1 m² quadrats) was established at each site. A random number generator was used to select quadrats within each plot in which to install wells (3 cm diameter, built following Lee et al. (2016)) to regularly assess water chemistry. Within each plot, triplicate wells were established at each of 3 depths (5, 10, and 30 cm). Every two months, wells were flushed with N₂, and water was sampled via syringe. A subsample (1 mL) was immediately preserved with zinc acetate (Otte and Morris 1994) for Σsulfide (H₂S, HS⁻, and S²⁻) analysis (Cline 1969). Another subsample (25 mL) was frozen (-20°C) until dissolved ion concentrations could be measured, as described in Section 2.4.

2.2. Soil Transplants

After well installation, soil (top 10 cm) was collected in the area adjacent to each plot and transported on ice to the laboratory. Soils (~10 kg per site) were homogenized, and large roots and debris were removed. Aliquots (~100 g wet weight) were then encased in nylon mesh bags (500 μm mesh, 15 x 25 cm), placed into individual airtight plastic bags, and stored in a cold room overnight. The following day, bags were transported on ice back to the field. Controls were deployed by reburying soil

at its site of origin (1 bag per 1 m² quadrant); these are referred to as Fresh (“F”), Oligo (“O”), and Meso (“M”) controls. In addition, bags containing soil from the Fresh site were buried at the Oligo (“FO”) and Meso (“FM”) sites to assess how the freshwater prokaryotic community would respond to two levels of increased salinity. Bags were buried horizontally at a depth of 10 cm and retrieved after 5 (June 2017), 10 (November 2017), 19 (August 2018), and 22 months (November 2018). A random number generator was used to determine which bags (n=5 per treatment) to retrieve at each sampling event.

2.3. Soil Processing

Redox and pH were measured immediately upon return to the lab using a Laqua Act Portable pH/ORP/ION probe (HORIBA Scientific, Irvine, CA, USA). Soil subsamples were then removed for analysis of prokaryotic community composition (10 g, archived at -80°C), porewater chemistry (35 g), and soil properties (25 g). The remaining soil was stored overnight (4°C) until construction of microcosms for measuring NO₃⁻ reduction rates. Soil moisture content was determined gravimetrically (72°C, 72 hr), and percent organic matter (OM) was calculated as mass loss on ignition (400°C, 16 hr). A subsample of dry soil (2 g) was ground and acidified (0.10 M HCl) for C:N analysis (Perkin Elmer CHNS-O analyzer, Waltham, MA, USA).

2.4. Porewater Chemistry

Porewater was extracted from each soil subsample by centrifugation (1,500 x g, 15 min) and then filtered (0.22 µm pore size). An aliquot (10 mL) was used to determine dissolved organic carbon (DOC) concentration (Shimadzu TOC-V 5,000, Columbia, MD, USA). The remaining porewater was frozen (-20°C) until being analyzed via ion chromatography for Cl⁻, NO₃⁻, and SO₄²⁻ (Thermo Scientific™ Dionex, Bremen, Germany). Salinity (ppt) was calculated based on Cl⁻ concentration (Bianchi 2007). In addition,

NH_4^+ concentrations were measured colorimetrically (Sinsabaugh et al., 2000) using a Synergy 2 plate reader (Biotech, Winooski, VT, USA).

2.5. NO_3^- Reduction Rates

We utilized soil microcosms and $^{15}\text{NO}_3^-$ additions to investigate how salinization affected microbially-mediated NO_3^- reduction (Huygens et al., 2015). Because preliminary screening failed to detect anammox (Supplemental Methods 1), we focused on denitrification and DNRA. Assays were performed for 3 soil bags from each treatment for the 10, 19, and 22-month sampling events. Denitrification was quantified by measuring the headspace accumulation of ^{15}N -enriched N_2O and N_2 , whereas DNRA was quantified by measuring the slurry accumulation of ^{15}N -enriched NH_4^+ .

2.5.1. Microcosm Construction

Microcosms (70 mL glass serum vials) were constructed by combining 10 g of soil with 10 mL of filter-sterilized deoxygenated water that mimicked the average salinity of the host environment (0.05, 1, and 10 ppt; diluted from Instant Ocean (Spectrum Brands, Blacksburg, VA, USA)). Microcosms were then hermetically sealed with a butyl rubber stopper, flushed with He (10 min), and placed on an incubated shaker table (28°C, 100 RPM) for 24 hr to allow microbial activity to deplete residual O_2 and NO_3^- . After pre-incubation, microcosms were again flushed with He (10 min). A syringe was then used to inject enough 99 atom% K^{15}NO_3 (Cambridge Isotope Laboratories, Andover, MA, USA) dissolved in filter-sterilized (0.22 μm pore size) deionized water to bring each microcosm to a final concentration of 100 μM $^{15}\text{NO}_3^-$. A subset of microcosms were immediately sampled to serve as the initial time point for rate calculations. The remaining microcosms were returned to the shaker and sampled after 6, 24, and 45 hr. Two technical replicates were constructed for each soil bag and each time point. For each soil bag, four

additional microcosms were constructed (no $K^{15}NO_3$ added) to assess the natural (background) abundance of ^{15}N in N_2 , N_2O , and NH_4^+ . These microcosms were also sampled at 0, 6, 24, and 45 hr.

2.5.2. Denitrification

Headspace gas samples were collected for determining denitrification rates. First, 10 mL of He was injected and mixed into each microcosm headspace, then 10 mL of headspace gas was removed and transferred into a helium-flushed Exetainer[®] (Labco, Lampeter, UK). Gas samples were shipped to the University of California, Davis Stable Isotope Facility to measure N_2 and N_2O concentrations and isotope ratios. However, N_2O was always below the analytical detection limit (< 150 pmoles); therefore only ^{15}N enrichment of N_2 was reported. Denitrification rates were determined using linear regression of $^{15}N_2$ production over time (mean $r^2=0.95$) and are reported as nanomoles ^{15}N g-OM⁻¹ hr⁻¹.

2.5.3. DNRA

After headspace sampling, microcosm contents were transferred into 160-mL specimen cups containing 100 mL of 2 M KCl and placed on a shaker table (1 hr, 120 RPM). Aliquots (50 mL) of the resultant KCl extracts were then decanted, filtered (0.22 μm pore size), and placed in new acid-washed specimen cups to perform microdiffusions following Fillery and Recous (2001). Briefly, 5-mm diameter diffusion disks were made from Whatman grade GF/F filters (Cytiva, Marlborough, MA, USA) and suspended above the filtered KCl extracts using stainless steel wires. Diffusion disks were acidified by pipetting 10 μL of 2.5 M $KHSO_4$ directly onto the disks, and then adding 0.7 g of MgO to the KCl extract. Specimen cups were immediately sealed, placed in an incubator (25°C), and left undisturbed for 10 days. Diffusion disks were removed from the microdiffusion chambers and placed in a desiccator to dry until mass remained constant (70°C, ~3 days). Microdiffusion disks were sealed in 5 × 9 mm tin capsules (Costech, Valencia, CA, USA) and shipped to the Boston University Stable Isotope Facility for ^{15}N analysis

(GV Instruments IsoPrime™ Isotope Ratio Mass Spectrometer, Manchester, UK). DNRA rates were determined using linear regression of $^{15}\text{NH}_4^+$ production over time (mean $r^2=0.90$) and are reported as nanomoles $^{15}\text{N g-OM}^{-1} \text{ hr}^{-1}$.

2.6. Genetic Analyses

2.6.1. DNA Extraction

Archived soil samples were centrifuged ($10,000 \times g$, 1 min) to remove excess water. A portion (0.25 g) of the residual soil was then washed with EDTA (Dang et al., 2019) before performing DNA extraction using the Qiagen DNeasy® Powersoil® Extraction Kit (Germantown, MD, USA) following the manufacturer's protocol. Extraction was confirmed via gel electrophoresis (1.5%) and quantified using the Quant-iT™ PicoGreen™ dsDNA Assay Kit (Invitrogen, Carlsbad, CA, USA). DNA extracts were stored at -20°C .

2.6.2. Functional Gene Abundance via qPCR

Quantitative polymerase chain reaction (qPCR) was used to target functional genes associated with both denitrification (*nirS*, *nirK* clade I (hereafter *nirK1*), and *nirK* clade II (hereafter *nirK2*)) and DNRA (*nrfA*). Amplifications (15 μL) were performed using SsoAdvanced™ Universal SYBR® Green Supermix (BioRad, Hercules, CA, USA) and a Bio-Rad CFX384™ Real-Time System (Bio-Rad, Hercules, CA, USA) following Table 1. Genomic DNA extracted from bacterial cultures (American Type Culture Collection, Manassas, VA, USA) was used for standard curves (all $r^2 > 0.97$). Reaction efficiencies were 92-102%. Amplification products were verified using gel electrophoresis (1.2%) and melt curves. Three technical replicates were performed for each sample, and abundances are reported as gene copies g-OM^{-1} .

2.6.3. *16s rRNA* Amplicon Sequencing

Prokaryotic community composition was monitored with amplicon sequencing of the V4 region of the *16s rRNA* gene using the 515f-806R primer pair (Caporaso et al., 2011). Library preparation followed the 16S Metagenomic Sequencing Library Preparation Protocol (Part # 15044223 Rev. B, Illumina, CA, USA) with modifications to the first stage PCR. The first stage PCR was performed using a 20 μ L reaction volume and consisted of 0.33 μ M of each primer, 6 ng DNA, and 10 μ L of iProof™ High Fidelity Master Mix (BioRad, Hercules, CA, USA). The thermocycling protocol was: 98°C for 1 min; 20 cycles of 98°C for 20 sec, 55°C for 30 sec, and 72°C for 30 sec; and final elongation at 72°C for 5 min. PCR products were verified using gel electrophoresis (1.5%). Duplicate PCRs were performed for each sample and pooled prior to purification using Agencourt® AMPure XP PCR solution (Beckman Coulter, Brea, CA USA). For the second stage PCR, the Nextera® XT Index Kit (Illumina, San Diego, CA, USA) was used. Amplicons were purified using the Agencourt® AMPure XP PCR solution, quantified using a Qubit® fluorometer (Invitrogen, Waltham, MA, USA), and pooled in equimolar concentration. The library included 5% PhiX control DNA (Illumina, San Diego, CA, USA) and was sequenced on an Illumina MiSeq® using 2x300 paired-end reads with the MiSeq® V3 reagent kit. Sequence data and corresponding metadata are available on the MG-RAST server project number 102115 as part of the “TC Soil Transplant” study.

2.6.4. Sequence Processing

Sequences were processed using Mothur v.1.44.0 (Schloss et al., 2009) following the MiSeq SOP (https://www.mothur.org/wiki/MiSeq_SOP). Reads were assembled using the *make.contigs* command, resulting in 12,887,867 sequences across 87 samples. Sequences were aligned using the SILVA database (Quast et al., 2013). VSEARCH was used to remove chimeric sequences (5.8%) (Rognes et al., 2016). Hierarchical classification was performed using Greengenes version 13_8 (McDonald et al., 2012) at 99%

similarity, and sequences classified as mitochondria, chloroplast, or unknown were removed from the data set using the *remove.lineage* command. Operational taxonomic units (OTUs) were clustered at a 0.03 cutoff with the OptiClust algorithm (Westcott and Schloss 2017) in the *cluster.split* command splitting by classification at level 6. Samples were rarefied to 42,568 reads using the *sub.sample* command, resulting in 96,591 OTUs across all samples. Consensus OTU classification was performed using SILVA v138.1.

2.6.5. Predictive Functional Profiling

Predictive functional profiling was performed using PICRUST2 (Phylogenetic Investigation of Communities by Reconstruction of Unobserved States) in python (Douglas et al., 2020). The accuracy of the predicted genomes was screened using the Nearest Sequenced Taxon Index (Langille et al., 2014). The unstratified predicted metagenome was constructed using EC (enzyme commission) data.

From this dataset, we selected two ECs for a more detailed analysis related to NO_3^- reduction. We considered EC 1.7.2.1, hereafter NIR, which corresponds to the nitric oxide-forming nitrite reductase used in denitrification. We also considered EC 1.7.2.2, hereafter NRF, which corresponds to the ammonia-forming nitrite reductase used in DNRA. In addition to comparing total abundance (reads) for each EC, PICRUST2 provides OTU contributions, which we used to investigate taxonomic shifts for community members predicted to contain NIR or NRF (Castellano-Hinojosa and Strauss 2021, Gaiero et al., 2021).

2.7. Statistical Analysis

Univariate data (e.g., soil properties, NO_3^- reduction rates, gene abundances, and diversity) were analyzed using SigmaPlot 14 (Systat Software Inc., San Jose, CA, USA) ($\alpha=0.05$). Data were screened for normality using Shapiro-Wilk's tests before proceeding with parametric testing. Two-factor ANOVAs

were performed to consider the effects of treatment (F, O, M, FO, and FM) and exposure length (5, 10, 19, and 22 months). All but 3 (of 19) of these two-way ANOVAs displayed a significant interaction ($p > 0.05$), indicating treatment effects varied based on exposure length. To account for this, we performed subsequent one-way ANOVAs analyzing treatment effects *separately* for each sampling event (Supplemental Table 1); Tukey's HSD was used for *post-hoc* comparisons using Copenhaver-Holland p -value adjustments. Note that DOC concentration and denitrification rates were not available for 22 months (November 2018) due to a laboratory processing error, so these comparisons had fewer time points.

To further investigate how functional predictors (qPCR gene abundances and EC abundances) changed in the transplant soils relative to the Fresh control soils, we calculated the standardized mean differences (SMD) at each sampling event using the *cohen.d* command with Hedges' correction in R via the MBESS package (Kelly 2007). Functional predictors were correlated to NO_3^- reduction rates using Pearson's coefficient.

Multivariate analysis of community data was performed using the vegan package in R (Oksanen et al., 2015). Non-metric multidimensional scaling (NMDS) ordinations based on Bray-Curtis dissimilarity were constructed for both OTU-level community data and predicted metagenome data using the *metaMDS* command; environmental vectors were fitted using the *envfit* command. PERMANOVA was performed using the *adonis* command. Potential correlation between community structure and the predicted metagenome was assessed using the *procrustes* command. From the Bray-Curtis matrix, we also calculated the percent dissimilarity of the two transplants (FO and FM) relative to the fresh control (F) at each sampling event.

Alpha diversity indices and taxa relative abundances were calculated using the phyloseq package (McMurdie and Holmes, 2013). In addition, family-level normalized relative abundance data were analyzed using linear discriminant analysis effect size (LEfSe) (Segata et al., 2011) to detect differentially-

abundant taxa among the Fresh control, FO transplant, and FM transplant soils. Data were analyzed via the Galaxy portal (<http://huttenhower.sph.harvard.edu/lefse>) using $\alpha=0.05$ for the Kruskal-Wallis test and a logarithmic linear discriminant analysis (LDA) threshold of 2.0. Once differentially abundant families were identified, heatmaps were constructed using the Heatmapper package (Babicki et al., 2016).

3. Results

3.1. Soil and Water Chemistry

Well water chemistry showed consistent patterns across the three sites (Supplemental Figure 1), with median salinity matching the expected values for freshwater (0.1 ppt), oligohaline (1.1 ppt), and mesohaline (14.5 ppt) wetlands. Concurrent with the salinity increase, we saw increased median concentrations of Σ sulfide (freshwater: not detected, oligohaline: 0.1, and mesohaline: 2.4 mM), SO_4^{2-} (< 0.1, 0.1, and 1.7 mM), NH_4^+ (3.3, 6.5, 14.6 μM), and NO_3^- (7.5, 8.5, and 12.1 μM). Though less pronounced, site differences were also evident in soil data (Table 2, controls). The greatest differences were for OM and redox, which were always significantly lower in Meso controls compared to Fresh and Oligo. The other soil properties (C:N and pH) did not differ across controls except for a slight pH increase for Meso at 22 months.

Porewater data indicate that transplanted freshwater soil bags equilibrated quickly to the host environments. Salinity increased to match oligohaline and mesohaline levels by the first sampling, and FO and FM were always significantly greater than the Fresh controls (Table 2; Supplemental Table 1). Concentrations of SO_4^{2-} , NH_4^+ , NO_3^- , and DOC in FO and FM bags also always matched their surroundings except for FM at 19 months. In those bags, NO_3^- and SO_4^{2-} concentrations were significantly higher in the

FM transplant soils than in the corresponding Meso controls, whereas DOC concentrations were significantly lower.

Soil chemistry of transplants was also altered, but usually required longer exposure than porewater chemistry for differences to manifest (Table 2). Organic matter content remained high and similar to Fresh controls until 22 months, at which point the FO transplant decreased to 35%, compared to 42% in the Fresh controls. The corresponding decrease was even greater in the FM transplants, and OM in those final bags (23%) was nearly the same as the Meso controls (21%). C:N ratio did not change significantly during these incubations, and pH was also fairly stable. The FM transplant experienced transient acidic conditions at the first sampling, dropping to 4.7 after 5 months of exposure, before stabilizing at a near neutral pH (6.5 to 6.9), intermediate between the Fresh and Meso controls, for the remainder of the experiment. Redox showed the fastest response of the soil transplants; both FO and FM were significantly lower than the Fresh controls for all comparisons except FO at 5 months.

3.2. DNRA and Denitrification Rates

DNRA rates were higher in the Meso controls compared to the Fresh and Oligo controls (Figure 1). This suggests a positive relationship between DNRA and salinity, though the difference across sites was only statistically significant for the 22 month sampling. When fresh soil was exposed to oligohaline conditions (FO), DNRA rates were stimulated. This effect was magnified in the FM transplants, which were significantly greater than the Fresh controls for both the 10- and 22-month sampling events. Data for the 19-month sampling event were similar, but with higher overall rates and greater variability.

In contrast, denitrification rates did not show consistent treatment effects, except that Meso soils always had the lowest rates of the controls (Figure 1). Data for 10 months of exposure suggest that salinization suppressed denitrification; rates in both FO and FM soils were significantly lower than Fresh

controls. This effect disappeared by the 19-month sampling. Instead, we observed increased denitrification rates in Oligo controls relative to all other treatments.

3.3. DNRA Functional Gene Abundance

Abundance of the DNRA gene, *nrfA*, showed a negative relationship to salinity across the three sites (Supplemental Table 2). The responses of transplanted soils were determined by calculating SMD relative to Fresh controls at each sampling event (Figure 2). This indicated that exposure to oligohaline conditions (FO) had no consistent effect on *nrfA* abundance, whereas exposure to mesohaline conditions (FM) led to a significant decrease at 10 months that persisted through the 22 month sampling event.

These qPCR results contrasted with those obtained via functional prediction modeling (i.e., the EC data), which instead showed a positive relationship with salinity. NRF abundance was consistently highest in the Meso soils (Supplemental Table 2), and SMD analysis indicated abundance was elevated in FM soils relative to the Fresh controls at 19 and 22 months (Figure 2).

3.4. Denitrification Functional Gene Abundance

In control soils, qPCR abundance of denitrification functional genes decreased with salinity for all sampling events (Supplemental Table 2). The difference was statistically significant for *nirS* and *nirK2*, which were both ~4-fold lower in Meso soil compared to Fresh. SMD analysis of both *nirK* genes showed initial decreases in abundance, followed by a return to levels comparable to the Fresh controls (Figure 2). This recovery was faster for FO (10 months for *nirK1*, 19 months for *nirK2*) compared to FM (22 months for both genes). Exposure to mesohaline conditions had a similar negative effect on *nirS*, which persisted for the remainder of the experiment.

NIR abundances showed a more complex pattern. Results for mesohaline conditions were similar to the qPCR assays; abundance was lowest in Meso controls (Supplemental Table 2) and suppressed in FM transplants (Figure 2). However, unlike the qPCR data, the greatest NIR abundances were consistently found in Oligo controls, and FO transplants did not change following salinity increases.

3.5. Alpha Diversity

Two-way ANOVAs revealed a significant treatment effect on both Shannon H' ($F=28.4$, $p<0.001$) and OTU richness ($F=28.4$, $p<0.001$). Because exposure length (H' : $F=2.2$, $p=0.09$; OTUs: $F=2.6$, $p=0.06$) and interaction (H' : $F=1.4$, $p=0.18$; and OTUs: $F=0.9$, $p=0.53$) effects were not significant, results were summarized across all sampling events (Figure 3). Diversity (H') was lowest in the Meso controls, but no differences were evident between Fresh or Oligo controls or either transplant (FO and FM). OTU richness was more affected by salinity; in addition to being significantly lower in Meso controls, richness was slightly decreased in both transplants.

3.6. Beta Diversity

Two-way PERMANOVA indicated a significant interaction between treatment and exposure length as effects on community structure (Treatment pseudo- $F=50.8$, $p<0.001$; Exposure length pseudo- $F=6.5$, $p<0.001$; Interaction pseudo- $F=3.5$, $p<0.001$). NMDS (stress=0.06) shows the three controls were distinct, with minimal temporal change (Figure 4A). Meso controls, which separated on axis 1, were most distinct, with Oligo and Fresh controls separating on axis 2. The Meso control communities were characterized by elevated salinity, SO_4^{2-} , and NO_3^- . In contrast, the Fresh and Oligo communities correlated with redox and OM.

In addition to separating the control soils, NMDS shows transplant communities migrating from the Fresh controls to match the respective host communities. The lower salinity transplant, FO, was

again most resistant; it remained clustered near the Fresh controls until the final (22 months) sampling event, at which point only one replicate moved to cluster with the Oligo controls. The FM transplant community responded quickly and diverged from the Fresh controls within 5 months. By the end of the experiment, the communities in the FM transplants converged with the Meso controls. This shift was characterized by an increase in salinity and dissolved ion concentrations (NH_4^+ , NO_3^- , and SO_4^{2-}) and a decrease in redox and OM.

Divergence of the transplant communities from the Fresh controls was also visualized by plotting the mean relative dissimilarity for each sampling event (Figure 4B), which was compared to the mean dissimilarity among all Fresh controls (solid horizontal line). Overall, FO soils were much more resistant than FM. It took 22 months for the FO community to separate appreciably from Fresh, whereas the FM community reached the same level within 5 months. FM transplants continued to diverge with longer exposure, and were 93% dissimilarity from the Fresh control community by the end of the experiment.

3.7. Predicted Metagenome

NMDS ordination of the predicted metagenome (stress=0.09) showed similar patterns to the ordination for community structure (Procrustes, $\text{RLs}=0.92$, $p=0.001$) and similar spread of environmental vectors (Figure 4C). Controls separated into three clusters, with Meso being most distinct due to elevated salinity, SO_4^{2-} , and NO_3^- . The transplanted communities changed over time to better match their host environment. This change was slowest for FO, which remained clustered with Fresh controls until the final sampling event. In contrast, FM transplants immediately diverged from Fresh controls, and restructured to fully match the Meso controls by 22 months.

Divergence of the transplant communities based on predicted metagenomes (Figure 4D) was similar to what was obtained for community composition but with much less overall change (note

Figures 4B and 4D scales). Even after 22 months under mesohaline conditions, FM soils were only 5-6% dissimilar from the Fresh control community in terms of overall predicted functional potential.

3.8. Phyla Overview

Differences in community composition in the three controls were observed at the phylum level (Supplemental Figure 2). Proteobacteria were dominant across all samples and sampling events, comprising 17.0-25.2% of the community. Relative abundance of Acidobacteria decreased across the salinity gradient, averaging 15.0 (\pm 0.5, S.E.), 8.8 (0.5), and 6.7 (0.2) % of the community for Fresh, Oligo, and Meso controls respectively. Other groups decreasing across the gradient include Nitrospirota (Fresh: 6.6 (0.6), Oligo: 7.2 (0.7), and Meso: 0.9 (0.1)), Methyloirabiolota (1.4 (0.1), 0.5 (0.1), and 0.1 (0.1)), MBNT15 (2.7 (0.2), 1.0 (0.1), and 0.7 (0.1)), and Sva0485 (2.5 (0.3), 1.7 (0.1), and 0.5 (0.1)). In contrast, abundance increased with salinity for Bacteroidota (7.7 (0.3), 10.6 (0.4), and 14.3 (0.8)), Desulfobacterota (6.9 (0.2), 11.0 (0.3), and 17.1 (1.1)), and Crenarchaeota (1.5 (0.1), 2.1 (0.2), and 2.4 (0.4)).

Dominant phyla in transplant soils were initially similar to the Fresh controls, but shifted in later sampling events to match the host communities. Changes in FO transplants were modest compared to FM. For example, the relative abundance of Acidobacteria in FO decreased from 17.6 (\pm 0.3, S.E.) % to 13.5 (3.0) % between the 5 and 22 month sampling events, whereas the corresponding decrease for FM was 15.8 (2.8) % to 5.2 (1.0) %. Incubation under more saline conditions also had a greater effect on relative abundance of Desulfobacterota (FO: 7.4 (0.3) increased to 9.6 (1.1); FM: 9.3 (1.4) increased to 15.1 (0.7)) and Bacteroidota (FO: 7.5 (0.2) to 9.2 (0.5); FM: 8.0 (0.6) to 13.3 (1.8)). Some phyla were affected by mesohaline but not oligohaline conditions. For example, Methyloirabiolota and MBNT15 still comprised >2% of the FO community after 22 months, but were completely absent from FM by the 19 and 22 month exposures, respectively. Similarly, Nitrospirota was still a dominant member of the FO

community after 22 months (7.7 (0.5) %) but had decreased to only 0.2 (0.1) % of the FM community by 22 months.

3.9. Differentially Abundant Taxa

To identify differentially abundant taxa responsible for reshaping the transplant communities, we performed LefSe analysis at the family level, focusing on the Fresh controls and the transplant soils. A total of 82 families (F=29, FO=8, FM=45) were identified as being differentially abundant among the three soils (Supplemental Table 4). Fresh controls (Figure 5A) were characterized by methane-cycling prokaryotes (e.g., Methanosaetaceae and Methanomassiliicoccaceae), multiple lineages from the phylum Myxococcota (e.g., Anaeromyxobacteraceae and Polyangiaceae), and nitrifiers (e.g., Nitrosomonadaceae and Nitrospiraceae). For FO transplant soils (Figure 5B), the loss of freshwater taxa was more discriminating than the gain of new transitional or oligohaline indicators; only eight families were found in greater relative abundance in FO soils than in the Fresh control and FM soils. Of the eight families, Methylospiraceae, Comamonadaceae, and Hydrogenophilaceae showed the greatest enrichment in the FO transplant community. The taxa that differentiated the FM community (Figure 5C) were largely sulfur-cycling taxa from the order Campylobacterales (e.g., Sulfurimonadaceae and Sulfurovaceae) and the phylum Desulfobacterota (e.g., Desulfurivibrionaceae and Desulfobulbaceae). In addition, multiple Gammaproteobacteria families (e.g., Halothiobacillaceae and Rhodobacteraceae) increased in relative abundance.

3.10. NIR and NRF Taxonomic Contributions

To gain more detailed knowledge regarding the response of the NO_3^- reducing prokaryotes, we examined the relative abundance of taxa that are predicted to be capable of DNRA (i.e., predicted to contain NRF) and denitrification (NIR). Distinct patterns were evident across the control samples (F, O,

and M in Figure 6), with many of the groups that had been identified as differentially abundant via LEfSe emerging as dominant taxa capable of NO_3^- reduction.

NRF taxonomic contributions (Figure 6B) in the Fresh community were dominated by Geobacteraceae, Bacteroidetes_vadinHA17, and an unclassified family from the order MBNT15. The Oligo control communities showed a similar pattern, though the contribution of Geobacteraceae and MBNT15 decreased, and the contribution of Syntrophobacteraceae increased. In the Meso controls, Geobacteraceae and MBNT15 were no longer found, and the community became dominated by Ignavibacteriaceae and an unclassified family belonging to the order Ignavibacteriales. Transplant soils were more variable over time, and showed both a loss of Fresh taxa and an increase in either Oligo (FO) or Meso (FM) taxa over the course of the experiment. For example, the FO community transition was characterized by a decrease in the relative abundance of Geobacteraceae and an increase in the abundance of Syntrophobacteraceae and Bacteroidetes_vadinHA17. The FM community transition also saw a decrease in Geobacteraceae (<1.5% by 22 months), which was replaced by Ignavibacteriaceae, Sva1033, and an unclassified family in the order Ignavibacteriales.

NIR taxonomic contributions (Figure 6A) in the Fresh community were dominated by Nitrosomonadaceae, Nitrospiraceae, Methylomonadaceae, and B1-7Bs. These taxa were considerably less abundant in the Oligo control community, which was instead dominated by Gallionellaceae and Hydrogenophilaceae. The Meso control community was dominated by Sulfurimonadaceae, Rhodanobacteraceae, and Rhodobacteraceae, with a small amount of Methylomonadaceae and Nitrosomonadaceae remaining. Transplant communities initially matched the Fresh controls but changed over time to match the host-site community, similar to the NRF transitions. For example, the relative abundance of Gallionellaceae and Hydrogenophilaceae (dominant in the Oligo control communities) dramatically increased in FO transplant soils by the final sampling event, while several taxa characteristic of the Fresh community remained (e.g., B1-7Bs, Burkholderiales, and

Nitrososphaeraceae). In FM transplant communities, Sulfurimonadaceae and Rhodanobacteraceae were enriched, together accounting for over 50% of NIR taxa by the 22 month sampling.

4. Discussion

4.1. Salinization Alters Soil and Water Chemistry

Analysis of soil properties and porewater chemistry showed distinct physicochemical conditions at the three sites, consistent with prior studies across salinity gradients (Morrissey et al., 2014, Martin and Moseman-Valtierra 2015, Zhao et al., 2020). Further, the changes observed in the transplanted soils indicate that the experiment successfully represented a salinization disturbance. The decrease in soil OM was especially striking. After 22 months of exposure, freshwater soil experiencing oligohaline salinity had 18% less OM than the freshwater controls, and soils experiencing mesohaline conditions had 46% less. The magnitude of soil OM loss in the transplant soils was surprisingly large. Broadly speaking, these findings are consistent with prior salinity manipulation studies (Neubauer et al., 2019, Weston et al., 2010, Chambers et al., 2013, Servais et al., 2019) as well as observational studies along salinity gradients (Wang 2016, Morrissey et al., 2014, Craft 2007). This consistent negative relationship between OM and salinity has been attributed to multiple factors, including variations in carbon input and content (Xia et al., 2021) and desorption of organic particles due to increased ionic strength (Servais et al., 2019, Servais et al., 2020). Unfortunately, our DOC data showed considerable variability throughout the experiment, even for controls, so it was not possible to assess the potential role of desorption in our system. Another mechanism of OM loss is increased decomposition due to greater availability of SO_4^{2-} , which serves as a terminal electron acceptor for heterotrophic metabolism (Weston et al., 2006, Weston et al., 2010, Chambers et al., 2019). In transplant soils, we measured increased concentrations of SO_4^{2-} (Table 2) and a greater abundance of SO_4^{2-} -reducing taxa (Supplemental Figure 2, Figure 5), which,

combined with a loss of methanogenic taxa, suggests that increased activity of SO_4^{2-} reducers contributed to OM loss.

Another physicochemical change associated with salinization is increased porewater NH_4^+ concentrations (Herbert et al., 2015). We observed this trend in both transplant soils (Table 2), although it was more pronounced under mesohaline conditions. The phenomenon is often attributed to desorption of NH_4^+ from soil due to cation displacement (Herbert et al., 2015), though this process is thought to occur over relatively short temporal scales (Liu and Lennartz 2019). Since prolonged exposure to increased salinity depletes soil pools of exchangeable NH_4^+ (Noe et al., 2013), this mechanism is an unlikely explanation for the elevated NH_4^+ that we observed at later sampling events. Instead, those elevated NH_4^+ concentrations may be due to greater N mineralization (associated with increased decomposition) or suppression of nitrification due to increased Σ sulfide concentrations (Joye and Hollibaugh 1995, Rysgaard et al., 1999). The higher DNRA rates in transplanted soils (Figure 1) may also contribute. Together, these environmental data agree well with prior wetland salinization studies and indicate our transplant experiments are a valuable system for studying how exposure length and salinity level impact prokaryotic communities.

4.2. Response of Soil Prokaryotic Communities to Salinization

Several prior studies observed a negative relationship between salinity and diversity in microbial communities (Zhao et al., 2020, Simachew et al., 2016, Xie et al., 2017), which also manifests in our data. In particular, we saw decreased diversity and lower richness in controls incubated at the mesohaline site, but no differences between freshwater or oligohaline controls. Given the unique community found at the mesohaline site, it was surprising to see no statistically significant change in diversity or richness in the transplanted FM community. One possible explanation is that 22 months of exposure to mesohaline conditions was not long enough for diversity differences to develop. Data from the final

sampling event show a small decrease in diversity (2.0%) and richness (7.1%) relative to the Fresh control community, which suggests that larger differences might have manifested if the experiment had been conducted for a third year.

Though salinization did not significantly impact alpha diversity in our transplant communities, it did impact beta diversity (Figure 4A) and caused a shift in the abundance of dominant taxa (Supplemental Figure 2, Figure 6). Freshwater communities incubated under oligohaline conditions were quite resistant to restructuring, and did not match the native oligohaline community even after 22 months of exposure. This suggests that a significant portion of the freshwater community was able to tolerate or adapt to the physiological stressors of low(er)-intensity salinization. Prior studies show similar community structures between freshwater and oligohaline environments (Herlemann et al., 2011) and find that aquatic freshwater communities display high resistance to oligohaline salinization (Berga et al., 2017). In contrast, the freshwater community quickly restructured when exposed to mesohaline conditions (FM in Figure 4B). Our results are supported by Dang et al. (2019), who performed a similar soil transplant using our mesohaline site but a different freshwater site. They found unique transitional communities within ~3 months, which persisted until the end of their experiment (1 year). We also observed unique transitional communities during the first 1.5 years (5, 10, and 19 month sampling events), and learned that it can take 2 years (22 months) of exposure for a freshwater community to restructure under mesohaline conditions. Our data suggest that communities experiencing oligohaline levels of salinization will take even longer to stabilize, though the overall change in community composition will be less.

Prokaryotic communities experiencing salinization are characterized by a decrease in abundance of methanogens and/or a shift in methanogen community composition (Dang et al., 2019, Morrissey and Franklin, 2015), a decrease in abundance of nitrifiers (Li et al., 2021), and an increase in abundance of SO_4^{2-} reducers (Mobilier et al., 2020). We detected all of these shifts in our transplant communities and

also made novel observations. We identified freshwater taxa that were the most sensitive to salinization (Figure 5A), which included methanogens and syntrophs (e.g., Syntrophaceae), as well as several N cycling prokaryotes. Besides nitrifiers, select families of DNRA-capable bacteria (Anaeromyxobacteraceae, Myxococcaceae, Opiritaceae, and Pedosphaeraceae) decreased in abundance due to salinization, as did the family Methylomonadaceae, which has the genetic capability to perform denitrification and methanotrophy (Grinsven et al., 2020).

We found that freshwater soils experiencing oligohaline levels of salinization predominately retain freshwater taxa. Any taxa that are specialized for oligohaline conditions are either relatively uncommon or take >22 months to become dominant community members. In contrast, we saw that freshwater soils experiencing mesohaline conditions acquired several new dominant taxa within only a few months (Figure 5C). In addition to SO_4^{2-} reducers (e.g., Desulfobacteraceae and Desulfuromonadaceae), we found an increased abundance of sulfur-cycling taxa capable of denitrification (e.g., Sulfurimonadaceae (Waite et al., 2017) and Sulfurovaceae (Chen et al., 2021)) and DNRA (e.g., Desulfurivibrionaceae (Anantharaman et al., 2018), Desulfobulbaceae (Anantharaman et al., 2018), Sva1033 (predicted to contain NRF), and Ignavibacteriaceae (Cheung et al., 2018)). Taxonomic shifts during salinization show freshwater N cycling prokaryotes are predominantly replaced by taxa that couple NO_3^- reduction to sulfur oxidation, or by SO_4^{2-} reducing bacteria with flexible metabolism including NO_3^- reduction. These shifts suggest a major change in the functional potential of the communities, which was reinforced by our metagenomic predictions (Figure 4C). Overall, the transitions we observed align with previous efforts to characterize prokaryotic community changes during salinization (e.g., Dang et al., 2019; Morrissey and Franklin, 2015; McBeth et al., 2013; Cheung et al., 2018) and with a recent meta-analysis by Chen et al. (2022).

4.3. Impact on NO_3^- Reducing Community

By assessing the prokaryotic community in tandem with measurements of NO_3^- reduction potential (i.e., rates and functional gene abundance), we gained a more nuanced understanding of how salinity level and exposure length impact N cycling communities in coastal freshwater wetlands. Metagenome predictions revealed diverse communities capable of denitrification and DNRA at all sites and suggest that denitrifiers may be more sensitive to salinization than DNRA taxa. This is supported by the fact that the dominant taxa of potential denitrifiers were distinct across all three sites (F, O, and M in Figure 6A), and even the modest increase in salinity associated with transplanting fresh soil to the oligohaline site caused a significant shift in denitrifier community composition.

The complexities of predicting how denitrifiers will respond to salinization are highlighted by our *nirS* and *nirK* qPCR results. Denitrifiers are typically classified by which of these nitrite reductase genes they possess, as *nirS* and *nirK* denitrifiers display different ecologies (Kou et al., 2021, Bowen et al., 2020). In our study, abundance of *nirS*-type denitrifiers did not change due to exposure to oligohaline conditions, but decreased under mesohaline conditions. The response of *nirK* denitrifiers depended on exposure length rather than salinity level. When the freshwater community was transplanted to either salinity level, abundance was initially suppressed but rebounded after 22 months of exposure. This could be due to the freshwater *nirK* community acclimating to the host-site conditions and recovering, or it could be due to the replacement of susceptible freshwater taxa with denitrifying taxa from the host-site. Our findings are in general agreement with *nirK*-type denitrifiers being more sensitive to salinity than *nirS*-type denitrifiers (Jones and Hallin, 2010, Wang et al., 2018); however, our data indicate that *nirK*-type denitrifiers may be more resilient to mesohaline levels of salinity than *nirS*-type denitrifiers.

Denitrification rates were affected by salinity (Figure 1) and highlight the importance of explicitly considering exposure length when drawing conclusions about salinization effects. For example, data from our 10-month sampling suggest that salinization suppresses denitrification, consistent with

the findings of Craft et al. (2009), Rysgaard et al. (1991), Smith et al. (2015), Neubauer et al. (2019), and Qi et al. (2021). However, the 19-month data suggest no effect, similar to Magalhães et al. (2005), because transplants were not significantly different from fresh controls. Other experimental manipulations of wetland soil salinity have found denitrification to increase (Marton et al., 2012, Marks et al., 2016), though those studies considered salinization over relatively short temporal scales (hours to days). The disparate findings from past studies contextualized with our new results suggest that efforts to reconcile and synthesize denitrification responses to salinization must carefully consider the duration of exposure. Further, our data demonstrate that denitrifier community responses to salinization are dynamic for *at least* 19 months (probably >22 months based on community composition changes (Figure 6A)) and suggest that salinization effects on ecosystem N removal may differ dramatically for short (days-weeks-months) vs. long (months-years) exposures.

One additional noteworthy finding from our denitrification data is the observation that rates in the oligohaline wetland were comparable to, if not greater than, rates at the freshwater site (contrast F and O controls in Figure 1). This was unexpected, as trends across salinity gradients generally find denitrification is suppressed at higher salinities (Craft et al., 2009, Rysgaard et al., 1991, Smith et al., 2015, Qi et al., 2021). Our NIR taxonomic analysis revealed the oligohaline community has a particularly high abundance of Hydrogenophilaceae (yellow bars in Figure 6A), which are known to perform chemolithoautotrophic denitrification by coupling sulfide oxidation with NO_3^- reduction (Orlygsson and Kristjansson 2014). These organisms can become stimulated at sulfide concentrations of ~ 0.1 mM (Murphy et al., 2020), which we observed in our oligohaline wells. Dominance of this group at the oligohaline site highlights the complex linkages of N and sulfur cycling, which must be explored further if we are to develop a truly mechanistic understanding how salinity affects NO_3^- removal. Sulfur availability and redox state are also key to many DNRA organisms (Burgin and Hamilton, 2007).

Prior studies of DNRA community structure find taxonomic transitions across salinity gradients, such as a decrease in Geobacteraceae and an increase in Ignavibacteraceae and Prolixibacteraceae (Hu et al., 2021, Song et al., 2014), which also manifest in our data (Figure 6B). Overall, DNRA taxa showed considerable overlap between freshwater and oligohaline environments and were distinct from mesohaline taxa, suggesting that mesohaline levels of salinization are required to reshape DNRA communities. We observed just this: transplant soils experiencing oligohaline conditions retained many freshwater DNRA taxa, whereas exposure to mesohaline conditions caused a strong shift after only 10 months. When considering DNRA rates, we also found mesohaline conditions were necessary to induce a significant change. These results agree with previous research efforts by Zhou et al. (2021), who found no difference in DNRA rates between freshwater and oligohaline wetlands, and Giblin et al. (2010), who found DNRA was stimulated in wetlands experiencing seasonal increases to mesohaline salinities. Together, these data suggest that DNRA rates and associated taxa may be resistant to moderate (oligohaline) intensities of salinization, but susceptible to higher levels (mesohaline).

Though we saw good agreement of our DNRA taxa and rate data with prior studies, *nrfA* qPCR data did not show the expected response. Instead of finding a positive relationship between *nrfA* and salinity levels, as has previously been found in both salinity gradients (Franklin et al., 2017) and salinity manipulations (Neubauer et al., 2019), we saw a negative relationship. Recent work by Cannon et al. (2019) indicate that the primers we used exclude certain taxa (ex. Clade I organisms), so it is likely our *nrfA* results are limited due to poor coverage. We did see a strong positive relationship between salinity with NRF abundance (Supplemental Table 2).

Lastly, we assessed how well our genetic data on functional potential correlated with our measured rates of NO_3^- reduction. For both DNRA and denitrification, EC abundance from predicted metagenomes performed better than qPCR data from functional genes (Supplemental Table 5). For DNRA, the low correlation of *nrfA* abundance to rates ($r=0.13$) was likely due to the primer design

discussed above. For denitrification, correlations with qPCR functional gene data were slightly better (0.32-0.54) but still much lower than NIR abundance ($r=0.73$). This could be due to the fact that NIR EC 1.7.2.1 accounts for both nitrite reductase enzymes (*nirS* and *nirK*), making it a broader integrator of denitrifier potential compared to any individual functional gene. To test this, we performed a multiple regression combining qPCR data from all three denitrification qPCRs (*nirS*, *nirK1*, and *nirK2*). Together, they explained 37% of the variance (adjusted R^2) observed in denitrification rates, compared to 53% for NIR. These results suggest that recent improvements to PICRUSt2 (Douglas et al., 2020) have made it a valuable tool for making functional predictions from amplicon sequencing of environmental samples, consistent with Raes et al. (2021).

5. Conclusions

While we have contextualized this study by focusing on salinization driven by sea-level rise, our findings are applicable to other coastal salinization events, including storm surges and seawater incursion following hydrologic manipulations (e.g., groundwater extraction or freshwater diversion for irrigation and industrial use) (Hebert et al., 2015, Tully et al., 2019). Our conclusions are also relevant to efforts to understand and mitigate the salinization of inland wetlands, which can occur due to irrigation, mining, and application of de-icing salts (Hintz et al., 2022). Our transplant experiment mimicked chronic salinization, which tends to have more long-lasting ecosystem effects compared to episodic salinization (Widney et al., 2019, Hebert et al., 2018). Overall, we found the microbial community response to be highly dependent on salinity level. Freshwater communities experiencing mesohaline conditions rapidly reorganized, whereas communities experiencing oligohaline conditions resisted restructuring. Though compositionally more stable, these fresh-to-oligohaline communities did change in function (e.g., decreased denitrification rates). This finding is consistent with Philippot et al. (2021), who posit that a

mild disturbance is likely to initially affect microbial functions but not microbial community composition. However, Philippot et al. (2021) caution that delayed compositional responses may be an artifact due to the detection of relic DNA (i.e., extracellular DNA or dead cells) when using DNA-based approaches. Given the relatively long intervals between our sampling events and the rapid changes we detected for community composition in the mesohaline transplant, we do not think this is a major factor. Our data highlight that microbial community structural and functional responses can be decoupled, and that both may take several years to stabilize in response to chronic salinization. Further, taking the temporal scale of microbial responses into account may help reconcile apparent discrepancies among studies investigating the impact of salinization on microbially-mediated ecosystem N removal.

Acknowledgments: We greatly appreciate David Berrier, Chansotheary Dang, Drashty Mody, Ella Balasa, Aoife Mahaney, Joseph Battistelli, Melissa Davis, and Michael Kammerman for their help with field and lab work. We thank Denise Wohlfahrt for assistance with sequence processing, and Dr. Robert Michener for logistical support during isotope analysis. We would like to give special thanks to Dr. Jeffrey Chanat for the R code he generously provided to parse predicted metagenome functions. This paper is a contribution from the VCU Rice Rivers Center.

Funding: Funding for this research was provided by the National Science Foundation (DEB 1355059), Virginia Sea Grant, the Virginia Water Resources Research Center, and the VCU Rice Rivers Center.

6. Tables and Figures

Table 1. Primers and thermal cycling conditions for qPCR assays.

Target	Primer Information			Template DNA (ng)	Standards (ATCC Strain #)	Thermal Conditions (°C)
	Names	Reference	μM			
<i>nirK1</i>	nirKC1F nirKC1R	Wei et al. (2015)	0.20	4.0	<i>Alcaligenes faecalis</i> (8750)	98° for 2 min, 40 cycles of 98° for 10 sec, 54° for 10 sec, 68° for 30 sec
<i>nirK2</i>	nirKC2F nirKC2R	Wei et al. (2015)	0.20	4.0	<i>Caulobacter segnis</i> (21756)	98° for 2 min, 32 cycles of 98° for 10 sec, 56° for 10 sec, 68° for 30 sec
<i>nirS</i>	cd3aF R3cd	Throbäck et al. (2004)	0.10	3.0	<i>Paracoccus denitrificans</i> (17741)	94° for 4 min, 35 cycles of 94° for 30 sec, 56° for 30 sec, 72° for 60 sec
<i>nrfA</i>	nrfAF2aw nrfAR1	Welsch et al. (2014)	0.43	1.5	<i>Escherichia coli</i> (11775)	95° for 5 min, 40 cycles of 95° for 30 sec, 53° for 30 sec, 72° 20 sec

Table 2. Mean (\pm standard error) for soil and porewater chemistry. Lower case letters indicate significant treatment effects on the corresponding parameter within each exposure length, detected via one-way ANOVA with subsequent post-hoc analysis using Tukey’s HSD. Missing data are denoted as “nd.”

Parameter	Treatment	Exposure Length			
		5 Months	10 Months	19 Months	22 Months
Salinity (PPT)	F	0.0 \pm 0.0 c	0.0 \pm 0.0 c	0.0 \pm 0.0 d	0.1 \pm 0.0 c
	FO	2.0 \pm 0.4 b	1.5 \pm 0.2 c	3.6 \pm 0.1 c	1.3 \pm 0.1 b
	O	3.7 \pm 0.9 b	5.4 \pm 0.4 b	1.6 \pm 0.1 d	1.9 \pm 0.1 b
	FM	10.4 \pm 0.6 a	10.4 \pm 0.5 a	7.1 \pm 0.9 b	11.7 \pm 0.9 a
	M	10.6 \pm 0.7 a	10.1 \pm 0.3 a	9.3 \pm 0.3 a	13.4 \pm 0.2 a
NO ₃ ⁻ (μ M)	F	5.5 \pm 1.0 -	16.6 \pm 2.2 ab	11.2 \pm 0.7 c	15.3 \pm 2.6 -
	FO	4.1 \pm 0.5 -	10.0 \pm 0.6 b	9.7 \pm 0.2 c	10.2 \pm 1.6 -
	O	8.7 \pm 3.0 -	7.1 \pm 0.3 b	15.2 \pm 1.8 c	8.2 \pm 0.6 -
	FM	1.8 \pm 0.4 -	25.4 \pm 3.9 a	39.2 \pm 3.9 a	10.3 \pm 1.0 -
	M	1.6 \pm 0.6 -	23.9 \pm 1.3 a	27.1 \pm 0.7 b	11.5 \pm 0.3 -
NH ₄ ⁺ (μ M)	F	52.5 \pm 8.3 -	21.2 \pm 4.5 b	8.4 \pm 2.4 b	8.8 \pm 3.6 -
	FO	64.2 \pm 8.1 -	31.2 \pm 11.2 b	25.6 \pm 4.3 bc	6.3 \pm 2.4 -
	O	48.2 \pm 15.0 -	35.9 \pm 17.9 b	17.6 \pm 3.7 b	1.9 \pm 0.8 -
	FM	57.0 \pm 11.4 -	234.5 \pm 56.7 a	125.5 \pm 28.2 a	2.2 \pm 1.1 -
	M	60.1 \pm 5.4 -	130.6 \pm 37.6 ab	89.7 \pm 21.2 ab	3.8 \pm 0.7 -
SO ₄ ²⁻ (mM)	F	0.0 \pm 0.0 b	0.0 \pm 0.0 b	0.1 \pm 0.0 c	0.2 \pm 0.1 b
	FO	0.2 \pm 0.1 b	0.2 \pm 0.1 b	1.0 \pm 0.2 c	0.7 \pm 0.2 b
	O	0.4 \pm 0.1 b	1.9 \pm 0.3 b	0.5 \pm 0.1 c	0.9 \pm 0.2 b
	FM	8.0 \pm 0.9 a	9.5 \pm 0.6 a	31.6 \pm 5.7 a	22.5 \pm 1.4 a
	M	6.0 \pm 0.7 a	10.2 \pm 2.1 a	18.4 \pm 2.5 b	27.4 \pm 2.9 a

DOC (mg L ⁻¹)	F	15.1 ± 3.9	-	48.7 ± 5.3	a	33.5 ± 6.1	b	nd
	FO	16.0 ± 1.8	-	24.5 ± 2.5	b	20.3 ± 3.5	b	nd
	O	18.5 ± 4.1	-	19.2 ± 1.9	b	22.3 ± 5.6	b	nd
	FM	30.1 ± 5.4	-	29.9 ± 3.7	bc	29.2 ± 2.8	b	nd
	M	27.8 ± 2.9	-	39.8 ± 3.6	ac	62.6 ± 5.1	a	nd
OM (%)	F	36.6 ± 0.3	a	36.0 ± 0.5	a	35.3 ± 0.5	a	42.3 ± 1.7 a
	FO	36.4 ± 0.4	a	35.7 ± 0.4	a	30.8 ± 3.8	a	34.8 ± 0.9 b
	O	35.7 ± 2.8	a	36.8 ± 4.7	a	39.9 ± 5.0	a	30.5 ± 0.3 bd
	FM	34.9 ± 1.1	a	34.8 ± 0.5	a	34.5 ± 0.8	a	22.7 ± 2.5 cd
	M	23.7 ± 3.0	b	20.2 ± 2.1	b	20.4 ± 1.2	b	20.8 ± 1.5 c
C:N	F	16.1 ± 0.5	-	14.5 ± 0.7	-	15.0 ± 0.3	-	14.9 ± 0.3 -
	FO	15.2 ± 0.5	-	15.2 ± 0.6	-	15.1 ± 0.2	-	15.2 ± 0.2 -
	O	14.5 ± 0.9	-	14.2 ± 0.7	-	14.3 ± 0.4	-	16.8 ± 1.9 -
	FM	14.9 ± 0.2	-	14.3 ± 0.2	-	15.8 ± 0.7	-	14.2 ± 0.7 -
	M	15.1 ± 1.0	-	13.7 ± 0.5	-	14.1 ± 0.6	-	14.5 ± 1.5 -
Redox (mV)	F	-123.4 ± 9.8	a	-72.4 ± 6.3	a	-44.6 ± 22.7	a	-62.6 ± 11.2 a
	FO	-152.2 ± 12.1	a	-178.8 ± 28.8	b	-160.6 ± 18.2	b	-262.0 ± 18.5 b
	O	-128.6 ± 8.3	a	-117.4 ± 9.3	ab	-143.2 ± 15.3	b	-101.3 ± 12.5 a
	FM	-77.2 ± 6.7	c	-302.8 ± 26.1	c	-212.6 ± 24.8	b	-248.1 ± 17.6 b
	M	-262.4 ± 14.0	b	-289.2 ± 24.1	c	-206.8 ± 21.0	b	-308.7 ± 8.7 b
pH	F	6.6 ± 0.1	ab	6.2 ± 0.1	ab	6.5 ± 0.0	ab	6.4 ± 0.1 a
	FO	6.6 ± 0.1	ab	5.9 ± 0.2	a	6.1 ± 0.1	a	6.3 ± 0.1 a
	O	6.4 ± 0.1	b	6.2 ± 0.0	ab	6.3 ± 0.1	a	6.5 ± 0.2 a
	FM	4.7 ± 0.1	c	6.5 ± 0.3	ab	6.6 ± 0.4	ab	6.9 ± 0.2 ab
	M	6.7 ± 0.0	a	6.7 ± 0.1	b	7.3 ± 0.2	b	7.5 ± 0.0 b

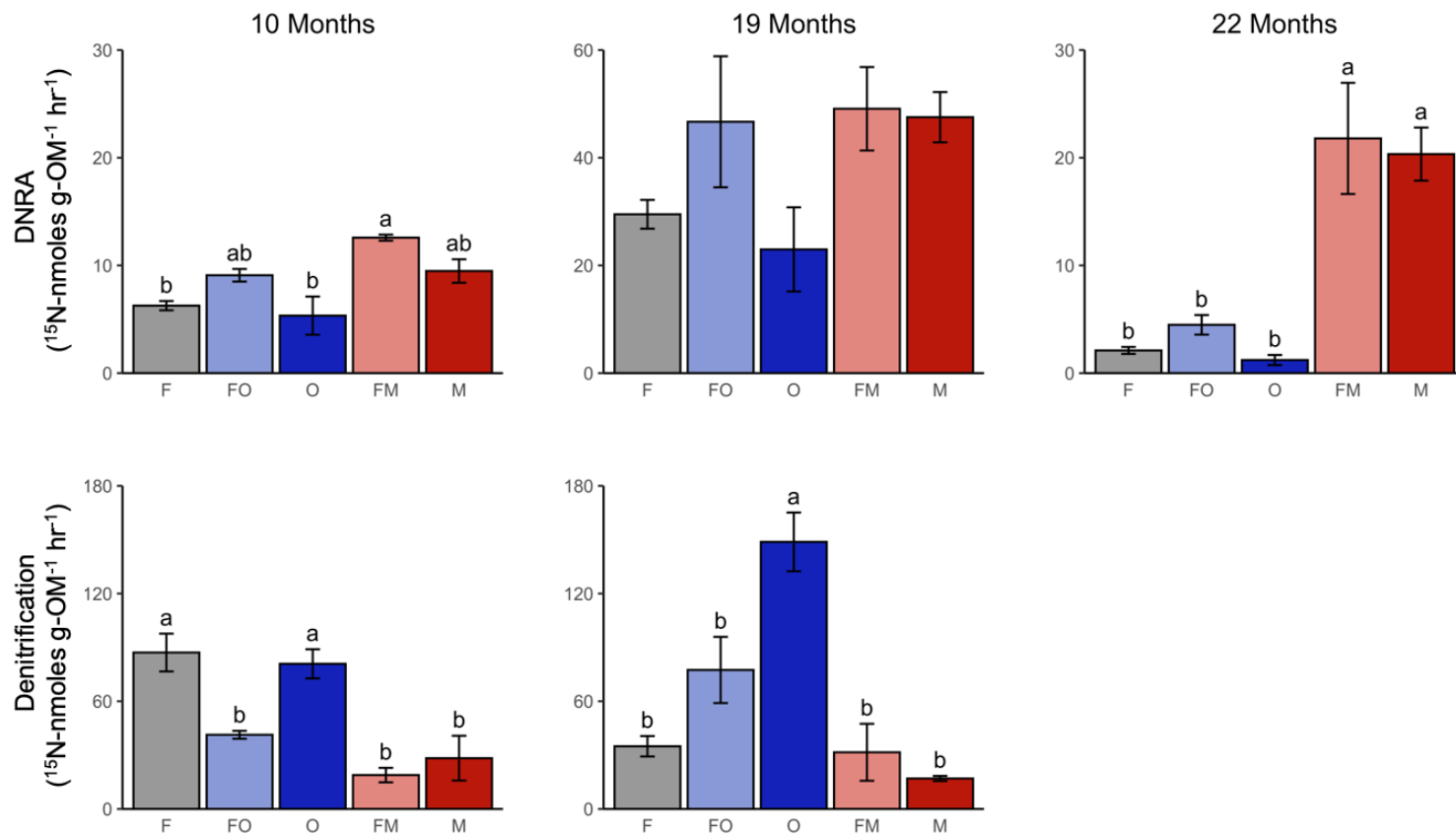


Figure 1. Mean (\pm standard error) rates of DNRA (top) and denitrification (bottom) for the various exposure lengths; no data are available for denitrification at 22 months. Lowercase letters indicate significant differences via Tukey's HSD *post-hoc* analysis. Note change in scale for DNRA at 19 months.

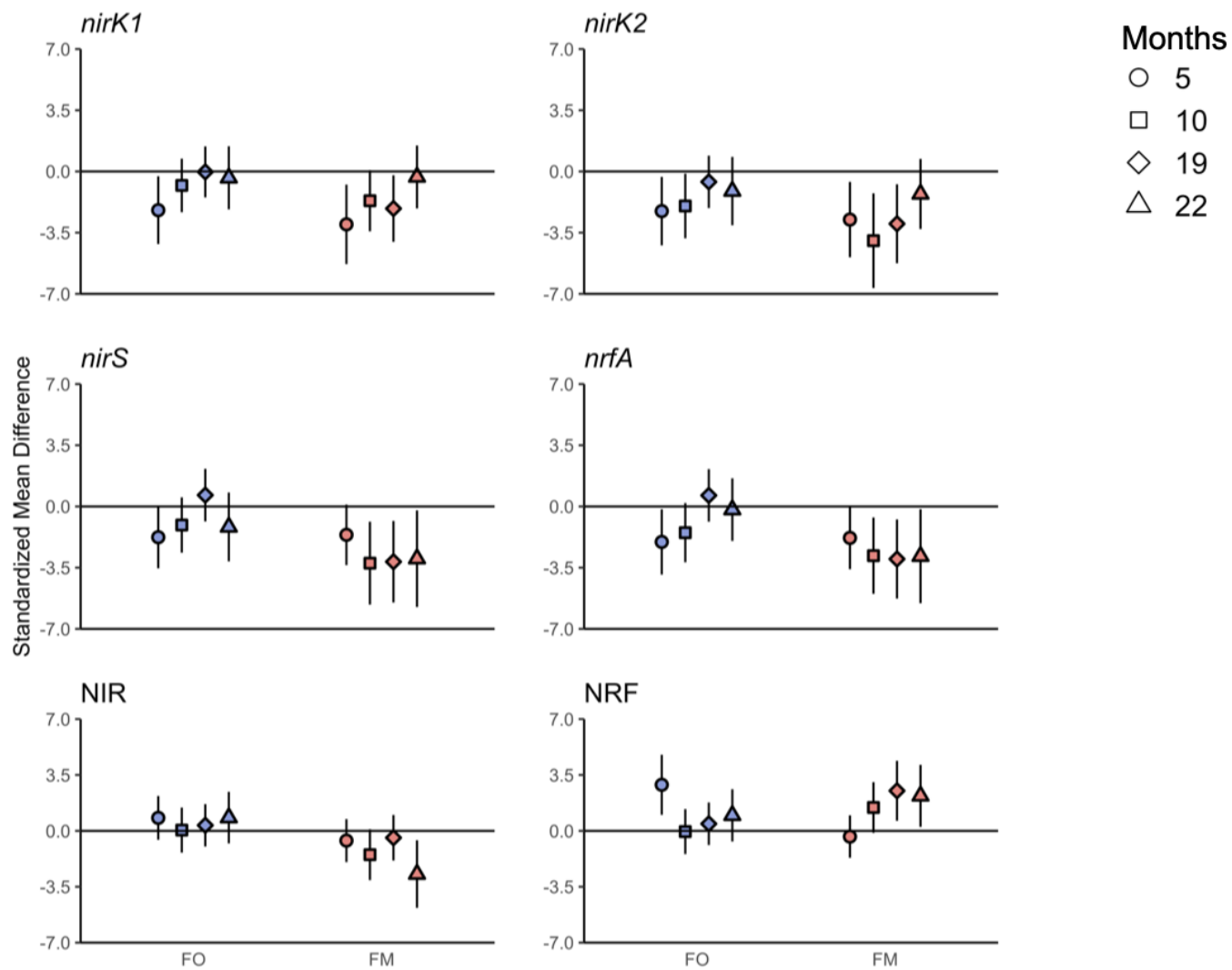


Figure 2. Standardized mean differences (Hedges' g) for transplanted soils relative to Fresh control soil for functional genes (*nirK1*, *nirK2*, *nirS*, and *nrfA*) and EC predictions (NIR and NRF). Bars represent 95% confidence intervals. Differences are considered significant if confidence intervals do not overlap with the zero line.

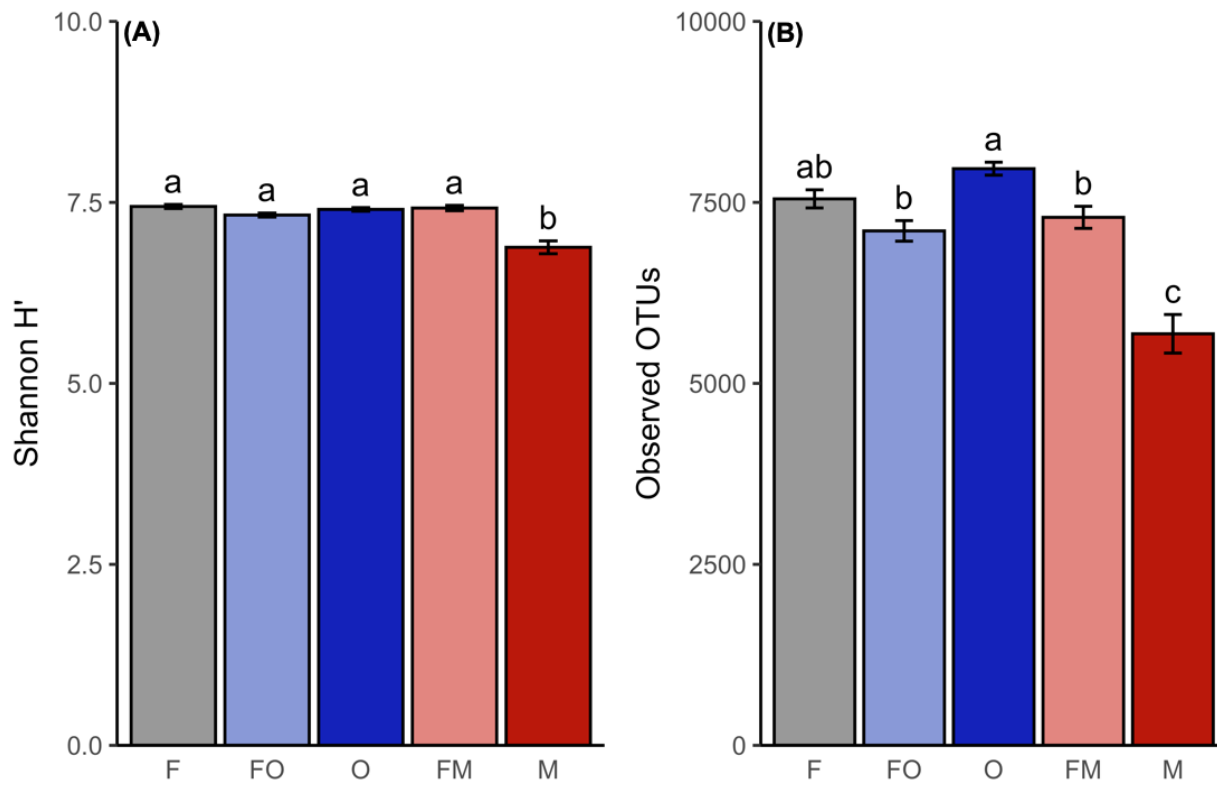


Figure 3. Mean (\pm standard error) of (A) Shannon diversity (H') and (B) Observed OTUs by treatment (all exposure lengths combined). Lowercase letters denote significant differences via Tukey's HSD *post-hoc* analysis.

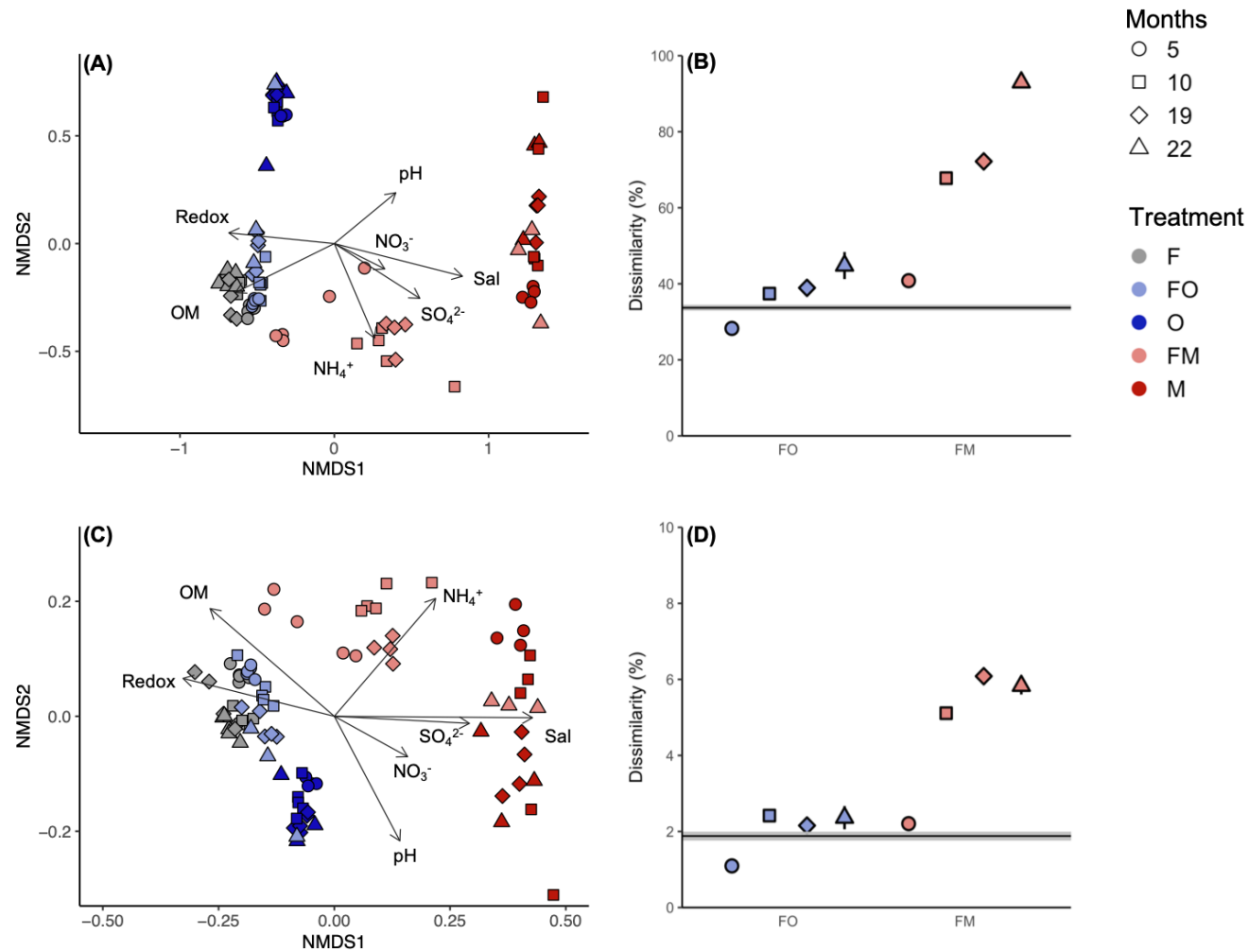


Figure 4. NMDS ordinations of (A) prokaryotic community structure and (C) predicted metagenome. Vectors represent environmental parameters that significantly correlated, with “Sal” corresponding to salinity. Also shown are the average (\pm standard error) Bray dissimilarity percentages calculated for transplant soils (either FO or FM) relative to Fresh (F) controls at each sampling event, for the (B) prokaryotic community and (D) predicted metagenome. The horizontal black lines represent the mean dissimilarity of all Fresh controls, and grey shading represents 95% confidence intervals.

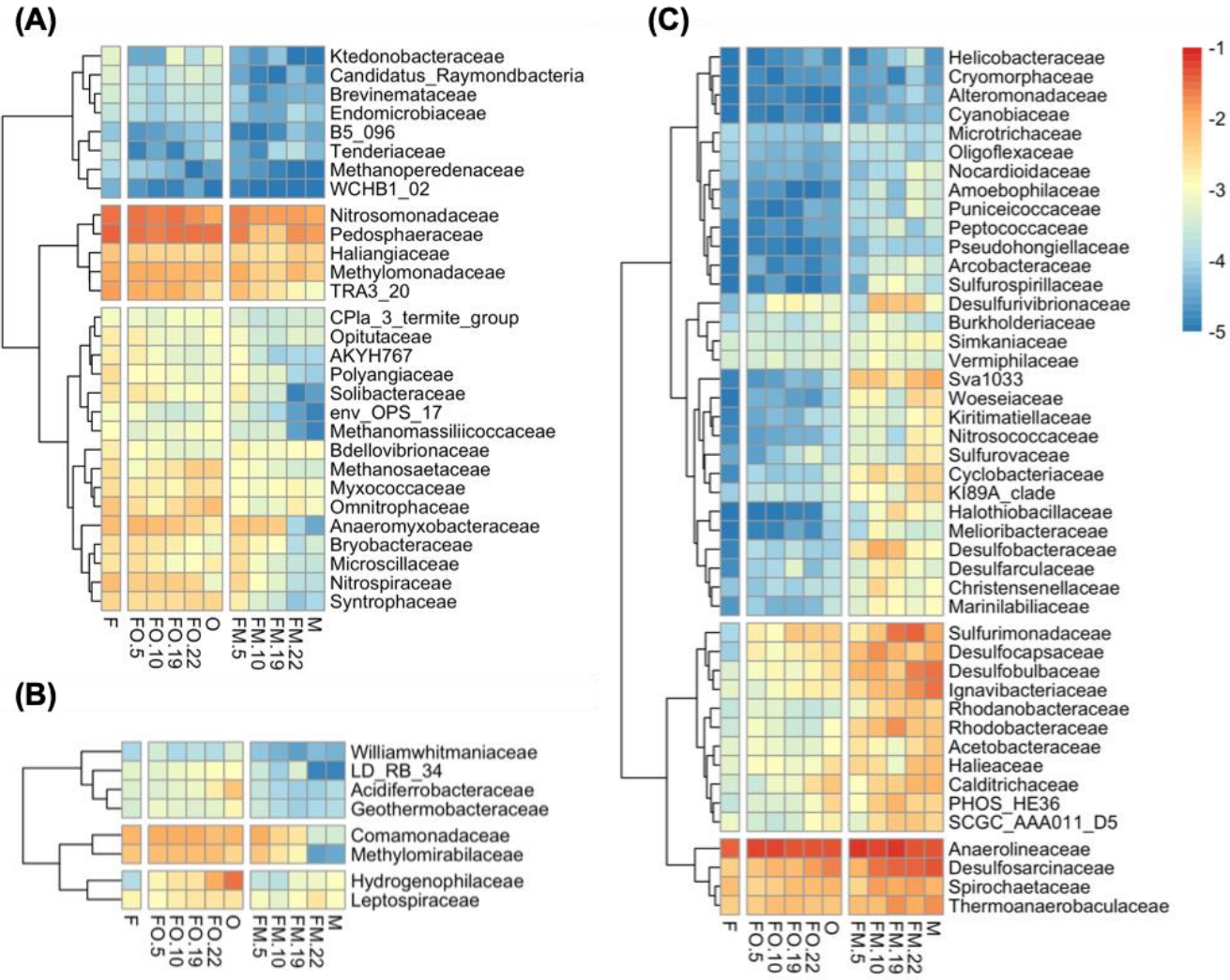


Figure 5. \log_{10} transformed relative abundance of the LfSe indicator families for Fresh control (A), FO transplant (B), and FM transplant (C). For the control sites (F, O, and M), abundance changed little during the course of the study, so all samples for all four exposure lengths were averaged and presented as a single column in the heatmap. For transplant soils, each column represents the mean of replicate samples, ordered chronologically from left to right with numbers corresponding to exposure length (months). Taxa were clustered by abundance patterns.

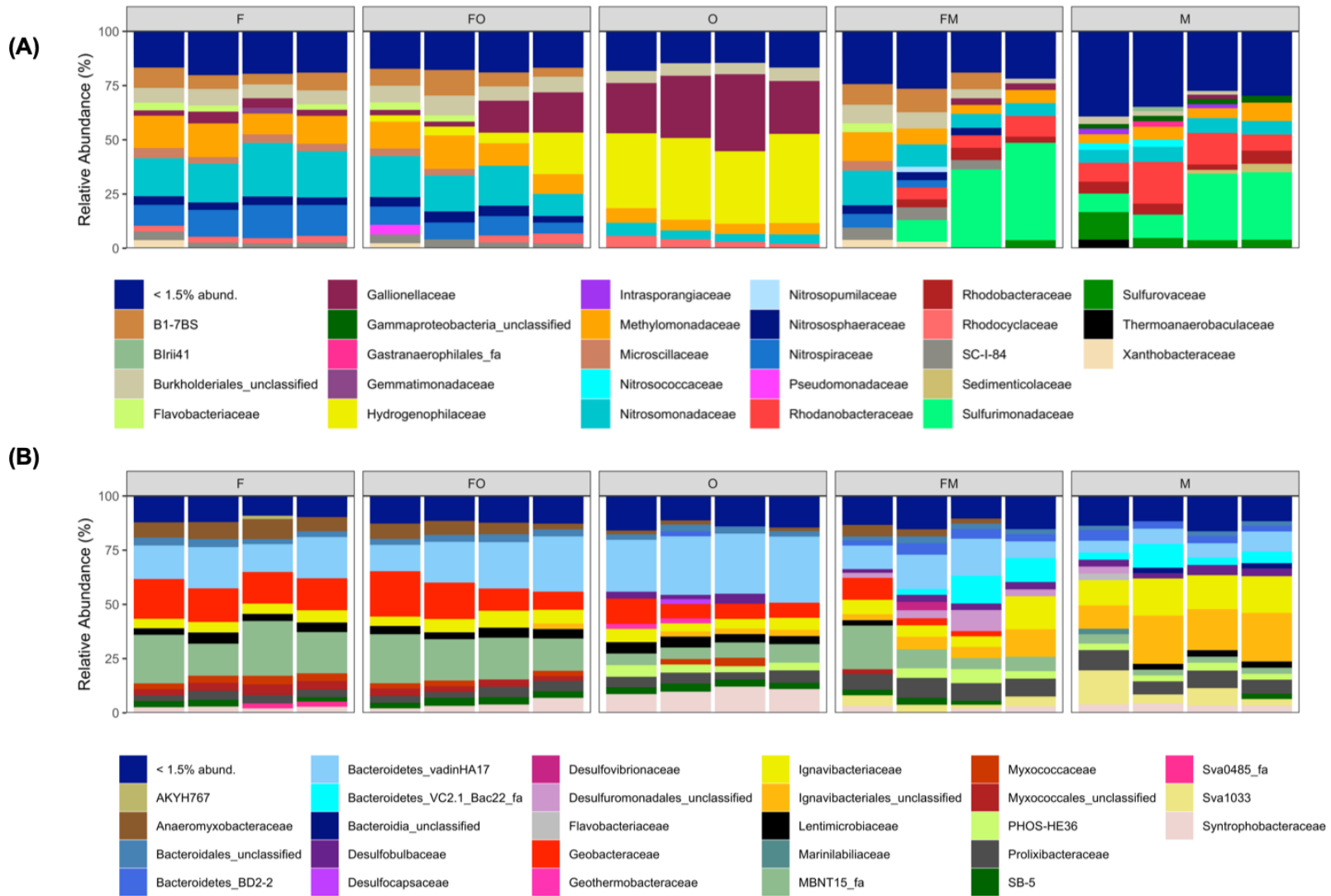


Figure 6. Mean relative abundance of top families contributing to NIR (A) and NRF (B) over the course of the experiment. Within each treatment, samples are ordered chronologically from left to right. Families that accounted for less than 1.5% were combined to form the < 1.5% group. Taxa with the suffix “unclassified” represent taxa that belong to unclassified families within the given order.

7. Supplemental Materials

Anammox Screening Method

Soils were screened for anaerobic ammonium oxidation (anammox) activity following the protocol of Huygens et al. (2015). Briefly, microcosms were constructed and incubated as described in the main document, but isotope treatments consisted of $^{15}\text{NH}_4\text{Cl}$, $^{15}\text{NH}_4\text{Cl}$ and K^{14}NO_3 , or K^{15}NO_3 (99 atom%, Cambridge Isotope Laboratories, Andover, MA, USA) with each brought to 100 μM concentration in the microcosms. Microcosms were sampled at 0, 24, and 45 hr. Gas samples were shipped to University of California, Davis Stable Isotope Facility for isotope analysis of $^{15}\text{N}_2$ (ThermoFinnigan GasBench and PreCon trace gas concentration system interfaced to a Thermo Scientific™ Delta V Plus isotope-ratio mass spectrometer, Bremen, Germany). $p^{29}\text{N}_2$ enrichment was not detected in the presence of $^{15}\text{NH}_4^+$ and $^{14}\text{NO}_3^-$, suggesting little to no anammox activity.

Supplemental Table 1. Test Statistic (F) for one-way ANOVAs comparing soil and porewater chemistry, rates of NO₃⁻ reduction, and genetic parameters across treatments for each sampling event. Corresponding p-values are indicated as: (*) for 0.01 < p < 0.05, (**) for 0.001 < p < 0.01, and (***) for p ≤ 0.001; all other p > 0.05. Missing data are denoted as nd.

Parameter		Incubation Length			
		5 Months	10 Months	19 Months	22 Months
Soil and Water	Salinity	72.0 ***	222.5 ***	76.8 ***	280.1 ***
	NO ₃ ⁻	3.0	12.1 ***	38.1 ***	2.1
	NH ₄ ⁺	0.4	11.7 ***	10.3 ***	1.3
	SO ₄ ²⁻	64.6 ***	25.4 ***	30.3 ***	108.7 ***
	DOC	3.3	10.9 ***	11.5 ***	nd
	OM	8.1 ***	9.0 ***	6.7 **	24.2 ***
	C:N	0.8	0.9	2.0	1.0
	Redox	43.5 ***	23.5 ***	10.8	65.7 ***
	pH	124.6 ***	4.2 *	5.1 **	10.7 ***
Rates	Denitrification	nd	13.6 ***	16.0 ***	nd
	DNRA	nd	8.3 **	1.9 ***	15.3 ***
Genetic	<i>nirS</i>	5.7 **	13.4 ***	7.3 ***	11.7 ***
	<i>nrfA</i>	6.5 **	20.0 ***	14.0 *	29.4 ***
	<i>nirK1</i>	4.5 **	3.6 *	12.4 *	0.2
	<i>nirK2</i>	15.0 ***	20.2 ***	8.9 ***	3.6 *
	NIR	49.6 ***	100.1 ***	33.4 ***	12.9 ***
	NRF	9.5 ***	8.0 ***	22.0 ***	9.4 **

Supplemental Table 2. Mean (\pm standard error) functional gene ($\times 10^8$ copies g-OM⁻¹) and EC ($\times 10^3$ counts sample⁻¹) abundances. Lower case letters indicate significant treatment effects on the corresponding parameter within each incubation length, detected via one-way ANOVA with subsequent *post-hoc* analysis using Tukey's HSD.

Parameter	Treatment	Incubation Length			
		5 Months	10 Months	19 Months	22 Months
<i>nirS</i>	F	2.1 \pm 0.4 ^a	1.3 \pm 0.2 ^a	5.6 \pm 0.8 ^a	4.7 \pm 0.7 ^a
	FO	0.7 \pm 0.2 ^b	0.9 \pm 0.1 ^{ac}	7.0 \pm 0.8 ^a	2.9 \pm 0.5 ^{ab}
	O	0.4 \pm 0.1 ^b	0.5 \pm 0.1 ^{bc}	5.0 \pm 1.8 ^{ab}	2.2 \pm 0.1 ^b
	FM	0.9 \pm 0.1 ^b	0.3 \pm 0.1 ^b	0.9 \pm 0.2 ^b	0.4 \pm 0.1 ^b
	M	0.8 \pm 0.3 ^b	0.2 \pm 0.1 ^b	1.5 \pm 0.4 ^b	1.0 \pm 0.2 ^b
<i>nirK1</i>	F	22.5 \pm 3.8 ^a	14.2 \pm 3.6 ^a	1.8 \pm 0.4 ^{ab}	2.6 \pm 0.7 ⁻
	FO	5.3 \pm 2.4 ^b	8.8 \pm 1.6 ^{ab}	1.8 \pm 0.2 ^{ab}	2.1 \pm 0.5 ⁻
	O	11. \pm 5.3 ^{ab}	7.4 \pm 1.4 ^{ab}	3.9 \pm 1.3 ^a	2.4 \pm 0.6 ⁻
	FM	2.2 \pm 0.6 ^b	3.4 \pm 1.1 ^b	0.3 \pm 0.1 ^b	2.1 \pm 0.5 ⁻
	M	10.2 \pm 3.2 ^{ab}	9.2 \pm 1.5 ^{ab}	1.2 \pm 0.3 ^{ab}	1.9 \pm 0.6 ⁻
<i>nirK2</i>	F	13.6 \pm 2.4 ^a	9.4 \pm 1.0 ^a	6.6 \pm 1.2 ^a	8.5 \pm 2.4 ^a
	FO	3.6 \pm 0.7 ^b	5.7 \pm 0.4 ^c	5.2 \pm 0.7 ^a	2.7 \pm 0.8 ^{ab}
	O	3.8 \pm 0.7 ^b	4.2 \pm 0.6 ^{bc}	4.7 \pm 1.4 ^{ac}	3.4 \pm 0.3 ^{ab}
	FM	1.8 \pm 0.3 ^b	1.9 \pm 0.5 ^b	0.8 \pm 0.3 ^b	2.0 \pm 0.3 ^{ab}
	M	3.6 \pm 0.7 ^b	2.6 \pm 0.8 ^b	1.2 \pm 0.3 ^{bc}	1.0 \pm 0.4 ^b
<i>nrfA</i>	F	1.0 \pm 0.2 ^a	0.6 \pm 0.1 ^a	1.1 \pm 0.8 ^a	0.9 \pm 0.1 ^a
	FO	0.3 \pm 0.1 ^b	0.3 \pm 0.0 ^b	1.5 \pm 0.4 ^a	0.9 \pm 0.1 ^a
	O	0.3 \pm 0.1 ^b	0.3 \pm 0.0 ^b	1.6 \pm 0.8 ^{ab}	0.6 \pm 0.1 ^a
	FM	0.4 \pm 0.1 ^b	0.1 \pm 0.0 ^c	0.2 \pm 0.0 ^b	0.1 \pm 0.0 ^b
	M	0.3 \pm 0.2 ^b	0.03 \pm 0.0 ^c	0.1 \pm 0.0 ^b	0.1 \pm 0.0 ^b
NIR	F	2.0 \pm 0.1 ^b	1.8 \pm 0.0 ^b	1.8 \pm 0.1 ^b	1.8 \pm 0.1 ^b
	FO	2.2 \pm 0.1 ^b	1.8 \pm 0.1 ^b	1.9 \pm 0.2 ^b	2.2 \pm 0.4 ^b
	O	3.2 \pm 0.2 ^a	3.4 \pm 0.1 ^a	3.2 \pm 0.2 ^a	2.9 \pm 0.4 ^a
	FM	1.8 \pm 0.1 ^c	1.4 \pm 0.1 ^c	1.7 \pm 0.2 ^c	1.1 \pm 0.2 ^c
	M	0.7 \pm 0.1 ^d	0.6 \pm 0.1 ^d	0.6 \pm 0.0 ^d	0.7 \pm 0.1 ^d
NRF	F	4.3 \pm 0.1 ^b	4.3 \pm 0.1 ^b	4.4 \pm 0.1 ^b	4.2 \pm 0.1 ^b
	FO	4.7 \pm 0.1 ^b	4.3 \pm 0.1 ^b	4.5 \pm 0.1 ^b	4.5 \pm 0.1 ^b
	O	4.8 \pm 0.3 ^{ab}	4.7 \pm 0.1 ^b	4.5 \pm 0.1 ^b	4.5 \pm 0.1 ^b
	FM	4.1 \pm 0.3 ^b	5.1 \pm 0.3 ^b	5.7 \pm 0.3 ^a	5.7 \pm 0.6 ^a
	M	5.8 \pm 0.2 ^a	7.2 \pm 0.8 ^a	6.1 \pm 0.2 ^a	5.7 \pm 0.1 ^a

Supplemental Table 3. Correlation coefficient (r^2) from the envfit model performed on prokaryotic community (OTU) and the predicted metagenome (EC). All p-values ≤ 0.005 .

Parameter	Prokaryotic Community	Predicted Metagenome
Salinity	0.71	0.73
Redox	0.47	0.44
OM	0.46	0.43
SO ₄ ²⁻	0.37	0.34
NH ₄ ⁺	0.26	0.36
pH	0.21	0.27
NO ₃ ⁻	0.12	0.12

Supplemental Table 4. Results of the LEfSe analysis, showing taxonomy from Phylum to Family level, ordered by treatment (trt). All p-values for the LDA scores were ≤ 0.001 except * indicates $0.01 < p < 0.05$, and ** indicates $0.001 < p < 0.01$.

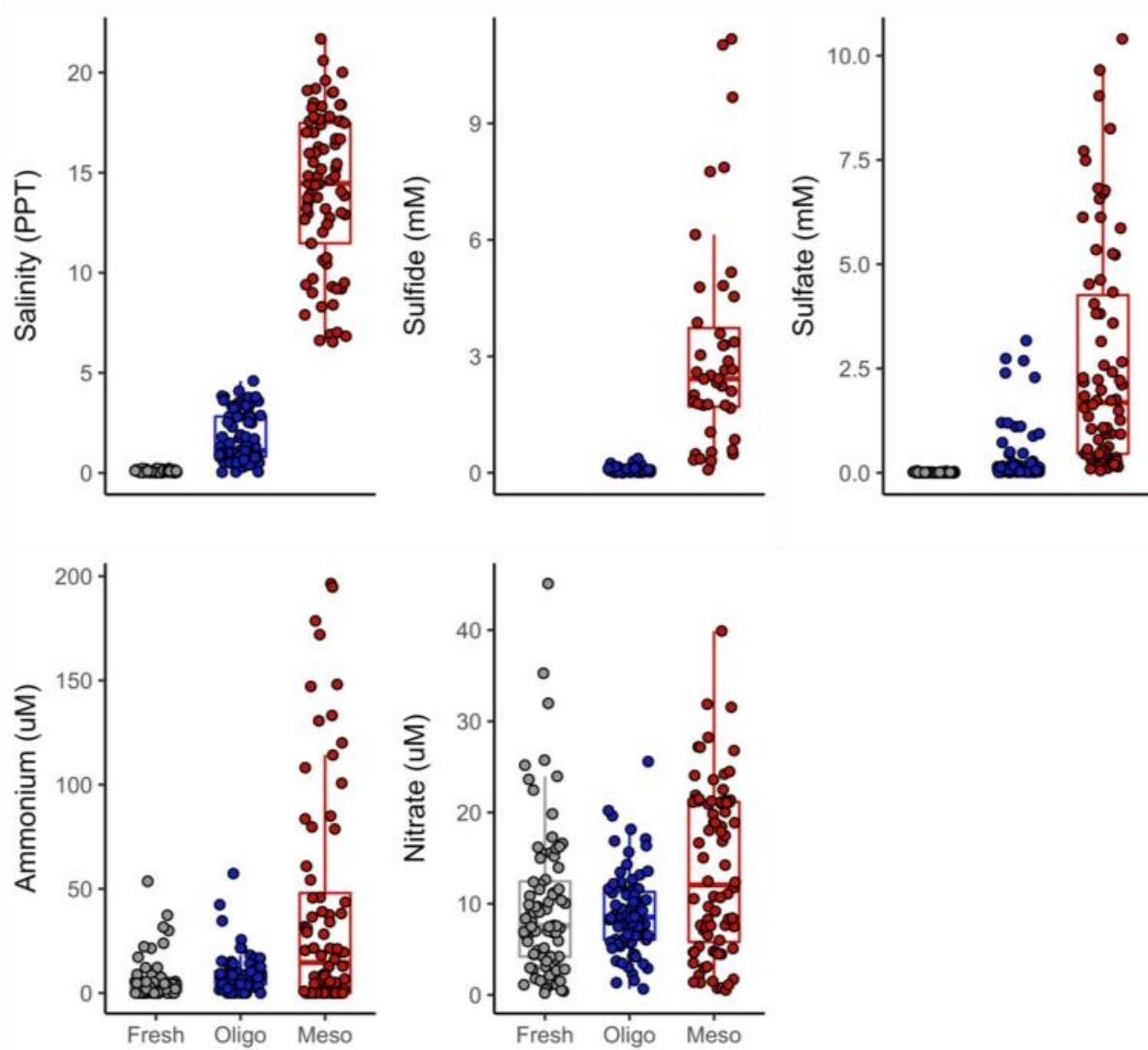
Family	Trt	LDA	Kingdom	Phylum	Class	Order
Methanoperedenaceae	F	2.4	Archaea	Halobacterota	Methanosarcinia	Methanosarciniales
Methanosaetaceae	F	3.0	Archaea	Halobacterota	Methanosarcinia	Methanosarciniales
Methanomassiliicoccaceae	F	2.6	Archaea	Thermoplasmata	Thermoplasmata	Methanomassiliicoccales
Bryobacteraceae	F	2.9	Bacteria	Acidobacteriota	Acidobacteriae	Bryobacterales
Solibacteraceae	F	2.9	Bacteria	Acidobacteriota	Acidobacteriae	Solibacterales
Microscillaceae	F	2.8**	Bacteria	Bacteroidota	Bacteroidia	Cytophagales
AKYH767	F	2.8	Bacteria	Bacteroidota	Bacteroidia	Sphingobacteriales
env_OPS_17	F	2.6	Bacteria	Bacteroidota	Bacteroidia	Sphingobacteriales
Bdellovibrionaceae	F	2.6	Bacteria	Bdellovibrionota	Bdellovibrionia	Bdellovibrionales
WCHB1_02	F	2.8	Bacteria	Caldisericota	Caldisericia	Caldisericales
Ktedonobacteraceae	F	2.4	Bacteria	Chloroflexi	Ktedonobacteria	Ktedonobacterales
Syntrophaceae	F	3.2	Bacteria	Desulfobacterota	Syntrophia	Syntrophales
Endomicrobiaceae	F	2.5	Bacteria	Elusimicrobiota	Endomicrobia	Endomicrobiales
B5-096	F	2.7	Bacteria	Fibrobacterota	Fibrobacteria	Fibrobacterales
Candidatus_Raymondobacteria	F	2.4	Bacteria	Fibrobacterota	Fibrobacteria	Fibrobacterales
Anaeromyxobacteraceae	F	3.3	Bacteria	Myxococcota	Myxococcia	Myxococcales
Myxococcaceae	F	2.9	Bacteria	Myxococcota	Myxococcia	Myxococcales
Haliangiaceae	F	3.2	Bacteria	Myxococcota	Polyangia	Haliangiales
Polyangiaceae	F	3.0	Bacteria	Myxococcota	Polyangia	Polyangiales
Nitrospiraceae	F	3.4	Bacteria	Nitrospirota	Nitrospira	Nitrospirales
CPla_3_termite_group	F	2.6	Bacteria	Planctomycetota	Phycisphaerae	Tepidisphaerales
Nitrosomonadaceae	F	3.8	Bacteria	Proteobacteria	Gammaproteobacteria	Burkholderiales
TRA3_20	F	3.7	Bacteria	Proteobacteria	Gammaproteobacteria	Burkholderiales
Methylomonadaceae	F	3.4	Bacteria	Proteobacteria	Gammaproteobacteria	Methylococcales
Tenderiaceae	F	2.0	Bacteria	Proteobacteria	Gammaproteobacteria	Tenderiales
Brevinemataceae	F	2.4	Bacteria	Spirochaetota	Brevinematia	Brevinematales
Omnitrophaceae	F	3.4	Bacteria	Verrucomicrobiota	Omnitrophia	Omnitrophales
Opitutaceae	F	2.8	Bacteria	Verrucomicrobiota	Omnitrophia	Omnitrophales
Pedosphaeraceae	F	4.1	Bacteria	Verrucomicrobiota	Verrucomicrobiae	Pedosphaerales
SCGC_AAA011_D5	FM	3.2	Archaea	Nanoarchaeota	Nanoarchaea	Woesearchaeales

Thermoanaerobaculaceae	FM	3.5	Bacteria	Acidobacteriota	Thermoanaerobaculia	Thermoanaerobaculales
Microtrichaceae	FM	2.1	Bacteria	Actinobacteriota	Acidimicrobiia	Microtrichales
Nocardioideaceae	FM	2.1	Bacteria	Actinobacteriota	Actinobacteria	Propionibacteriales
Marinilabiliaceae	FM	2.7	Bacteria	Bacteroidota	Bacteroidia	Bacteroidales
Amoebophilaceae	FM	2.1	Bacteria	Bacteroidota	Bacteroidia	Cytophagales
Cyclobacteriaceae	FM	3.1	Bacteria	Bacteroidota	Bacteroidia	Cytophagales
Cryomorphaceae	FM	2.6**	Bacteria	Bacteroidota	Bacteroidia	Flavobacteriales
Ignavibacteriaceae	FM	3.6	Bacteria	Bacteroidota	Ignavibacteria	Ignavibacteriales
Melioribacteraceae	FM	2.5	Bacteria	Bacteroidota	Ignavibacteria	Ignavibacteriales
PHOS_HE36	FM	3.3	Bacteria	Bacteroidota	Ignavibacteria	Ignavibacteriales
Oligoflexaceae	FM	2.3	Bacteria	Bdellovibrionota	Oligoflexia	Oligoflexales
Calditrichaceae	FM	3.2	Bacteria	Calditrichota	Calditrichia	Calditrichales
Arcobacteraceae	FM	2.4	Bacteria	Campylobacterota	Campylobacteria	Campylobacterales
Helicobacteraceae	FM	2.1**	Bacteria	Campylobacterota	Campylobacteria	Campylobacterales
Sulfurimonadaceae	FM	3.9	Bacteria	Campylobacterota	Campylobacteria	Campylobacterales
Sulfurospirillaceae	FM	2.4	Bacteria	Campylobacterota	Campylobacteria	Campylobacterales
Sulfurovaceae	FM	2.6	Bacteria	Campylobacterota	Campylobacteria	Campylobacterales
Anaerolineaceae	FM	4.0	Bacteria	Chloroflexi	Anaerolineae	Anaerolineales
Cyanobiaceae	FM	2.7	Bacteria	Cyanobacteria	Cyanobacteriia	Synechococcales
Vermiphilaceae	FM	2.3	Bacteria	Dependentiae	Babeliae	Babeliales
Desulfarculaceae	FM	2.8	Bacteria	Desulfobacterota	Desulfarculia	Desulfarculales
Desulfobacteraceae	FM	3.5	Bacteria	Desulfobacterota	Desulfobacteria	Desulfobacterales
Desulfosarcinaceae	FM	4.0	Bacteria	Desulfobacterota	Desulfobacteria	Desulfobacterales
Desulfobulbaceae	FM	3.8	Bacteria	Desulfobacterota	Desulfobulbia	Desulfobulbales
Desulfocapsaceae	FM	3.7	Bacteria	Desulfobacterota	Desulfobulbia	Desulfobulbales
Desulfurivibrionaceae	FM	3.4	Bacteria	Desulfobacterota	Desulfobulbia	Desulfobulbales
Sva1033	FM	3.4	Bacteria	Desulfobacterota	Desulfuromonadia	Desulfuromonadales
Christensenellaceae	FM	2.8	Bacteria	Firmicutes	Clostridia	Christensenellales
Peptococcaceae	FM	2.3	Bacteria	Firmicutes	Clostridia	Peptococcales
Acetobacteraceae	FM	2.8	Bacteria	Proteobacteria	Alphaproteobacteria	Acetobacterales
Rhodobacteraceae	FM	3.6	Bacteria	Proteobacteria	Alphaproteobacteria	Rhodobacterales
Burkholderiaceae	FM	2.4	Bacteria	Proteobacteria	Gammaproteobacteria	Burkholderiales
Alteromonadaceae	FM	2.4	Bacteria	Proteobacteria	Gammaproteobacteria	Enterobacterales
Halothiobacillaceae	FM	2.8	Bacteria	Proteobacteria	Gammaproteobacteria	Halothiobacillales

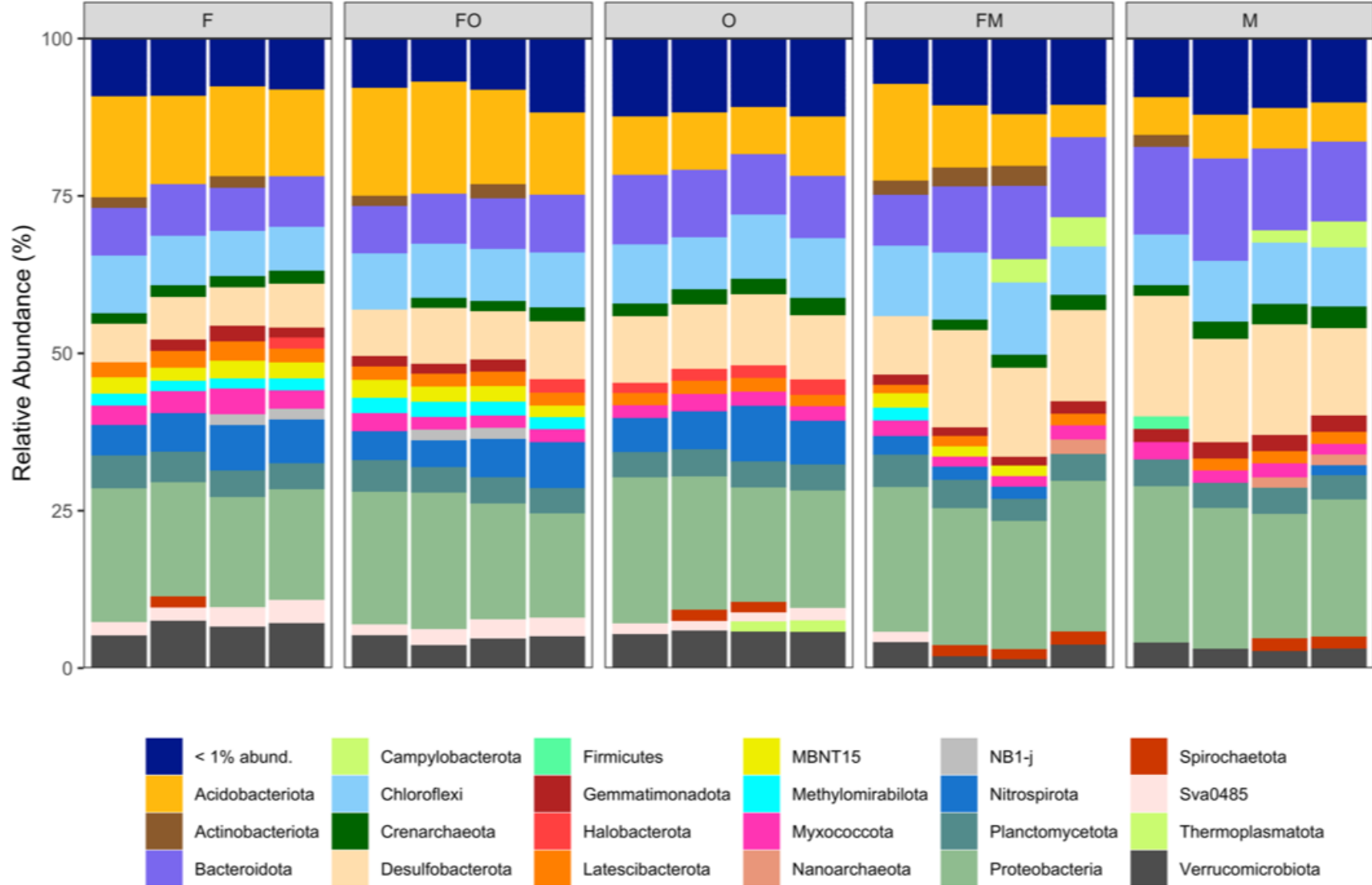
Nitrosococcaceae	FM	2.5	Bacteria	Proteobacteria	Gammaproteobacteria	Nitrosococcales
Haliaceae	FM	3.1	Bacteria	Proteobacteria	Gammaproteobacteria	Pseudomonadales
KI89A_clade	FM	2.8	Bacteria	Proteobacteria	Gammaproteobacteria	Pseudomonadales
Pseudohongiellaceae	FM	2.5	Bacteria	Proteobacteria	Gammaproteobacteria	Pseudomonadales
Woeseiaceae	FM	2.8	Bacteria	Proteobacteria	Gammaproteobacteria	Steroidobacterales
Rhodanobacteraceae	FM	3.2	Bacteria	Proteobacteria	Gammaproteobacteria	Xanthomonadales
Spirochaetaceae	FM	3.3*	Bacteria	Spirochaetota	Spirochaetia	Spirochaetales
Simkaniaceae	FM	2.5	Bacteria	Verrucomicrobiota	Chlamydiae	Chlamydiales
Kiritimatiellaceae	FM	2.6	Bacteria	Verrucomicrobiota	Kiritimatiellae	Kiritimatiellales
Puniceicoccaceae	FM	2.1	Bacteria	Verrucomicrobiota	Verrucomicrobiae	Opitutales
Williamwhitmaniaceae	FO	2.2**	Bacteria	Bacteroidota	Bacteroidia	Bacteroidales
LD_RB_34	FO	2.5	Bacteria	Bacteroidota	Ignavibacteria	Ignavibacteriales
Geothermobacteraceae	FO	2.4	Bacteria	Desulfobacterota	Desulfuromonadia	Desulfuromonadales
Methylomirabilaceae	FO	3.4	Bacteria	Methylomirabilota	Methylomirabilia	Methylomirabiales
Acidiferrobacteraceae	FO	2.5	Bacteria	Proteobacteria	Gammaproteobacteria	Acidiferrobacterales
Comamonadaceae	FO	3.5	Bacteria	Proteobacteria	Gammaproteobacteria	Burkholderiales
Hydrogenophilaceae	FO	3.2	Bacteria	Proteobacteria	Gammaproteobacteria	Burkholderiales
Leptospiraceae	FO	2.5**	Bacteria	Spirochaetota	Leptospirae	Leptospirales

Supplemental Table 5. Results of Pearson correlation analysis between functional predictors and measured function.

Approach	Denitrification (n=30)			DNRA (n=45)		
	Predictor	r	p	Predictor	r	p
EC	NIR (1.7.2.1)	0.73	<0.001	NRF (1.7.2.2)	0.61	<0.001
qPCR	<i>nirS</i>	0.54	0.002	<i>nrfA</i>	0.13	0.41
	<i>nirK1</i>	0.32	0.09			
	<i>nirK2</i>	0.55	0.002			



Supplemental Figure 1. Boxplot of well water chemistry data collected over the course of the experiment, combined for all depths (5, 10, and 30 cm).



Supplemental Figure 2. Mean relative abundance of prokaryotic phyla. Within each treatment, samples are ordered chronologically from left to right based on increasing incubation length. Phyla that accounted for less than 1% were combined

CHAPTER 3: PROKARYOTIC COMMUNITY DYNAMICS DURING A THREE-YEAR *IN-SITU* SALINITY MANIPULATION IN A TIDAL FRESHWATER WETLAND

Joseph C. Morina¹, Georgios Giannopoulos², Bonnie L. Brown³,

Scott C. Neubauer¹, and Rima B. Franklin¹

¹Department of Biology, Virginia Commonwealth University, Richmond, VA 23284 USA

²Laboratory of Soil Science, School of Agriculture, Aristotle University of Thessaloniki, Thessaloniki, Greece

³Department of Biological Sciences, University of New Hampshire, Durham, NH, 03824 USA

1. Introduction

While wetland ecosystems cover only ~8 percent of the Earth's surface, they hold an estimated 20-30% of the global soil carbon stock (Lal 2008, Mitsch and Gosselink 2015). The saturated conditions of wetland soils dramatically reduce rates of organic matter (OM) mineralization by shifting microbial respiration from aerobic to anaerobic pathways. The carbon storage ability of wetlands allows them to act as a global carbon sink; however, anthropogenic disturbances such as salinization threaten the functioning of these ecosystems (Herbert et al., 2015). Tidal freshwater wetlands are especially vulnerable to salinization, which can occur through multiple pathways, including sea-level rise, alteration to hydrology management, and major storm events (Tully et al., 2019). Salinization has the potential to alter pathways of OM mineralization by acting upon the prokaryotic communities responsible for OM mineralization.

Salinity is a known driver of prokaryotic community structure (Lozupone and Knight 2007, Auguet et al., 2010) and can impact communities via indirect and direct effects. The direct effect of increased osmotic pressure will select for community members that are more tolerant of saline conditions. However, indirect effects of salinity appear vital to our understanding of how salinization events will alter microbial metabolisms. For example, the introduction of sulfate (SO_4^{2-}) has been shown to drastically shift the mineralization pathways of wetland soils by stimulating the activity of SO_4^{2-} reducing bacteria (SRB), who can directly compete with methanogens or their associated syntrophs for carbon substrates (Berrier et al., 2022). Furthermore, reduced sulfur species produced from SO_4^{2-} reduction can have both inhibitory and stimulatory effects on different guilds of prokaryotes, such as nitrate (NO_3^-) reducers (Murphy et al., 2020, Joye and Hollibaugh 1995, Burgin and Hamilton 2007), making predictions regarding respiratory pathways challenging. However, it is generally accepted that salinization and increased sulfide concentrations favor dissimilatory NO_3^- reduction to ammonium (DNRA) over denitrification (Giblin et al., 2010, Murphy et al., 2020).

The terminal end products of soil OM mineralization, CO₂ and CH₄, are frequently measured in response to salinization. When considering how the production of these greenhouse gases is altered after salinization, studies generally find the suppression of CH₄ production (Marton et al., 2012, Chambers et al., 2011, Neubauer et al., 2013, Weston et al., 2006). However, the effect of salinity on CO₂ production does not show a consistent response. Results suggests that both salinity level and exposure length are critical factors when predicting the response of CO₂ production. For instance, Chambers et al. (2011) found no difference in CO₂ production in freshwater soil exposed to salinities of 3.5 and 14 ppt, but found a suppression when salinities were raised to 35 ppt. Neubauer et al. (2013) observed that after a short term exposure (3 days) to oligohaline salinities, CO₂ production increased, but when considering soils that had longer exposures (3.5 years) to oligohaline salinities, CO₂ production was suppressed. The differential response of CO₂ production over time and across salinities levels, even within individual studies, highlights the difficulty in predicting how salinization will impact the end products of OM mineralization. Furthermore, many studies investigating the response of CO₂ and CH₄ production during salinization do not assess metrics of microbial community structure (Neubauer et al., 2013, Weston et al., 2006, Chambers et al., 2011, Marton et al., 2012), therefore the direct examination of soil microbial communities in tandem with functional measurements will better our understanding of CO₂ dynamics during salinization events.

The few studies that have profiled microbial communities have added to our depth of understanding of how these communities respond, such as characterizing the dominant phyla associated with shifts in salinity (Chen et al., 2022) and the formation of transitional communities during these disturbance events (Dang et al., 2019). To further link microbial communities to functional responses of salinization events, we performed a three year *in-situ* watering experiment. We profiled the soil prokaryotic community using *16s rRNA* amplicon sequencing, in tandem with quantifying key functional genes involved with microbial respiratory pathways. Furthermore, we measured rates of

anaerobic CO₂ and CH₄ production over the course of three years and characterized shifts to NO₃⁻ reduction pathways during the final sampling event.

2. Methods

2.1. Experimental Design and Sample Collection

This experiment was performed in the Cumberland Marsh Preserve located on the Pamunkey River near New Kent, Virginia (USA). Cumberland Marsh Preserve is a tidal freshwater wetland located 35 river-km upstream from the salt front of the York River Estuary. An automated irrigation system servicing ~100 m² was constructed for *in-situ* salinization at 37° 33' 26.1" N, 76° 58' 21.9" W. The plant community in this area was dominated by common aquatic macrophytes of the region, *Peltandra virginica*, *Pontederia cordata*, and *Zizania aquatica*, with a total of 19 species. Surface soils are ~35% organic with a bulk density of ~0.14 g cm⁻³.

The design and schematics of the automated irrigation system are reported in detail in Lee et al. (2016). Briefly, the system was designed to collect site water, and dispense it onto the experimental plots. The pumping station allows for both application of site water (freshwater, ~0.1 ppt salinity) and saltwater (10 ppt, made by mixing Instant Ocean Sea Salt with site water). Fifteen plots (1 × 2 m) were established: 5 replicate "Control" plots, which received no water additions; 5 "Fresh" plots, which received 25 L of site water every low tide; and 5 "Salt" plots, which received 25 L of saltwater every low tide. In addition, 4 wells (3 cm diameter, PVC) were installed in each plot to collect well water across multiple depths (5, 10, and 25 cm) (Lee et al., 2016). Wells were sampled approximately twice each month while the watering system was in operation, and during each sampling event, to assess temporal variations in salinity. Well water was collected using a syringe and transported back to the laboratory on ice.

The experimental manipulation was initiated in May of 2015 and is ongoing; this paper describes results from the first (2015), second (2016), and third (2017) years. The irrigation system was turned off during colder months to prevent freezing of pipes (December 2015 through April 2016, December 2016 through February 2017). Excluding winter, soil sampling was conducted seasonally, and a total of seven events are included in this analysis: [1] 07/21/2015 (Summer '15), [2] 10/29/2015 (Fall '15), [3] 04/11/2016 (Spring '16), [4] 07/05/2016 (Summer '16), [5] 10/06/2016 (Fall '16), [6] 04/12/2017 (Spring '17), and [7] 08/28/2017 (Summer '17). For each sampling event, one soil core (> 50 cm) was collected from each plot using a PVC corer (Giannopoulos et al., 2019) and then subdivided in the field into three depth increments: 3-8 cm, 8-13 cm, and 48-53 cm. This analysis focused only on the top depth increment (3-8 cm). In the field, a subsample (~5 g) of soil to be used for genetic analysis was preserved in a sterile 50-mL conical tube using 10 mL of LifeGuard Solution. The remainder of each soil sample was placed in an airtight plastic bag and transported to the lab on ice for processing.

2.2. Soil and Water Chemistry

Soils preserved in LifeGuard solution were immediately frozen (-80°C) for future genetic analysis. From the remaining soil, an aliquot (~0.5 g) was used to determine gravimetric soil moisture content (H₂O %) by heating to 45°C until a constant mass was achieved (> 72 hr). Dried soil was then ground and combusted to determine organic matter content (OM %) based on mass loss on ignition at 550°C for 6 hours. Another aliquot (7 g) was used for the soil CO₂ and CH₄ production assays. For the final sampling event (08/28/2017), an additional aliquot (~50 g) of soil (stored overnight at 4°C) was set aside for the ¹⁵NO₃⁻ reduction assays.

After the various aliquots were collected, any remaining soil (usually ~30 g) was placed into a 50-mL conical tube and centrifuged (1,500 x g, 15 min) to extract soil porewater. After centrifugation, the supernatant was decanted and filtered using a mixed cellulose ester filter (0.22-µm pore size). Both this

soil porewater and the well water were frozen (-20°C) until being analyzed via ion chromatography for Cl⁻, NO₃⁻, and SO₄²⁻ concentrations (Thermo Scientific™ Dionex™ Integrion™ HPIC™ System, Bremen, Germany). Ammonium (NH₄⁺) concentrations were determined colorimetrically (Sinsabaugh et al., 2000) using a Synergy 2 plate reader (Biotech, Winooski, VT, USA). Salinity (ppt) was calculated based on Cl⁻ concentration (Bianchi 2007).

2.3. Microbial Community Analysis

The soil-LifeGuard slurry was thawed, and an aliquot (~1.5 mL) was centrifuged (10,000 × g, 1 min). The LifeGuard solution and excess water were decanted, and the remaining soil pellet (~0.5 g) was extracted using the Qiagen DNeasy® Powersoil® Extraction Kit (Germantown, MD, USA) following the manufacturer's protocol. Successful DNA extraction was confirmed via agarose gel electrophoresis (1.5%) and was quantified using the Quant-iT™ PicoGreen™ dsDNA Assay Kit (Invitrogen, Carlsbad, CA, USA). DNA extracts were stored at -20°C.

For this study, we assessed how the abundance of key functional groups of the soil microbial community changed after salinization by monitoring the abundance of four genes involved with key OM breakdown pathways, specifically: denitrification (*nirS*), DNRA (*nrfA*), methanogenesis (*mcrA*), and SO₄²⁻ reduction (*dsrA*). In addition, we monitored total bacterial abundance via the *16s rRNA* gene. These gene abundances were determined using quantitative polymerase chain reaction (qPCR) on a Bio-Rad CFX384™ Real-Time System (Bio-Rad, Hercules, CA, USA) using SsoAdvanced™ Universal SYBR® Green Supermix (BioRad, Hercules, CA, USA). Reaction conditions, primer references, standard organisms, and reaction efficiencies are presented in Table 1. The amplification of a single product was verified using agarose gel electrophoresis (1.2%) and melt curve analysis. All qPCR assays were performed with three technical replicates for each sample. Abundances are reported as gene copies g dry soil⁻¹.

To profile changes to soil prokaryotic community composition over time, we sequenced the V4

region of the *16s rRNA* gene following the 16S Metagenomic Sequencing Library Preparation Protocol (Part # 15044223 Rev. B, Illumina, CA, USA). The only modification was to the first stage PCR, which was performed using a 20 µl reaction volume and consisted of 0.33 µM of the forward and reverse primers (515f - 806R, following Caporaso et al. (2011)), 6 ng DNA, and 10 µl of iProof™ High Fidelity Master Mix (BioRad, Hercules, CA, USA). The thermocycling protocol was: initial denaturation (98°C for 1 min) followed by 20 cycles of denaturation (98°C for 20 sec), primer annealing (55°C for 30 sec), and amplicon elongation (72°C for 30 sec). After the 20 cycles were complete, a final elongation step was performed (72°C for 5 min). PCR products were verified using agarose gel electrophoresis (1.5%). These first stage PCRs were performed in duplicate and pooled for each sample. For the second PCR, the Nextera® XT Index Kit (Illumina, San Diego, CA, USA) was used to attach dual indices and Illumina sequencing adapters. Amplicons were purified after both PCR stages using Agencourt® AMPure XP PCR purification solution (Beckman Coulter, Brea, CA USA) following the manufacturer's protocol. After the second PCR, the amplicons were quantified using Qubit™ dsDNA HS Assay on the Qubit® fluorometer (Invitrogen, Waltham, MA, USA) and were pooled in equimolar concentration. The library consisted of 5% PhiX control DNA (Illumina, San Diego, CA, USA), and was sequenced on an Illumina MiSeq® sequencing platform in the VCU Forensic Biology Laboratory using 2 x 300 paired-end reads, and the MiSeq® V3 reagent kit, following the manufacturer's protocol.

Sequences were processed using Mothur v.1.44.0 (Schloss et al., 2009) following the MiSeq SOP (https://www.mothur.org/wiki/MiSeq_SOP). Reads were assembled into contigs using the *make.contigs* command, resulting in a total of 12,887,867 sequences across all samples. Sequences were aligned using the SILVA reference database (Quast et al., 2013). VSEARCH was used to remove chimeric sequences (5.8%) (Rognes et al., 2016). Hierarchical classification was performed using Greengenes version 13_8 (McDonald et al., 2012) at a 99% similarity, and sequences classified as mitochondria, chloroplast, or unknown were removed from the data set using the *remove.lineage* command, leaving only bacterial

and archaeal lineages. Operational taxonomic units (OTUs) were clustered at a 0.03 cutoff with the OptiClust algorithm (Westcott et al., 2017) in the *cluster.split* command splitting by classification at level 6. All samples were rarefied to 75,024 reads using the *sub.sample* command. Consensus OTU classification was performed using SILVA v138.1 (Quast et al., 2013). Indices of alpha diversity were calculated using the *estimate_richness* command (McMurdie and Holmes, 2013) in R.

2.4. Microcosm Assays

2.4.1 CO₂ and CH₄ Production

Anaerobic microcosms were used to determine CO₂ and CH₄ production rates from soil slurries as described in Neubauer et al. (2013). Briefly, soil slurries were prepared inside an anaerobic chamber by adding 7 mL of deoxygenated water to 7 g of soil into 125 mL serum bottles. For microcosms constructed for both the Control and Fresh treatments, site water (~0.1 ppt) was added. For the Salt treatment, site water mixed with Instant Ocean was added to achieve a salinity of 2 pp, which was representative of the average *in situ* salinity in the Salt plots. Two microcosms (technical replicates) were constructed for each sample. The microcosms were hermetically sealed while inside the chamber, and their headspaces were flushed with N₂ for 15 minutes. Bottles were left overnight to equilibrate and for any residual O₂ to be depleted. The following day, the headspaces of the bottles were flushed again with N₂, and an initial (t = 0) sample of headspace gas was collected. Bottles were then incubated in the dark at 25°C, and additional samples were collected after 4, 24, 28, and 48 hours.

To obtain headspace gas samples, N₂ (9 mL) was first injected and mixed into the bottle before immediately collecting the gas samples (9 mL). Gas samples were injected into N₂ flushed Exetainer® vials (Labco, Lampeter, UK). Concentrations of CO₂ and CH₄ were determined using a Shimadzu GC-14A gas chromatograph with methanizer and flame ionization detector (Shimadzu Scientific Instruments, Columbia, MD, USA). Rates of CO₂ and CH₄ production were calculated using linear regression of gas

concentrations over time. For CO₂ production, the minimum $r^2 = 0.81$ and the average $r^2 = 0.97$; for CH₄, the minimum $r^2 = 0.77$ and the average $r^2 = 0.94$. Rates of CH₄ and CO₂ production are reported as $\mu\text{mol g dry soil}^{-1} \text{ hr}^{-1}$.

2.4.2 NO₃⁻ Reduction Assays

For the final sampling event (08/28/2017), microcosms were also constructed to measure rates of denitrification and DNRA. This time, soil slurries were prepared by adding 10 mL of filter-sterilized (0.22- μm pore size) water to 10 g of soil in 70 mL serum vials. Two technical replicates were constructed for each sample at each time point. For microcosms constructed for both the Control and Fresh treatments, site water was added. For the Salt treatment, site water mixed with Instant Ocean to reach a salinity of 5 ppt was added. Serum vials were hermetically sealed with a butyl rubber stopper and then flushed with He (10 min). Samples were then placed on an incubated shaker table (28°C, 100 RPM) in the dark for 24 hours to allow for microbial activity to deplete residual O₂ and NO₃⁻. After incubation, microcosms were flushed again with He (10 min). A syringe was used to inject the microcosms with 99 atom% K¹⁵NO₃ (Cambridge Isotope Laboratories, Andover, MA, USA), dissolved in filter-sterilized deionized water, to bring each microcosm to a final concentration of 100 μM ¹⁵NO₃⁻. A subset of microcosms was immediately sampled to serve as the initial time point for rate calculations. The remaining microcosms were placed back on the incubated shaker table and sampled at 0.5, 24, and 45 hours. In addition to the microcosms receiving K¹⁵NO₃, a second set of samples received no isotope additions to assess the natural (background) ¹⁵N composition of N₂, N₂O, and NH₄⁺. Production of ¹⁵N-labeled N₂ and N₂O was quantified to determine rates of denitrification, and production of ¹⁵N-labeled NH₄⁺ was used for DNRA; details of these measurements are presented below. Rates for both denitrification and DNRA are reported as nanomoles ¹⁵N g dry soil⁻¹ hr⁻¹.

To collect gas samples for determining rates of denitrification, 10 mL of He was injected and

mixed into each microcosm headspace immediately before removing 10 mL of headspace for analysis. The 10 mL sample was injected into a He flushed Exetainer® (Labco, Lampeter, UK), which was then shipped to the University of California, Davis Stable Isotope Facility to measure N₂ and N₂O gas concentrations and isotope ratios. Rates of denitrification were calculated by determining the δ¹⁵N of the N₂ and N₂O in the headspace of the microcosm after correcting for He dilutions. Both N₂ and N₂O were measured. However, N₂O was always below the analytical detection limit (< 150 pmoles N₂O), so only ¹⁵N enrichment of N₂ is reported. Rates of denitrification were calculated using linear regression of ¹⁵N₂ production over time (mean r² = 0.96).

After headspace sampling, microcosm contents were transferred into 160-mL specimen cups containing 100 mL of 2 M KCl and placed on a shaker table (1 hr, 120 RPM). Aliquots (50 mL) of the resultant KCl extracts were then decanted, filtered (0.22 μm pore size), and placed in new acid-washed specimen cups to perform microdiffusions following Fillery and Recous (2001). Briefly, 5-mm diameter diffusion disks were made from Whatman grade GF/F filters (Cytiva, Marlborough, MA, USA) and suspended above the filtered KCl extracts using stainless steel wires. Diffusion disks were acidified by pipetting 10 μL of 2.5 M KHSO₄ directly onto the disks, and then adding 0.7 g of MgO to the KCl extract. Specimen cups were immediately sealed, placed in an incubator (25°C), and left undisturbed for 10 days. Diffusion disks were removed from the microdiffusion chambers and placed in a desiccator to dry until mass remained constant (70°C, ~3 days). Microdiffusion disks were sealed in 5 × 9 mm tin capsules (Costech, Valencia, CA, USA) and shipped to Boston University Stable Isotope Facility for ¹⁵N analysis (GV Instruments IsoPrime™ Isotope Ratio Mass Spectrometer, Manchester, UK). Rates of DNRA were determined using linear regression of ¹⁵NH₄⁺ production over time (mean r² = 0.96).

2.5. Statistical Analyses

Environmental variables failed to meet parametric assumptions of normality based on Shapiro-Wilk's tests; therefore, we performed Kruskal-Wallis tests with Dunn's post-hoc comparisons to assess how treatment affected each variable at each sampling event. Rate data, alpha diversity indices, and log-transformed qPCR data met parametric assumptions, so an ANOVA approach was used. We first performed two-way ANOVAs with Tukey's HSD post-hoc testing to assess the effects of treatment and sampling date. Whenever a significant interaction effect was observed, we performed one-way ANOVAs to assess treatment effects separately for each sampling event. For rates of denitrification and DNRA, data were only collected for the final sampling event, so one-way ANOVAs were adequate. All statistical analyses described above were performed using the PAST software package (Hammer et al., 2001).

Multivariate analysis of community data was performed in R v.4.0.3 (R Core Team, 2013) using the *vegan* package. Nonmetric multidimensional scaling (NMDS) ordinations were constructed using OTU-level community data based on Bray-Curtis dissimilarity using the *metaMDS* command. Environmental vectors were fitted onto the NMDS ordination using the *envfit* function. PERMANOVA was performed using the *adonis* command to assess if community structure was impacted by treatment or sampling date. To further investigate community structure, we assessed multivariate dispersions using the *betadisper* (a multivariate test for homogeneity of variance) to assess community structure variation within each treatment. We then performed Kruskal-Wallis and subsequent Dunn's post-hoc tests on the variance of each treatment to assess significant differences in community variation. Lastly, to determine the enrichment or suppression of prokaryotic taxa by treatment effects (Salt vs. Control; Fresh vs. Control), differentially abundant OTUs were identified using *DeSeq2* (Love et al., 2014). For all statistical analyses, an α of 0.05 was used.

3. Results

3.1. Soil and Water Chemistry

Well water salinities in Salt plots were elevated relative to Fresh and Control plots throughout the experiment (Figure 1). Salinity of near-surface wells (5 cm), which corresponds best to the soil samples we analyzed, showed some variation over time in the Salt plots, which were greater on average in 2015 (1.5 ppt) and 2016 (1.4 ppt) than 2017 (0.7 ppt). Despite these differences, the Salt plots were consistently more saline than both Control (0.2, 0.1, and 0.1 ppt) and Fresh (0.2, 0.1, and 0.1 ppt) plots over the three-year period.

When considering treatment effects on porewater chemistry, we found no differences between Control and Fresh plots, but did observe consistently elevated salinity and SO_4^{2-} concentrations in the Salt plots (Table 2). In addition, we found NH_4^+ concentrations were elevated in Salt plots for all sampling events except the first, though the increase was not always statistically significant. No clear trend could be discerned for NO_3^- concentrations, as there was only one sampling event where a treatment effect was observed (concentrations were ~2-fold greater in the Control porewater relative to the two treatments).

Lastly, both measured soil properties, OM (%) (all $H < 1.86$, all $p > 0.39$) and H_2O (%) (all $H < 1.38$, all $p > 0.21$), were unchanged by treatment over the course of the experiment (Table 2). Average soil OM (%) by treatment over the course of the experiment was 33.3 ± 0.01 % (Control), 33.6 ± 0.01 % (Fresh), and 35.2 ± 0.01 % (Salt); average H_2O was (%) 80.6 ± 0.01 % (Control), 82.2 ± 0.01 % (Fresh), and 81.4 ± 0.01 % (Salt).

3.2. Prokaryotic Communities

3.2.1 Response of Prokaryotic Functional Groups

Two-way ANOVAs applied to gene abundance data revealed no significant interactions between treatment and time for any of the genes considered (all $F < 1.2$, all $p > 0.29$). Further, gene abundances were largely unaffected by treatment; the only significant result was for the DNRA gene, *nrfA* ($F_{\text{treatment}} = 6.0$, $p = 0.003$; $F_{\text{date}} = 2.2$, $p = 0.06$). Abundances were elevated in the Salt treatment relative to Fresh ($p = 0.002$) but not Control soils ($p=0.24$), and no difference was detected between Control and Fresh soils. For all other genes, temporal effects exerted a stronger influence (Figure 2, Table 3). Abundance of the bacterial *16s rRNA* gene were only affected by date ($F_{\text{date}} = 13.0$, $p < 0.001$; $F_{\text{treatment}} = 2.3$, $p = 0.10$). Abundance of *nirS* was also affected by date ($F_{\text{date}} = 9.1$, $p < 0.001$; $F_{\text{treatment}} = 0.2$, $p = 0.79$), and exhibited a similar temporal pattern to bacterial *16s rRNA* (Table 3). Broadly, these two genes decreased in abundance during April 2016, July 2016, and August 2017. This decrease was more pronounced for *nirS* than *16s rRNA* during August 2017. Abundance of the dissimilatory SO_4^{2-} reduction gene, *dsrA*, was also only affected by date ($F_{\text{treatment}} = 1.8$, $p = 0.31$; $F_{\text{date}} = 2.4$, $p = 0.04$), and post-hoc testing revealed that *dsrA* abundances were only different between two sampling events, where abundances were greater in July 2016 than August 2017 (Table 3). Similarly, the abundance of *mcrA* was controlled only by date ($F_{\text{date}} = 15.3$, $p < 0.001$; $F_{\text{treatment}} = 1.1$, $p = 0.34$), wherein abundances were the lowest during the April and July 2016 sampling events.

Overall, SO_4^{2-} reducers (*dsrA*) were the most abundant functional guild (10^9 gene copies g dry soil⁻¹) quantified in our study. When comparing the abundance of NO_3^- reducers, the DNRA-capable organisms (*nrfA*) were more abundant (10^8 gene copies g dry soil⁻¹) than the denitrifiers (*nirS*) (10^7 gene copies g dry soil⁻¹). The methanogens (*mcrA*) displayed similar abundance to DNRA organisms (10^8 gene copies g dry soil⁻¹).

3.2.2 Alpha Diversity

Two-way ANOVAs show that richness but not diversity was affected by treatment (Table 4). Specifically, observed OTU richness ($F_{\text{treatment}} = 5.0$, $p = 0.01$; $F_{\text{date}} = 2.2$, $p = 0.06$; $F_{\text{interaction}} = 0.3$, $p = 0.98$) was higher in the Fresh treatment than the Salt treatment ($p=0.007$), but the Control community was not significantly different from either of the other two treatments (Fresh $p=0.19$; Salt $p=0.37$). For Shannon's H ($F_{\text{date}} = 3.0$, $p = 0.01$; $F_{\text{treatment}} = 2.5$, $p = 0.09$; $F_{\text{interaction}} = 0.7$, $p = 0.81$), only one temporal difference was detected post hoc, where diversity was greater during the April 2016 relative to the August 2017 sampling event (Table 3).

3.2.3 Community Structure

While no clear clustering by treatment was observed on the NMDS ordination (stress = 0.15) (Figure 3), PERMANOVA results suggest that both date (pseudo-F = 2.6, $p = 0.01$) and treatment (pseudo-F = 1.8, $p = 0.02$) controlled community composition, with no interaction between the two factors (pseudo-F = 1.0, $p = 0.35$). This manifested on the NMDS ordination as less variation within the community composition in the Salt treatment relative to the Fresh and Control community. This was supported by the results of multivariate dispersion analysis, which found a significant difference in community structure variation across treatments ($H = 7.9$, $p = 0.02$), with Salt having significantly less variation than the Control community ($p = 0.005$), but not Fresh ($p = 0.07$). Variation did not differ between Fresh and Control communities ($p = 0.28$). Lastly, none of the measured environmental variables significantly correlated with overall community structure (all $p > 0.08$; Table 5).

3.2.4 Taxonomic Shifts

Dominant phyla of the Fresh and Salt treatments were similar to those found in the Control community (Figure 4). Across all treatments, the most abundant phyla were Proteobacteria (16.9 ± 0.9 %), Chloroflexi (11.7 ± 0.5 %), Acidobacteriota (10.6 ± 0.2 %), and Bacteroidota (10.1 ± 0.3 %). The

phylum Desulfobacterota, which contains SO_4^{2-} reducing taxa, showed no enrichment in the Salt community relative to the Fresh and Control communities (Control = $9.7 \pm 0.6 \%$, Fresh = $10.9 \pm 1.6 \%$, Salt = $10.9 \pm 1.6 \%$). The phyla that contain methanogens (Euryarchaeota and Bathyarchaeota) always comprised $<1\%$ of the community.

For a higher resolution analysis on taxa that were responsive to our treatments, we assessed differentially abundant taxa at the OTU level using Deseq2 analysis. Of the 109,916 OTUs we detected across all our samples, only 1 was differentially abundant between Control and Fresh communities (Thermodesulfovibrionia; not shown), and only 50 were differentially abundant between the Control and Salt communities (Figure 5). Overall, we found that more taxa were suppressed by saline water additions (33) than were enriched (17). Taxa that were suppressed include members of the Acidobacteriota (6), Chloroflexi (3), Crenarchaeota (3), Verrucomicrobiota (1), and Planctomycetota (1). Taxa belonging to the phylum Proteobacteria were also suppressed (11), except for one OTU that was identified as a member of the family Hydrogenophilaceae and was enriched under saline conditions. Other taxa that were enriched in the Salt treatment were from the phylum Desulfobacterota (4), Fibrobacterota (1), and Nitrospirota (3). Numerous taxa from the phyla Bacteroidota were suppressed (6) and enriched (6).

3.3. Functional Response

3.3.1 CO_2 and CH_4 Production

Our analysis found a significant treatment effect for CH_4 production and $\text{CO}_2:\text{CH}_4$, but not CO_2 (Figure 6). Instead, CO_2 production was controlled by date ($F_{\text{date}} = 4.9$, $p < 0.001$; $F_{\text{treatment}} = 2.2$, $p = 0.12$; $F_{\text{interaction}} = 0.7$, $p = 0.77$) wherein the final two sampling events, while not different from one another, were significantly lower than July 2015, October 2015, and July 2016 (Table 3). Rates of CH_4 production were predominantly controlled by treatment ($F = 8.7$, $p < 0.001$) and date ($F = 4.3$, $p < 0.001$), with no

interaction between the two factors ($F = 1.1$, $p = 0.40$). Post-hoc analysis revealed CH_4 production from the Salt treatment was significantly lower than both Fresh ($p < 0.001$) and Control ($p < 0.001$) soils, which did not differ from each other ($p = 0.65$). We found that CH_4 production was significantly elevated during October 2015 compared to all other events except July and October 2016 (Table 3). Lastly, $\text{CO}_2:\text{CH}_4$ was altered significantly by treatment ($F_{\text{treatment}} = 31.9$, $p < 0.001$; $F_{\text{date}} = 1.7$, $p = 0.14$; $F_{\text{interaction}} = 0.9$, $p = 0.53$), and post-hoc testing revealed the Salt treatment was significantly elevated relative to Control (< 0.001) and Fresh (< 0.001), with the ratio unchanged between Control and Fresh ($p = 0.74$).

3.3.2 Rates of NO_3^- Reduction

Denitrification was the dominant NO_3^- reduction pathway observed across all treatments (Control = 98%, Fresh = 96%, Salt = 94%). Neither denitrification ($F = 3.6$, $p = 0.06$) nor DNRA ($F = 2.0$, $p = 0.18$) were significantly different across the three soils (Figure 7), however we did see a suppression of denitrification, and elevated rates of DNRA in both treatment soils. The denitrification: DNRA was significantly different ($F = 7.3$, $p = 0.008$) wherein the ratio was elevated in the Control soil relative to Fresh ($p = 0.02$) and Salt ($p = 0.01$) treatments, with no difference between the two treatments ($p = 0.92$).

4. Discussion

4.1. Response of Soil and Water Chemistry to Salinization

Our experimental design successfully elevated salinity in the Salt plots to oligohaline levels. Well water salinity matched soil porewater salinity, with the average of the Salt treatment (2.0 ppt) being more than an order of magnitude higher than the Control (0.1 ppt) and the Fresh treatments (0.1 ppt). In agreement with salinity, SO_4^{2-} concentrations were concomitantly elevated in the Salt treatment relative to the Control and Fresh treatments, further indicating that an oligohaline level of salinization was successfully achieved throughout the experiment.

A consistent trend in wetland salinization studies is the increased concentration of NH_4^+ in soil porewater, which was also evident in this study. This increase can be caused by multiple factors associated with salinization, including increased mineralization of OM, increased rates of DNRA, and the desorption of NH_4^+ from soil particles due to increased ionic strength (Herbert et al., 2015). Increased mineralization of OM seems unlikely to explain the change we observed since there were no treatment effects on CO_2 production and no changes to soil OM content during our experiment. Similarly, no treatment effect was observed on rates of DNRA, though they were only measured during the final sampling event. This suggests that the transient increase in NH_4^+ in our Salt treatment was most likely due to the ionic displacement from soil particles or another unmeasured mechanism.

Salinization increases the availability of the SO_4^{2-} ion, theoretically increasing the mineralization of soil OM by stimulating SRB (Weston et al., 2006). The negative relationship between soil OM and salinity has been observed in studies experimentally manipulating salinity in wetland soils (Neubauer et al., 2019, Weston et al., 2010, Chambers et al., 2013, Servais et al., 2019), further supporting increased rates of OM mineralization, potentially attributed to the stimulation of SRB. Thus, our finding that soil OM remained unchanged in our Salt treatment throughout the 3-year experiment was an unexpected result. One possible explanation is that SRB were not enriched for in the Salt treatment. This is supported by our findings that the SRB abundances (*dsrA*) were never elevated in the Salt community, nor did our bioinformatic analyses identify any pronounced taxonomic shift or enrichment for SRB. However, we cannot rule out that the activity of SRB increased in our Salt treatment, as this would not be captured in our DNA-based community profiling.

4.2. Prokaryotic Community Resists Structural Changes during Salinization

Overall, this study found that freshwater community structure is largely resistant to oligohaline ranges of salinization. Our analysis suggests that the oligohaline level of salinization altered the

microbial community by reducing the variability, rather than restructuring the prokaryotic community to form a novel or transitional community as observed under mesohaline conditions in Chapter 2 or as reported in Dang et al. (2019). Our findings are not unique, as growing evidence suggests that microbial communities of aquatic and coastal systems can resist moderate levels of salinity stress (Herlemann et al., 2011, Berga et al., 2017, Nelson et al., 2015). In Chapter 2, we found that the prokaryotic community of a nearby freshwater wetland also largely resisted structural changes during a two-year incubation at an oligohaline wetland. The finding that overall community structure resisted structural changes after three years of *in-situ* salinization is furthered by the paucity of differentially abundant OTUs, as < 0.001% of OTUs were differentially abundant between the Salt and Control communities. Nevertheless, the taxonomic transitions we observed agreed quite well with past studies profiling prokaryotic communities during experimental manipulations of salinity and with observational studies along salinity gradients. For instance, the enrichment of taxa belonging to Ignavibacteriaceae, Hydrogenoiphilaceae, and Desulfosarcinaceae to increased salinity has been reported by prior studies (Chapter 2, Cheung et al., 2018, Chen et al., 2022). Furthermore, our findings that certain freshwater prokaryotes increase in abundance when exposed to increased salinity demonstrates that there are taxa native to freshwater environments that are adapted to tolerate a range of salinities.

Wetland salinization studies often find changes in the abundance and distribution of methanogenic archaea and SRB (Dang et al., 2019, Morrissey and Franklin 2015, Chapter 2). While we observed a stark suppression of CH₄ production in our Salt treatment, we did not detect any major changes in abundance of methanogens or SRB, affirmed by both functional gene quantification and bioinformatics analysis. When predicting how a given disturbance event will affect ecological communities, prior disturbance exposure is known to influence the response of the microbial communities (Hawkes and Keitt 2015, Renes et al., 2020). Cumberland Marsh, VA was specifically chosen for this study because its location, 35 river-km upstream from the salt front, reduces the chance

or frequency with which this site experiences salinization. However, we cannot rule out that this site has experienced salinization events before, which could prime the prokaryotic community to resist salinity stress. Furthermore, the lack of immigration from prokaryotes adapted to saline environments was likely an important explanatory factor as to why the community did not show major changes over the course of this experiment. Community coalescence (i.e., the mixing of two different communities) has been shown to impact estuarine microbial communities in both structure and functional metrics (Rocca et al., 2019, Castledine et al., 2020). Dang et al. (2019) allowed for the immigration of host-soil community members by utilizing mesh bags, and Neubauer et al. (2019) allowed for immigration by irrigating with water from a nearby salt marsh to salinize freshwater wetland soils. In this study, artificial sea salts were added to Cumberland Marsh water, thereby not allowing for immigration to occur. Future studies considering the response of wetland microbial communities to salinization should consider treatments with and without immigration in their experimental designs to better isolate the effects community mixing has on the restructuring of freshwater prokaryotic communities.

4.3. Salinization Alters the Fate of C and N

Overall, our results suggest that salinization will alter the profile of respiratory products produced by microbial communities of tidal freshwater wetlands, as we observed a drastic shift in $\text{CO}_2:\text{CH}_4$ production in Salt soils throughout our study. Similarly, we observed that denitrification:DNRA was altered; however, this was observed in both Fresh and Salt treatments which suggests that increased inundation (water additions) alone was enough to cause a shift in the partitioning of NO_3^- . The tidal range of this stretch of the Pamunkey is ~ 0.9 m (tidesandcurrents.noaa.gov), thus the 25 L watering additions represented a minuscule change in inundation, and likely impacted rates through alterations to soil redox conditions.

Prior investigations into the effect of salinization on CO_2 production from wetland soils have

found disparate results, with some studies indicating stimulation of CO₂ production (Chambers et al., 2011, Marton et al., 2012, Dang et al., 2019), whereas other efforts have found a negative relationship (Neubauer 2013, Ardón et al., 2018, Ury et al., 2020). Progress has been made to identify important factors determining how CO₂ production responds to increased salinity, potentially explaining these disparate findings. For instance, both salinity level (Marton et al., 2012) and length of salinity exposure (Chambers et al., 2011) can dictate the production of CO₂ production in salinized soils.

Two studies performed by our research group used similar methodologies to assess the impact of salinization on CO₂ production, utilizing a soil transplant approach with freshwater soil from Cumberland Marsh (freshwater to mesohaline, Dang et al., 2019) and an *in-situ* watering experiment very similar to the experimental design of this study (freshwater to oligohaline, Neubauer et al., 2013). Dang et al. (2019) considered a temporal scale ranging from one week to one year and found the CO₂ production was consistently elevated relative to their fresh control soils. Neubauer et al. (2013) considered two exposure lengths, measuring CO₂ from soils experiencing the experimental manipulation for 3.5 years, and soils that were salinized in the laboratory for 48 hours. When comparing CO₂ production from the long-term and short-term experiments, contrasting findings were observed. CO₂ production was suppressed in their long-term exposure, but increased in their short-term exposure. Results of the current study contrast both of these manipulative studies, as we observed no treatment effect at any time point. In regards to Dang et al. (2019), the higher salinity level (mesohaline) used in that experiment compared to this experiment (oligohaline) could be an explanatory factor, as the origin community and soil properties were that of Cumberland Marsh. In Neubauer et al. (2013), the edaphic characteristics of the tidal freshwater wetland were considerably different. Soil OM content is a known driver of mineralization (Morrissey et al., 2014, Xu et al., 2015, Wallenius et al., 2011, Wen et al., 2019), and thus soils with different edaphic characteristics, such as organic matter quantity and quality (Sutton-Grier et al., 2011), would likely display differential responses to disturbances such as salinization (Wen et

al., 2019). Soils from the Neubauer et al. (2013) study had approximately 2-fold more OM content than the soils of Cumberland Marsh (63.5 % vs. 34.1 %), which could, in part, explain the discrepancies between our studies despite similar experimental designs. As discussed above, the lack of immigration of taxa adapted to more saline conditions could also help explain why we did not see changes in CO₂ production (i.e., SRB could not immigrate into the system to stimulate SO₄²⁻ reduction, thus increasing CO₂ production). In addition, the absence of treatment effects on CO₂ production could be a result of functional redundancy, wherein numerous community members are capable of performing a given function (Allison and Martiny, 2008), as CO₂ is the end product of multiple respiratory pathways. While the broad function of CO₂ production was not affected by salinization in our study, the production of CH₄ was significantly suppressed by salinization.

The production of CH₄ is generally suppressed when freshwater soils are exposed to increased salinities (Neubauer 2013, Neubauer et al., 2013, Weston et al., 2006, Wen et al., 2019). The proposed mechanism to explain this phenomenon is that methanogens are outcompeted for substrates by SRB due to more favorable thermodynamics, resulting in lower rates of CH₄ production and higher rates of CO₂ production via SO₄²⁻ reduction (Lovley et al., 1982, Oremland and Polcin 1982). Our findings agree with previous studies that found the suppression of methanogenesis in wetland soils post-salinization (Neubauer 2013, Neubauer et al., 2013, Weston et al., 2006, Marton et al., 2012), although, as addressed above, we did not observe increased rates of CO₂ production in our Salt treatment.

We observed no effect of salinity or increased inundation on the abundance of the *mcrA* gene, demonstrating that methanogens were able to tolerate oligohaline levels of salinity without decreasing in abundance, and that temporal effects exerted greater control over methanogen abundances than treatment effects. The reduced activity of methanogens (CH₄ production), despite no change in methanogen abundances, suggest that methanogens may have become dormant when exposed to increased salinities (Shade et al., 2012). Prior studies have shown suppression of CH₄ production via

increased osmotic pressure in the absence of SO_4^{2-} (Peng et al., 2017, Baldwin et al., 2006, Chambers et al., 2011). We cannot entirely rule out that SRB activities were stimulated in the Salt treatment via the introduction of SO_4^{2-} . However, if this was the case, the thermodynamic advantage of SO_4^{2-} reduction over methanogens did not result in long-term (3 years) changes to the abundances of either functional group.

Rates of denitrification and DNRA were unaltered after three years of *in-situ* salinization. The abundance of *nirS*-type denitrifiers remained unchanged by treatment throughout our experiment. The same primer pair used in this study has been used by our research group before in a similar *in-situ* watering experiment, and treatment effects were observed (Neubauer et al., 2019), where *nirS* abundance was significantly lower in the Salt treatment relative to the Control soils. The aforementioned study also used the same *nrfA* primers, and found a treatment effect wherein *nrfA* was significantly greater in the Salt treatment than in the Control soils. The *nrfA* gene was the only functional gene in our study that showed a treatment effect, in which abundances were elevated in response to salinity. While not statistically significant, both the Fresh and Salt showed elevated rates of DNRA, and suppressed rates of denitrification relative to the Control. Research into how NO_3^- reduction pathways are altered post-salinization predicts the suppression of denitrification and the enhancement of DNRA (Giblin et al., 2010, Zhou et al., 2021). However, more recent efforts have found the response of denitrification to not always follow this trend, with some findings that denitrification is stimulated or unaffected by salinization (Chapter 2, Fear et al., 2005, Li et al., 2019). While we did not detect a statistically significant difference across treatments for either of the individual pathways, we did find the denitrification:DNRA ratio was significantly elevated in the Control soils relative to both treatment soils, suggesting that altered hydrology (i.e., water additions), rather than ionic composition, was important for the partitioning of NO_3^- into the two reduction pathways at our study site.

5. Conclusions

Our results suggest that the composition of prokaryotic communities in tidal freshwater wetlands are resistant to moderate (oligohaline) levels of salinization over relatively long temporal scales (3 years), with salinization reducing variability in community structure. Results of this study affirm previous findings that CH₄ production is suppressed and rates of DNRA are stimulated under more saline conditions. When considering the results of our microbial community analysis, it is important to acknowledge that our data can inform on the abundance and composition of the targeted microbial groups, but do not capture the activity (e.g., either dormancy or increased activity) of the microorganisms. The fact that the overall prokaryotic community resisted structural changes, and that methanogen abundances were unaffected by salinization despite clear suppression of CH₄ production throughout the experiment, highlight the limitations of DNA-based approaches, and suggest that incorporation of RNA-based methodologies would give a more detailed assessment of salinization disturbance impacts the activities of different microbial functional guilds.

Funding: Funding for this research was provided by the National Science Foundation (DEB 1355059), Virginia Sea Grant, the Virginia Water Resources Research Center, and the VCU Rice Rivers Center.

6. Tables and Figures

Table 1. Primers and thermal cycling conditions for qPCR assays. The DNA column represents the concentration of template DNA used for the respective qPCR reaction. Reaction efficiencies (E) and standard curve fit (r^2) are reported in the r^2/E column.

Gene	Primer	Primer (μ M)	DNA (ng/ μ L)	Standards (ATCC Strain #)	r^2/E (%)	Thermal Conditions ($^{\circ}$ C)	Reference
16s	Eub 338	0.10	1.2	<i>Escherichia coli</i> (11775)	98.0/98.0	98 $^{\circ}$ C for 2 min, 40 cycles of 95 $^{\circ}$ C for 30 sec, 55.5 $^{\circ}$ C for 60 sec, 72 $^{\circ}$ C for 60 sec	Fierer et al., 2005
	Eub 517	0.10					
mcrA	mlas	0.26	2.0	<i>Methanococcus voltae</i> (BAA-1334D-5)	99.3/97.0	98 $^{\circ}$ C for 2 min, 50 cycles of 95 $^{\circ}$ C for 20 sec, 59 $^{\circ}$ C for 20 sec, 72 $^{\circ}$ C for 45 sec	Steinberg and Regan 2009
	mcrA-rev	0.35					
nirS	cd3aF	0.10	3.0	<i>Paracoccus denitrificans</i> (17741)	96.3/97.5	94 $^{\circ}$ C for 4 min, 35 cycles of 94 $^{\circ}$ C for 30 sec, 56 $^{\circ}$ C for 30 sec, 72 $^{\circ}$ C for 60 sec	Throbäck et al., 2004
	R3cd	0.10					
nrfA	nrfAF2aw	0.43	1.5	<i>Escherichia coli</i> (11775)	99.3/97.5	95 $^{\circ}$ C for 5 min, 40 cycles of 95 $^{\circ}$ C for 30 sec, 53 $^{\circ}$ C for 30 sec, 72 $^{\circ}$ C for 20 sec	Welsch et al., 2014
	nrfAR1	0.43					
dsrA	dsrA290F	0.30	2.0	<i>Desulfovibrio desulfuricans</i> (27774)	98.9/100.3	95 $^{\circ}$ C for 5 min, 55 cycles of 94 $^{\circ}$ C for 40 sec, 62 $^{\circ}$ C for 30 sec, 72 $^{\circ}$ C for 30 sec	Pereyra et al., 2010
	dsrA660R	0.30					

Table 2. Mean (\pm standard error) for porewater chemistry and soil OM. Lower case letters indicate significant treatment effects within each sampling event (row), detected via Kruskal–Wallis and Dunn’s *post hoc*. Corresponding p-values for each H-statistic are indicated as: (*) for $0.01 < p < 0.05$ and (**) for $0.001 < p < 0.01$; all other $p > 0.05$.

Parameter	Event	Control	Fresh	Salt	H
Salinity (ppt)	Jul ‘15	0.1 \pm 0.1 a	0.1 \pm 0.1 a	1.6 \pm 0.4 b	11.8 **
	Oct ‘15	0.3 \pm 0.1 a	0.3 \pm 0.1 a	2.1 \pm 0.5 b	8.2 *
	Apr ‘16	0.1 \pm 0.1 a	0.1 \pm 0.1 a	2.3 \pm 0.3 b	9.4 **
	Jul ‘16	0.1 \pm 0.1 a	0.1 \pm 0.1 a	2.9 \pm 0.8 b	10.2 **
	Oct ‘16	0.1 \pm 0.1 a	0.1 \pm 0.1 a	1.2 \pm 0.6 b	9.5 **
	Apr ‘17	0.1 \pm 0.1 a	0.1 \pm 0.1 a	3.2 \pm 0.9 b	8.1 *
	Aug ‘17	0.3 \pm 0.2	0.3 \pm 0.2	1.1 \pm 0.2	3.4
SO ₄ ²⁻ (mM)	Jul ‘15	1.3 \pm 0.5 a	1.6 \pm 0.4 a	4.5 \pm 0.7 b	7.3 *
	Oct ‘15	2.0 \pm 0.5 a	2.8 \pm 0.8 ab	6.0 \pm 1.2 b	6.6 *
	Apr ‘16	0.3 \pm 0.1 a	0.3 \pm 0.1 ab	2.0 \pm 0.4 b	9.8 **
	Jul ‘16	0.2 \pm 0.1 a	0.2 \pm 0.1 a	1.7 \pm 0.4 b	9.1 *
	Oct ‘16	0.8 \pm 0.4 a	0.9 \pm 0.2 a	3.2 \pm 0.4 b	9.1 *
	Apr ‘17	0.3 \pm 0.1 a	0.4 \pm 0.1 a	3.0 \pm 0.4 b	8.1 *
	Aug ‘17	0.1 \pm 0.1	0.1 \pm 0.1	0.1 \pm 0.1	1.3
NH ₄ ⁺ (μ M)	Jul ‘15	6.1 \pm 3.0	3.6 \pm 2.6	5.6 \pm 5.1	0.5
	Oct ‘15	1.8 \pm 1.2	20.3 \pm 13.4	32.1 \pm 18.6	1.0
	Apr ‘16	18.9 \pm 8.6	10.6 \pm 1.6	25.0 \pm 4.7	4.8
	Jul ‘16	3.2 \pm 1.8 a	13.6 \pm 4.5 a	22.7 \pm 3.1 b	8.7 *
	Oct ‘16	36.5 \pm 13.1	27.1 \pm 8.7	60.6 \pm 39.8	0.01
	Apr ‘17	15.5 \pm 4.0 a	13.3 \pm 10.8 a	74.4 \pm 26.9 b	7.9 *
	Aug ‘17	32.3 \pm 10.4	33.7 \pm 3.4	60.0 \pm 10.9	3.3
NO ₃ ⁻ (μ M)	Jul ‘15	25.2 \pm 9.0	13.9 \pm 1.7	28.1 \pm 7.6	2.7
	Oct ‘15	33.0 \pm 9.7	11.4 \pm 2.0	13.7 \pm 4.3	5.4
	Apr ‘16	8.9 \pm 0.8	18.0 \pm 3.9	10.9 \pm 2.2	5.4
	Jul ‘16	14.8 \pm 1.8 a	7.9 \pm 0.1 b	7.8 \pm 0.1 b	8.1 *
	Oct ‘16	8.6 \pm 0.5	8.0 \pm 0.3	8.2 \pm 0.5	1.0
	Apr ‘17	10.7 \pm 1.3	9.6 \pm 1.0	7.5 \pm 0.4	4.0
	Aug ‘17	10.3 \pm 4.7	5.3 \pm 3.1	5.9 \pm 3.4	0.3
Soil OM (%)	Jul ‘15	37.6 \pm 1.2	35.9 \pm 1.3	38.8 \pm 2.5	1.9
	Oct ‘15	32.7 \pm 1.5	31.7 \pm 2.6	34.8 \pm 2.0	1.0
	Apr ‘16	32.6 \pm 1.7	35.6 \pm 3.1	32.9 \pm 2.3	0.8
	Jul ‘16	31.7 \pm 4.4	32.8 \pm 1.7	35.9 \pm 1.8	1.1
	Oct ‘16	32.7 \pm 4.4	32.2 \pm 3.7	37.3 \pm 1.5	1.1
	Apr ‘17	30.4 \pm 4.0	35.9 \pm 1.7	33.9 \pm 4.9	0.7
	Aug ‘17	33.2 \pm 1.9	30.5 \pm 2.0	31.3 \pm 2.2	1.0

Table 3. Corresponding p-values from Tukey's *post hoc* test examining temporal effects after a significant two-way ANOVA.

Parameter	Event	Oct '15	Apr '16	Jul '16	Oct '16	Apr '17	Aug '17
<i>16s rRNA</i>	Jul '15	0.17	<0.001	0.43	0.60	0.25	1.00
	Oct '15		<0.001	0.001	0.98	1.00	0.04
	Apr '16			0.20	<0.001	<0.001	0.001
	Jul '16				0.01	0.001	0.72
	Oct '16					1.00	0.27
	Apr '17						0.07
<i>nirS</i>	Jul '15	0.48	0.69	0.61	1.00	0.17	0.44
	Oct '15		0.02	0.01	0.87	1.00	0.01
	Apr '16			1.00	0.32	0.002	1.00
	Jul '16				0.26	0.001	1.00
	Oct '16					0.56	0.16
	Apr '17						0.001
<i>dsrA</i>	Jul '15	1.00	1.00	0.99	1.00	1.00	0.21
	Oct '15		0.94	1.00	1.00	0.91	0.06
	Apr '16			0.89	0.97	1.00	0.41
	Jul '16				1.00	0.84	0.03
	Oct '16					0.94	0.07
	Apr '17						0.52
<i>mcrA</i>	Jul '15	1.00	<0.001	<0.001	0.003	0.34	0.68
	Oct '15		<0.001	<0.001	0.001	0.14	0.37
	Apr '16			1.00	0.31	0.002	<0.001
	Jul '16				0.16	0.001	<0.001
	Oct '16					0.53	0.23
	Apr '17						1.00
Shannon H'	Jul '15	1.00	0.85	1.00	0.87	0.14	1.00
	Oct '15		0.55	1.00	1.00	0.58	0.95
	Apr '16			0.55	0.23	0.006	0.99
	Jul '16				0.99	0.41	0.96
	Oct '16					0.92	0.71
	Apr '17						0.08
CO ₂ Production	Jul '15	1.00	0.57	1.00	0.23	0.04	0.009
	Oct '15		0.61	1.00	0.25	0.04	0.01
	Apr '16			0.54	1.00	0.82	0.53
	Jul '16				0.21	0.03	0.008
	Oct '16					0.99	0.88
	Apr '17						1.00
CH ₄ Production	Jul '15	0.03	1.00	0.96	1.00	0.98	0.95
	Oct '15		0.005	0.28	0.08	0.002	0.001
	Apr '16			0.74	0.95	1.00	1.00
	Jul '16				1.00	0.55	0.45
	Oct '16					0.85	0.76
	Apr '17						1.00

Table 4. Mean (\pm standard error) for Shannon diversity (H') and richness (observed OTUs) for each sampling event. Temporal variation of H' is summarized in Table 3.

	Event	Control	Fresh	Salt
Richness (Observed OTUs)	Jul '15	6864 \pm 175	6965 \pm 185	6549 \pm 208
	Oct '15	6494 \pm 30	6857 \pm 232	6183 \pm 121
	Apr '16	6957 \pm 212	7333 \pm 365	6588 \pm 232
	Jul '16	6663 \pm 217	6755 \pm 274	6568 \pm 163
	Oct '16	7192 \pm 34	7248 \pm 452	6464 \pm 317
	Apr '17	6193 \pm 754	6658 \pm 209	6535 \pm 749
	Jul '17	6245 \pm 235	6620 \pm 159	6022 \pm 222
Shannon Diversity (H')	Jul '15	7.5 \pm 0.1	7.5 \pm 0.1	7.4 \pm 0.1
	Oct '15	7.4 \pm 0.1	7.5 \pm 0.1	7.3 \pm 0.1
	Apr '16	7.6 \pm 0.1	7.7 \pm 0.1	7.4 \pm 0.1
	Jul '16	7.4 \pm 0.1	7.4 \pm 0.1	7.4 \pm 0.1
	Oct '16	7.6 \pm 0.1	7.5 \pm 0.2	7.4 \pm 0.1
	Apr '17	7.2 \pm 0.3	7.4 \pm 0.1	7.4 \pm 0.2
	Jul '17	7.3 \pm 0.1	7.3 \pm 0.1	7.2 \pm 0.1

Table 5. Correlation coefficient (r^2) and p-values from the envfit model performed on prokaryotic community structure.

Variable		r^2	p
Porewater	Salinity	0.03	0.31
	NH ₄ ⁺	0.07	0.08
	NO ₃ ⁻	0.01	0.96
	SO ₄ ²⁻	0.01	0.98
Soil	H ₂ O %	0.01	0.89
	OM %	0.02	0.46

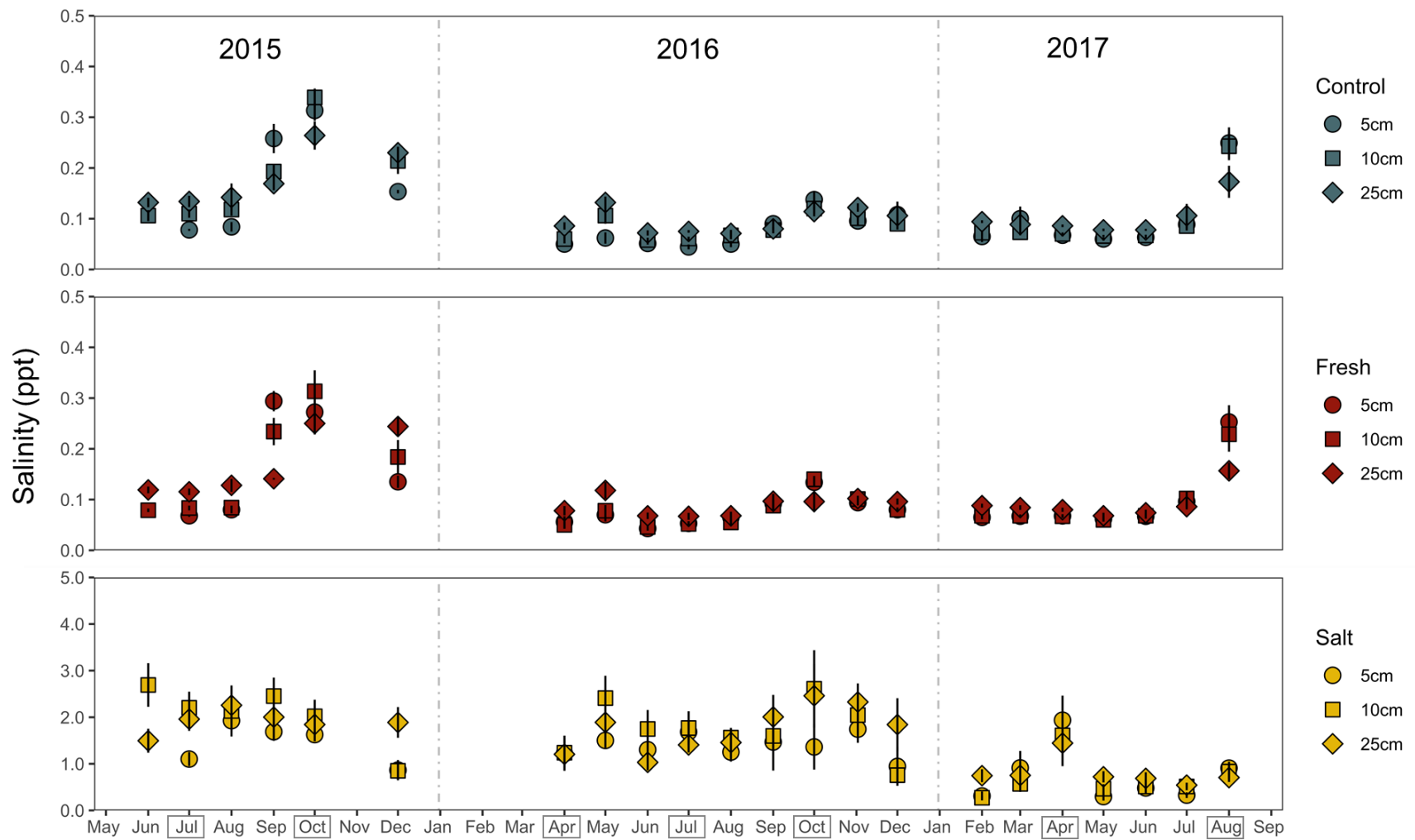


Figure 1. Monthly mean (\pm standard error) salinity for well water over the course of the experiment. Sampling events occurred during months that are boxed. Note change in scale of y-axis for Salt treatment.

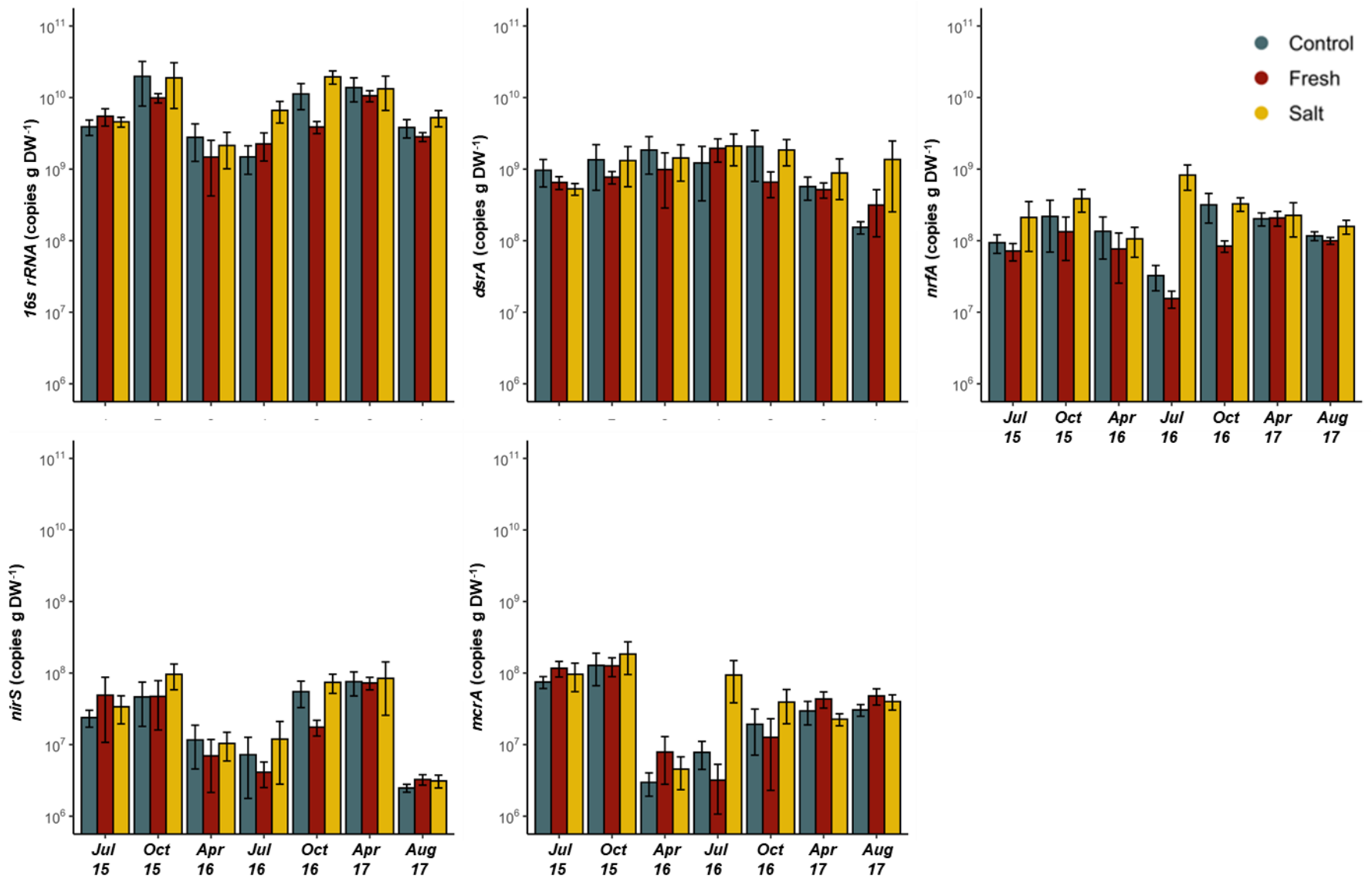


Figure 2. Mean (\pm standard error) abundance of bacteria (*16s rRNA*) and targeted functional genes.

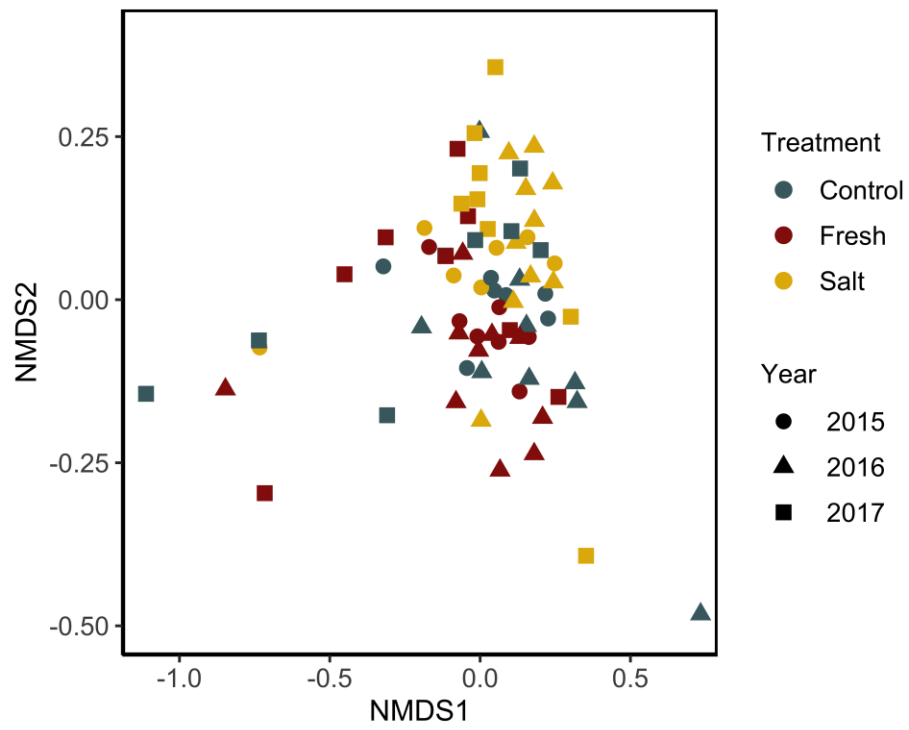


Figure 3. NMDS ordination of the prokaryotic community structure using Bray-Curtis dissimilarity.

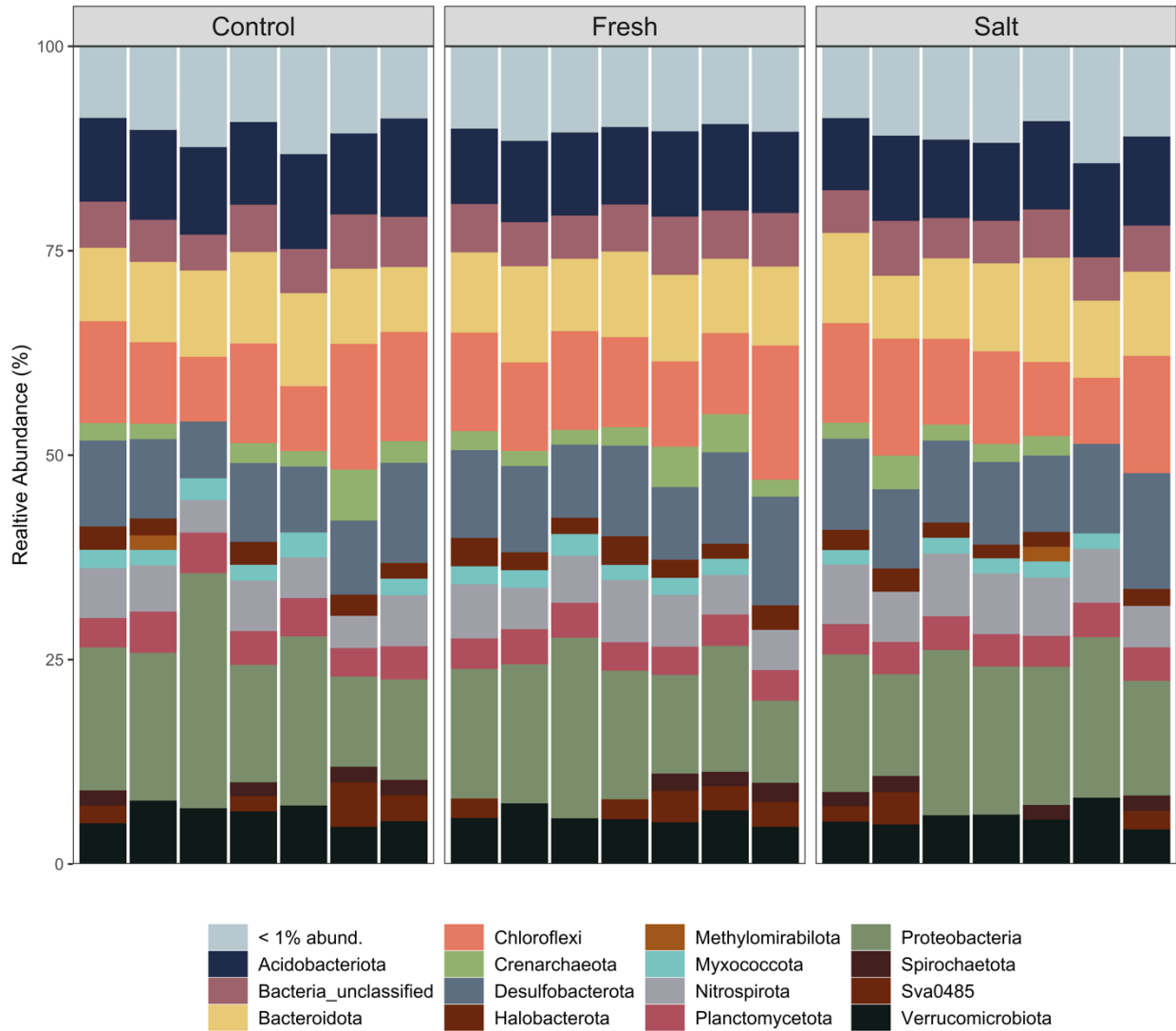


Figure 4. Mean relative abundance of prokaryotic phyla by sampling event. Within each treatment, samples are ordered chronologically from left to right. Phyla that accounted for less than 1% were combined.

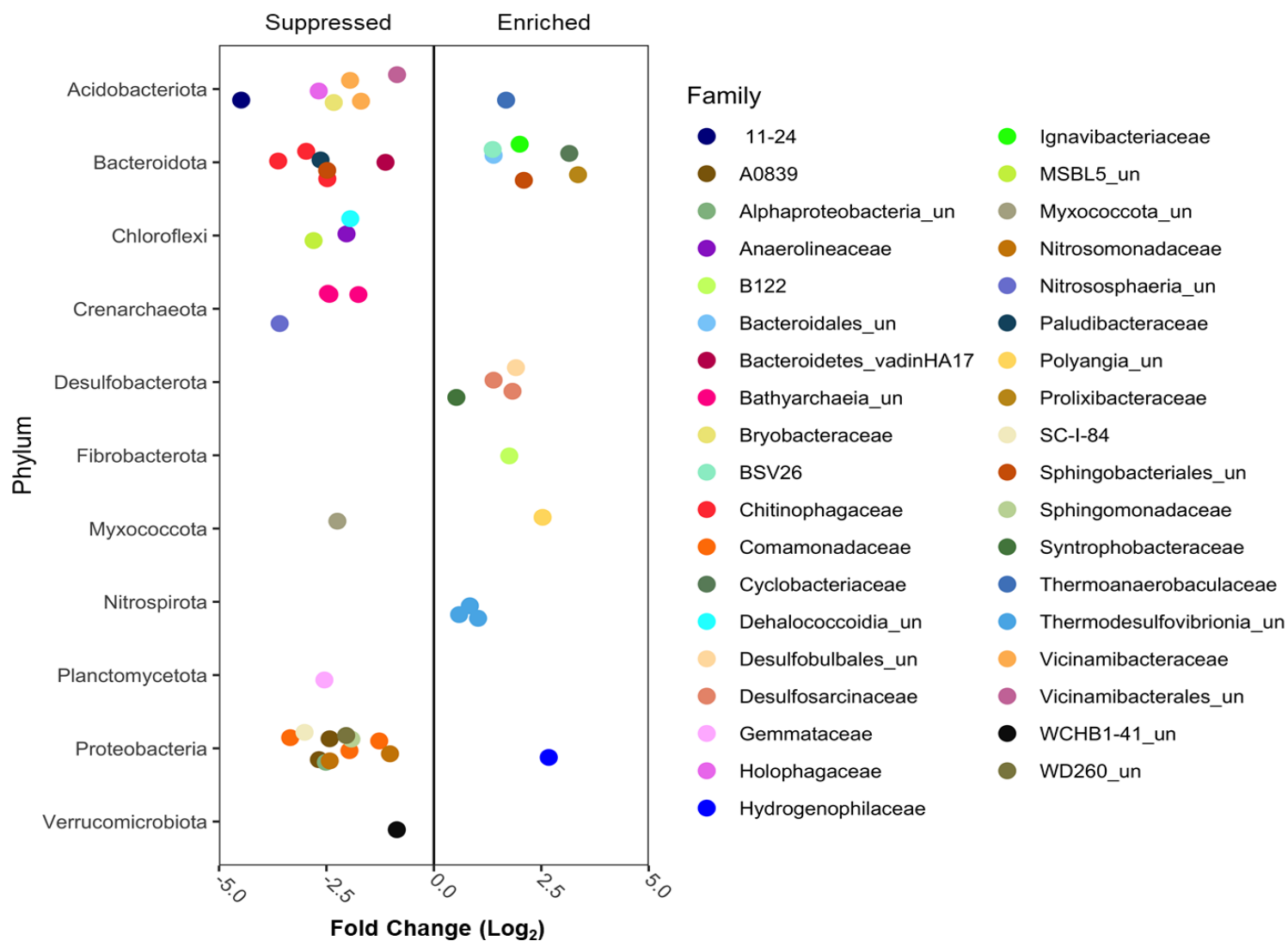


Figure 5. Fold change (Log₂) of taxa that were enriched (positive values) and suppressed (negative values) under saline conditions as identified by Deseq2. Color represents the highest level classification down to the Family level (ex. Bacteroidales_un represents an OTU that belongs to an unclassified family of the Order Bacteroidales).

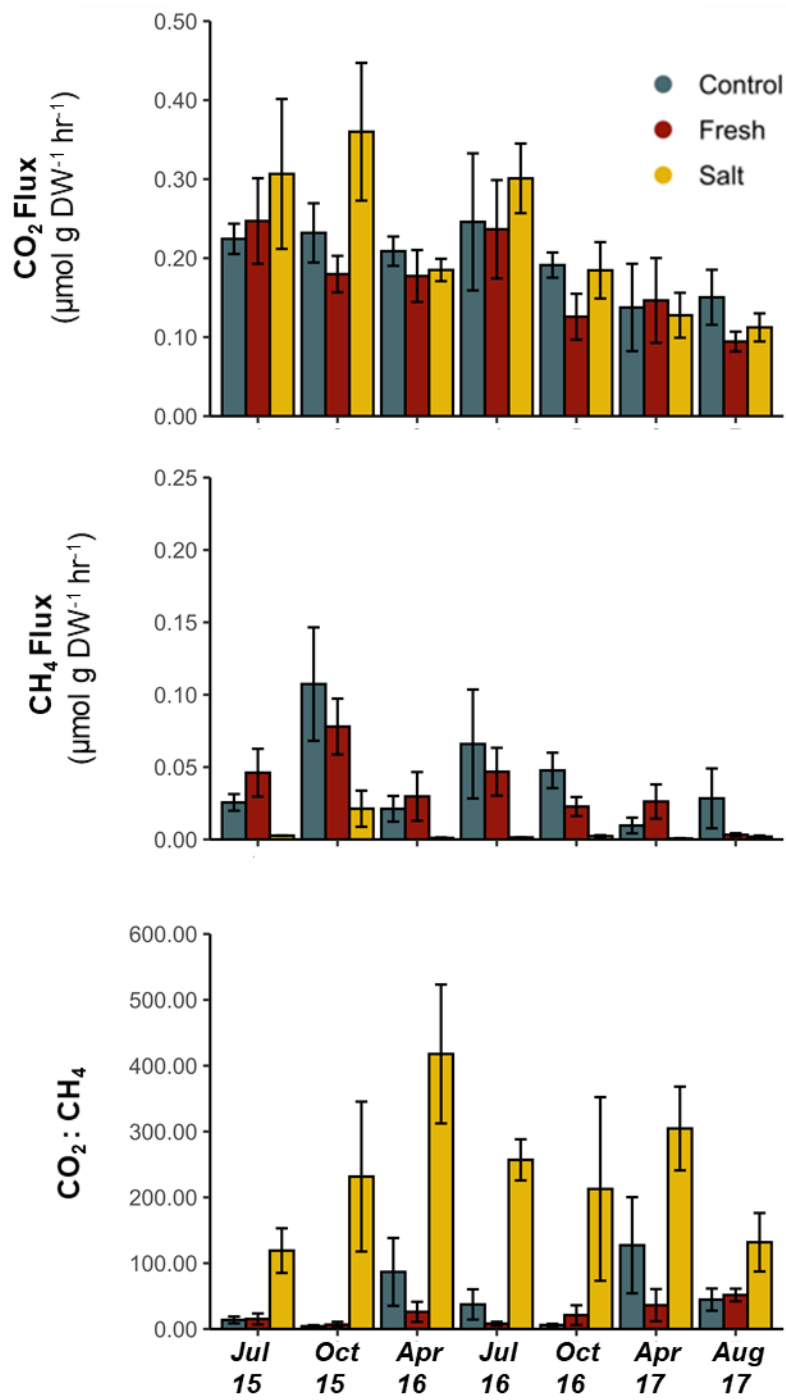


Figure 6. Mean (\pm standard error) rates of CO₂ production, CH₄ production, and the ratio of CO₂:CH₄.

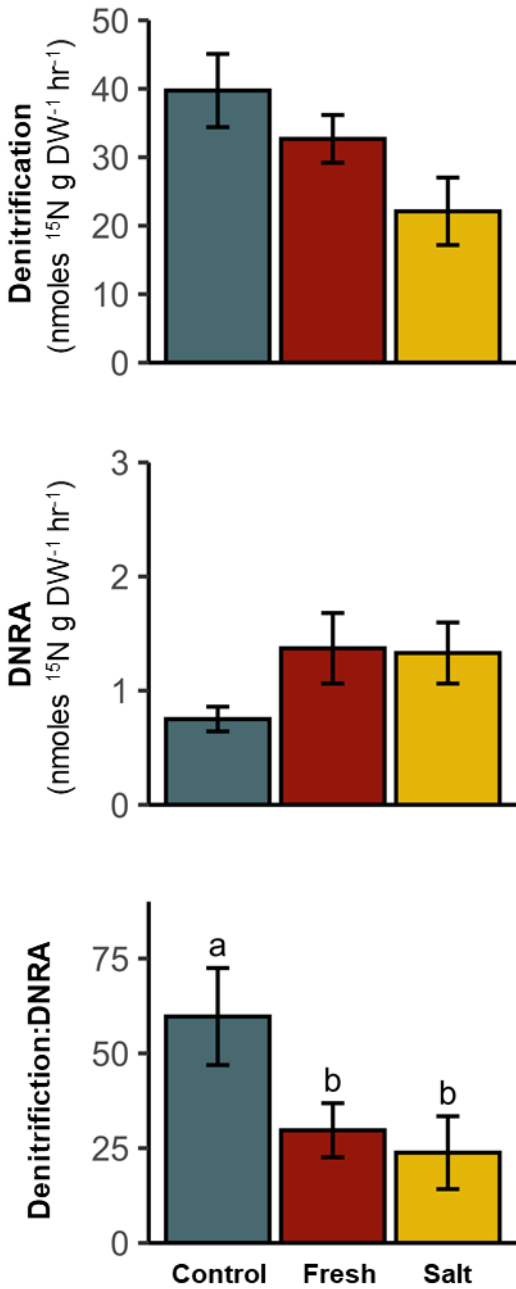


Figure 7. Mean (\pm standard error) rates of denitrification and DNRA, and the ratio of denitrification:DNRA during the August 2017 sampling event. Lowercase letters indicate significant differences via Tukey's HSD post-hoc analysis.

CHAPTER 4: RECONSIDERING ASSAYS OF ENZYME ACTIVITIES IN WETLAND SOILS

Joseph C. Morina¹, Chansotheary Dang², and Rima B. Franklin¹

¹Department of Biology, Virginia Commonwealth University, Richmond VA 23284 USA

²Division of Plant and Soil Sciences, West Virginia University, Morgantown, WV 26506

1. Introduction

Soil enzyme activity regulates the decomposition of soil organic matter. Because of this, enzymes are commonly used to evaluate soil quality and nutrient status, especially in agricultural systems (Bünemann et al., 2018; Trasar-Cepeda et al., 2008), and to assess soil functional diversity (Caldwell, 2005). In addition, enzyme activity is the foundation of several conceptual and mathematical models of microbial decomposition (e.g., see Allison et al. (2010), Moorhead and Sinsabaugh (2006), and Schimel 2003)), and efforts to include explicit representation of enzyme kinetics in broad-scale models of terrestrial carbon biogeochemistry are growing (e.g., see Chen et al. (2019), Wang et al. (2013), and Wieder et al. (2013)). The increasingly widespread use of soil enzyme assays is due, in part, to the development of protocols for microplate readers (Marx et al., 2001, Saiya-Cork et al., 2002, Jackson et al., 2013, Wirth and Wolf 1992, Kremer 1994), which have drastically reduced the time and cost of these analyses. This affords researchers greater replication and larger sample sizes, and increases the diversity of enzymes and ecosystems that can be studied. Despite these advances, our ability to make robust cross-ecosystem comparisons remains limited (e.g., consider meta-analyses by Jian et al. (2016), Ren et al. (2017), and Xiao et al. (2018)) due to differences in sample preparation and processing across the various microplate protocols. Calls for the development of standardized protocols are numerous, but there is considerable debate in the literature as to how this should be accomplished (German et al., 2011, Dick 2011, Dick et al., 2018, Marx et al., 2001, DeForest 2009). Much of this debate centers on the effects of pH and substrate concentrations and whether assay conditions should try to mimic *in situ* soil conditions (German et al., 2011, Saiya-Cork et al., 2002) or be optimized to determine maximum/peak reaction rates (Dick et al., 2018).

In addition to choosing if soil enzymes should be assayed under optimal or field conditions, there are other logistical/procedural issues that need to be considered such as sample storage, substrate concentration, incubation times, and soil slurry preparation. For the latter, most prior research

has focused on soil homogenization and determining the best way to separate aggregates and disperse enzymes in solution while minimizing lysis of microbial cells (Burns et al., 2013). The suspension solution used for homogenate preparation is important because, through pH and ionic strength effects, it can influence enzyme sorption to soil particles, enzyme conformation and stability, and solubility of substrates and cofactors (Turner 2010). Further, the choice of suspension solution can affect the chemistry in subsequent steps of the enzyme assay once the slurry is moved to the microplate and mixed with the buffered substrate; the slurry itself can make up 10% (Marx et al., 2001) to 80% (Saiya-Cork and Sinsabaugh 2002) of the total assay volume. Unfortunately, there is no agreed-upon suspension solution for the microplate assay across the published protocols, and little mention of suspension solution in the review articles that focus on methods development and optimization (Deng et al., 2011).

Because microplate assays require an aqueous soil suspension, the use of a laboratory solution (e.g., deionized water, acetate/acetic acid buffer, or phosphate buffer) is generally unavoidable in upland ecosystems. Inundated soils, such as those found in wetlands, are an exception. Porewater from these soils could be used as a suspension solution to prepare soil slurries for enzyme assays. This creates a unique opportunity to assess the impact of suspension solution on enzyme activity assays by comparing results obtained using a “natural” solution with the various laboratory solutions. Though the microplate approach is commonly used to assess enzyme activity in wetland soil (Corstanje et al., 2007, Dunn et al., 2014, Neubauer et al., 2013, Servais et al., 2019, Rietl et al., 2015, Penton and Newman 2007), no one uses porewater for preparing slurries. Instead, deionized water (Dang et al., 2019, Neubauer et al., 2013, Chambers et al., 2013) and acetate buffer (Servais et al., 2020, Jackson and Vallarie 2009) are commonly used. There have been few efforts to optimize enzyme assays specifically for wetland systems (Dunn et al., 2014); thus, it remains unclear how our understanding of mediating factors like pH and conductivity, primarily tested in upland soils, apply to saturated wetlands soils.

Information about conductivity could be particularly important for efforts to assess the impact salinity/salinization has on soil enzyme activity and carbon cycling in wetlands (Morrissey et al., 2014, Dong et al., 2022, Bai et al., 2021), and it is possible that the suspension solutions used could mask site effects in these studies.

In this paper, we present the results of three experiments that examine the methodological approaches to soil enzymology in wetland ecosystems. First, we explored the use of wetland porewater as a suspension solution, specifically examining whether the use of porewater would artificially increase enzyme activities due to the presence of enzymes within the porewater itself. In our second experiment, we considered how the choice of suspension solution can affect interpretations of wetland salinity gradient studies, specifically by testing if suspension solution alone could mask site effects. Lastly, to better understand the response of wetland enzymes to changes in salinity, we performed a manipulative experiment to investigate the role conductivity has on enzyme activities. All three experiments were conducted in parallel using soil from two wetland ecosystems along a salinity gradient (freshwater and mesohaline), and results are presented for seven enzymes involved in the cycling of C, N, P, and S.

2. Methods

2.1 Site Description and Sampling

Soil was sampled from two wetlands along the salinity gradient of Taskinas Creek (York River State Park, Virginia, USA) during low tide. The first site (37.399°N, -76.721°W), hereafter referred to as “fresh,” was a non-tidal freshwater wetland dominated by *Typha angustifolia*. The second site (37.414°N, - 76.716°W) was a tidal mesohaline marsh vegetated with a monoculture of *Spartina alterniflora*, hereafter referred to as the “salt” site. These sites correspond to the Fresh and Meso sites used in Chapter 2.

At each wetland, we collected five soil cores (10 cm × 10 cm) from within a 25 m² plot of uniform vegetation. Cores were sealed in air-tight plastic bags and placed on ice for transport to the laboratory. In addition, we collected bulk soil samples (3 L), which we later centrifuged (2,500 × *g*, 20 min) to extract porewater for the preparation of soil slurries.

2.2 Soil Properties and Porewater Chemistry

Upon return to the laboratory, pH (following Thomas (1996)), redox potential (Laqua Act Portable pH/ORP/ION meter D-73, Irvine, California, USA), and conductivity (Hach Pocket Pro+ Multi 2, Loveland, Colorado, USA) were immediately measured for each soil core. A subsample (~20 g) of soil was then removed to determine gravimetric water content (moisture %; 50°C for 7 days), organic matter (OM%; loss on ignition at 400°C for 16 hours), and C:N (acidified with 0.10 M HCl, analyzed using a Perkin Elmer CHNS-O analyzer, Waltham, Massachusetts, USA). The remainder of each soil core was reserved for enzyme assays (4°C, completed within one week). Soil properties are presented in Table 1.

Porewater samples were analyzed for conductivity and pH (Laqua probe), filtered (0.22 μm pore-sized mixed cellulose ester, EMD Millipore, Darmstadt, Germany), and then frozen (-20°C) for later analysis of dissolved organic carbon (DOC, Shimadzu TOC-V 5000, Columbia, Maryland, USA). Porewater chemistry is presented in Table 2.

2.3 Suspension Solutions

For all three experiments, we followed the enzyme protocol described below, with the only change being the suspension solution used to prepare the soil slurries. We first focused on the use of site-specific porewater, which was obtained by centrifugation and either: (i) used directly, (ii) filtered (using both GF/C and GF/F filters (Whatman, Pittsburgh PA, USA)), or (iii) autoclaved (121 PSI, 25 min). We then measured enzyme activity of these three porewater formulations and of soil slurries prepared

using each formulation.

We used soil from the two wetlands to prepare soil slurries with site-specific porewater and four commonly-used laboratory solutions: sterile deionized (DI) water (similar to Dunn et al., 2014, Lehman and O'Connell 2002, Deng et al., 2011), phosphate-buffered saline (PBS) (Phillips and Leonard 1976, Prosser et al., 2011)), sodium acetate buffer (NaOAc)(Saiya-Cork et al., 2002, Jackson and Vallaire 2009, Olander and Vitousek 2000, McClaugherty and Linkins 1990; Sinsabaugh and Findlay 1995; Allison et al., 2006, Frossard et al., 2012)), and physiological saline solution (0.85% w/v NaCl (Sun et al., 2020, Larson et al., 2002)). All solutions were filter sterilized (0.22- μ m pore size) and stored at room temperature before performing the assays, and the pH and conductivity of each solution are reported in Table 3.

Lastly, to assess the response of enzyme activities to changes in salinity, we used Instant Ocean (Spectrum Brands, Blacksburg, VA, USA) dissolved in deionized water to prepare solutions targeting 2, 4, 6 and 10 parts per thousand. This range is environmentally-relevant for freshwater wetlands experiencing salinization, and it is representative of the salinity gradient for our two sites (fresh: <0.1 ppt, salt: ~5 ppt). Furthermore, this range is comparable to the laboratory suspension solutions utilized in this study. However, because conductivity is the parameter that can be most directly compared with previous enzymology papers, especially ones that evaluate suspension solutions, we hereafter refer to these treatments based on their conductivity (4, 7, 10, 16 mS cm⁻¹).

2.4 Slurry Preparation

Soil slurries were prepared by mixing 1.0 g (\pm 0.2 S.E.) of soil with 100 mL of suspension solution in sterile 125 mL Erlenmeyer flasks. Slurries were sonicated at 15 W for 2 min (Misonix Sonicator 3000, Farmingdale, New York, USA) and then transferred to a shaker table (160 rpm) to maintain the suspension while enzyme assays were prepared. The conductivity and pH of each slurry were measured at this time.

2.5 Soil Enzyme Assays

We measured the activity of seven enzymes (Table 4) using microplate assays as described in Morrissey et al. (2014) and Neubauer et al. (2013). All hydrolytic enzymes were measured fluorometrically (360 nm excitation/460 nm emission) using 4-methylumbelliferone (MUB) except LLAP, which used 7-amino-4-methylcoumarin (AMC). Labeled substrates were dissolved in ethylene glycol monomethyl ether (EGME) and brought up to desired concentration with MES (0.1 M, pH 6.1). For the LLAP assay, Trisma (50 mM, pH 7.8) buffer was used. Phenol oxidase activities were measured colorimetrically (460 nm, using an empirically determined micromolar extinction coefficient of 7.9 per μmol) with L-3,4-dihydroxyphenylalanine (L-DOPA, 6.5 mM) using sodium bicarbonate buffer (50 mM, pH 6.1). For both fluorometric (6.5 hour incubation) and colorimetric (6 hour incubation) assays, 50 μl of soil slurry in a total reaction volume of 200 μl . All substrates and reagents were obtained from Sigma-Aldrich Co. Ltd. (Saint Louis, Missouri, USA), and all measurements were made using a Synergy 2 plate reader (Biotek, Winooski, Vermont, USA).

2.6 Statistical Analyses

For our first experiment, we used analysis of variance (ANOVA) and Tukey's HSD *post hoc* tests for each soil to determine if porewater formulation affected rates of enzyme activities, followed by Pearson correlation to assess congruity when all enzyme data were combined. For our second experiment, we first performed a two-way ANOVA to assess if the choice of suspension solutions altered the observed site effect. Due to the significant interactions observed in our two-way ANOVAs (discussed below), we performed a series of t-tests to compare enzyme activities at each site based on suspension solution. In our third experiment, we determined if soil enzyme activities from our two different sites were altered by changes in conductivity by performing one-way ANOVAs on enzyme activities under the

different conductivity levels for site. All statistical analyses were performed using PAST 3.2 (Hammer et al., 2001). We used an α of 0.05 except for t-tests, which used a more conservative α of 0.01 to account for multiple comparisons.

3. Results

3.1 Porewater Enzyme Activity

Enzyme activity was measured for untreated porewater as well as porewater that was subsequently filtered or autoclaved (Figure 1). For all three formulations, we were able to detect activity via the fluorometric assays. Rates were always low (all $< 0.0032 \text{ pmol } \mu\text{l}^{-1} \text{ h}^{-1}$), and the average across all enzymes and porewater formulations was only $0.00014 \text{ pmol } \mu\text{l}^{-1} \text{ h}^{-1}$ (± 0.00005 S.E.). For the colorimetric assay, POX activity was similarly low (maximum: $0.0013 \text{ pmol } \mu\text{l}^{-1} \text{ h}^{-1}$; average: 0.0012 ± 0.00001). Overall, porewater rates were 10^4 - to 10^6 -fold lower than the corresponding soil slurries (Table 5).

Slurries prepared using filtered or autoclaved porewater usually had lower activity compared to slurries prepared using untreated porewater; this difference was statistically significant for about half of the cases considered (Table 6). The largest decreases in activity were associated with the breakdown of more labile substrates (BG, CHB, LLAP, and PHOS). When data from all the enzymes and sites were pooled ($n = 70$), the activity of soil slurries prepared using untreated porewater was highly correlated with slurries prepared using both the filtered (Pearson correlation: $r = 0.98$) and autoclaved solutions ($r = 0.99$). On average, slurries prepared using filtered porewater had rates 25.6% ($\pm 3.8\%$) lower than slurries prepared using untreated porewater, whereas slurries prepared using autoclaved porewater were 12.8% ($\pm 5.3\%$) lower. Because of the high correlation between porewater formulations, and the extremely low enzyme activities observed across all treatments, we chose the untreated porewater to

use in our subsequent experiment that assessed if the choice of suspension solution impacted conclusions based on site effect.

3.2 Site Effects When Using Different Suspension Solutions

We next compared the activity of soil slurries prepared using untreated porewater and four common suspension solutions. Two-factor ANOVA revealed a significant interaction ($p < 0.01$) between soil type and suspension solution for all enzymes except LLAP ($p = 0.15$) and SULF ($p = 0.21$), indicating that efforts to compare enzyme activity of soil from our two sites will be impacted by the choice of suspension solution. Because of significant interactions in the ANOVAs, t-tests were used to test for site effects (fresh vs. salt) for each solution individually (Figure 2).

For three of the enzymes, BG, POX, and SULF (Figure 2A, 2B, and 2C), patterns across sites were consistent regardless of which suspension solution was used. For BG, activity was always greater in slurries prepared using soil from the fresh site; for POX and SULF, activity was always greater for the salt site. However, solution type did influence the *magnitude* of these cross-site differences. For example, the activity of BG from fresh soil was 5-fold greater than in salt soil when porewater was used to prepare the suspension, but only ~2-fold when other solutions were used (DI water: 2.0, NaOAc: 1.7; PBS: 1.5; Saline: 1.8).

For XYLO and LLAP (Figure 2F and 2G), results obtained using porewater matched two of the four laboratory solutions. The activities of these enzymes showed no site effect when slurries were prepared using either site-specific porewater, deionized water, or NaOAc buffer. However, site effects did manifest when slurries were prepared using the suspension solutions with greater conductivities (PBS (19.9 mS cm^{-1}) and physiological saline (16.1 mS cm^{-1})); specifically, activity measurements associated with salt soil increased in the solutions with high conductivity.

For CHB and PHOS (Figure 2D, and 2E), the use of porewater for slurry preparation gave markedly different results compared to all the laboratory solutions. For example, estimates of CHB activity for soil from the salt site were all quite similar when laboratory solutions were used to prepare the soil slurry but increased by a factor of 5 when site-specific porewater was used to prepare the soil slurry. For PHOS, the situation was reversed; the use of laboratory solutions would have led one to conclude that enzyme activities of fresh and salt soils differed, whereas differences were not evident when site-specific porewater was used to prepare the soil suspensions.

In addition to soil enzyme activities, we also measured the pH and conductivity of each solution and corresponding soil slurry (Table 3). Solution pH ranged from 5.6 (NaOAc buffer) to 8.0 (porewater from salt site). Except for physiological saline, slurry pH was generally similar to solution pH, and did not differ much across the two soil types. Solution conductivity ranged from ~ 0 (DI) to 20 mS cm^{-1} (PBS and porewater from salt site) and, as with pH, slurry conductivity tracked solution conductivity. Correlation analysis (Pearson) revealed several strong positive correlations of enzyme activities with pH and consistently negative correlations with conductivity for soils from the fresh site (Figure 3). Correlations for soil from the salt site were generally much smaller with BG and SULF activities displaying a negative correlation with slurry pH and conductivity, whereas CHB and LLAP activities showed a positive correlation to pH and conductivity.

3.3 Effect of Suspension Solution Salinity on Soil Enzyme Activities

The effect of suspension solution salinity was examined by comparing slurries prepared using deionized water (conductivity ~ 0) to ones made using Instant Ocean with conductivities of 4, 7, 10, and 16 mS cm^{-1} . The conductivity of soil slurries was similar to solutions, and did not differ much between fresh and salt soils. Slurry pH also remained relatively constant for both soils, and ranged from 6.3 to 6.7.

One-way ANOVAs (Table 7) show that only one enzyme measured for the fresh site was affected by conductivity; specifically, POX was stimulated under low and intermediate conductivities (4, 7, and 10 mS cm⁻¹). For all other enzymes, activity for fresh soil was positively correlated with conductivity, albeit not significantly (results not presented, Pearson r ranged from 0.22-0.42). When assessing enzyme activities for the salt soil, four of the seven responded to changes in conductivity (Table 7). The activity of POX was again elevated at lower conductivities (4 and 7 mS cm⁻¹) relative to the 16 mS cm⁻¹ treatment. BG activity was significantly lower in DI water than in the 16 mS cm⁻¹ slurry. Similarly, the activity of PHOS was lower in DI than in slurries with conductivities > 7 mS cm⁻¹. Lastly, LLAP activity was only suppressed in DI when compared to the 4 mS cm⁻¹ treatment. Except for POX, the activity of all enzymes was always lowest in DI compared to the solutions with elevated salinity.

4. Discussion

4.1 Porewater as a Suspension Solution

The use of porewater as an alternative to laboratory suspension solutions for creating soil slurries is predicated on the assumption that the enzyme activity of porewater is negligible compared to that of bulk soil. This assumption appears valid for the enzymes and sites that we considered. For all three of the porewater formulations that we tested, enzyme activity was minute in comparison to soil slurry activities. This finding agrees with similar studies comparing enzyme activity for freshwater peatland soils and porewater (Romanowicz et al., 2015) and for marine sediments and benthic waters (Arnosti 2000). These studies found enzyme activities for water were at least two orders of magnitude lower than enzyme activities in sediments and soils. The low(er) activity in the aqueous phase likely reflects the affinity of enzymes to bind with soil components such as organic matter and clays (Wallenstein and Burns 2011, Burns et al., 2013) and the fact that sorbed enzymes may be better protected from degradation than dissolved enzymes (Arnosti et al., 2014). Taken together, our results

suggest that porewater may be a valid option for preparing soils slurries and measuring enzyme activity for saturated soils. Nevertheless, we recommend that other investigators perform similar preliminary studies for each new system they wish to sample to confirm porewater enzyme activity is low.

When initially designing this experiment, we were concerned that “background” enzyme activity in porewater might inflate slurry estimates relative to the use of sterile laboratory solutions. Thus, we included the filtration and autoclaving treatments as possible ways of reducing porewater enzyme concentrations (e.g., via enzyme adherence to filters or destruction/deactivation due to heat) prior to slurry preparation. In the end, the activity of porewater was 10,000 to 1,000,000 times lower than corresponding slurries, essentially making the background activity imperceptible (Table 5). Given this, we were somewhat surprised to occasionally find significant differences in slurry activity when different porewater formulations were used for preparing the soil suspensions (Table 6). These differences were likely due to indirect effects of filtration and autoclaving on porewater chemistry. Though neither conductivity nor pH changed much as a result of these manipulations, we did find an increase in DOC concentration at the fresh site due to autoclaving (Table 2). This could be problematic given that prior researchers have linked porewater DOC concentrations with enzyme activity in wetland ecosystems (Peacock et al., 2014, Romanowicz et al., 2015). Future researchers considering pre-treatment options for porewater may wish to test different times/temperatures for autoclaving or experiment with different membrane types and/or pore sizes for filtration. Performing more detailed chemical analyses considering specific constituents known to serve as inhibitors and activators of soil enzyme activity (Tabatabai 1994) could also be useful. For subsequent aspects of this study, we elected to use untreated porewater, rather than filtered or autoclaved, as it should best represent *in situ* conditions.

4.2 Effect of Suspension Solution on Soil Enzyme Activities

We compared enzyme activity in soil slurries prepared using four common laboratory solutions, as well as site-specific porewater, and discovered that the choice of suspension solution can alter the perceived site effect, at least for our two wetlands (Figure 2). This is noteworthy given that suspension solution only accounted for 20-25% of the final reaction volume of our actual enzyme assays, and has important implications for ongoing efforts to develop consistent microplate protocols that facilitate cross-study comparisons. Most prior research has focused on optimization of *assay* conditions, with less attention to the potential impact of sample treatment prior to the actual rate measurements. Our results demonstrate that the choice of suspension solution for slurry preparation can have a significant impact on enzyme activities that must also be considered when optimizing and standardizing extracellular enzyme assays.

When comparing the enzyme activity profiles associated with the different suspension solutions, a few patterns emerge. Considering first the laboratory solutions, we found that PBS and physiological saline generally had similar results as did DI and NaOAc (Figure 2). This pattern mirrors the pH and conductivity results (Table 3), and is reasonable given prior research documenting the strong effects of pH and conductivity on enzyme activity (Tabatabai 1994, Turner 2010, Frankenberger and Bingham 1982, Saviozzi et al., 2011). Some prior studies have also suggested that enzyme activities are different under buffered vs. unbuffered conditions (Zantua and Bremner 1975, Taylor et al., 2002), but we did not find this to be a large effect. This may be due to the fact that, regardless of which suspension solution was used, all enzyme *assays* were buffered.

The suspension solutions used most commonly in wetland enzyme studies of salinity gradients are DI water and NaOAc (Dang et al., 2019, Neubauer et al., 2013, Chambers et al., 2013, Servais et al., 2020, Jackson and Vallaire 2009). In our second experiment, we found consistent site effects between these two suspension solutions. This suggests that wetland gradient studies using these two suspension

solutions are likely comparable, assuming all other aspects of the method are standardized between studies. However, we did observe discrepancies in site effects between porewater and these two suspension solutions (DI and NaOAc) for four of the enzymes we considered (CHB, PHOS, XYLO, and LLAP), implying that activities measured using these laboratory solutions may not be representative of activities under field conditions. It is also important to note that even when conclusions regarding site effects (i.e., is activity greater at the fresh or salt site?) were similar across suspension solutions, differences in magnitude were evident (e.g., Figure 2A), which could impact modeling results. These more nuanced differences are also likely to affect the interpretation of site effects when considering large numbers of sites. Regarding the use of site-specific porewater, these assays yielded enzyme activities similar in magnitude, variability, and dynamic range to the other solutions, suggesting porewater is a suitable solution for preparing soil suspensions when trying to mimic *in situ* conditions. While we can find no evidence that porewater, soil water, or site water has previously been used to prepare soil enzyme assays in wetland studies, this approach is common in several other assays of microbial function, including biogeochemical rates (Neubauer et al., 2013, Marton et al., 2012, Herbert et al., 2020) as to be more representative of field conditions.

The use of a site-specific solutions such as porewater may be particularly useful when comparing environments that differ in ways that directly affect enzyme physicochemistry (e.g., pH or conductivity). For example, the sites we considered differ markedly in conductivity, and using any of the candidate laboratory solutions could have a disproportional effect on samples from one of the sites (e.g., salt site enzymes being more susceptible to changes in conductivity than fresh) – changing its conductivity and possibly affecting enzyme stability, and thus assay rates, in a way that masks our ability to detect cross-site differences. To explore this issue further, we conducted a correlation analysis to compare slurry pH and conductivity with soil enzyme activities for each site (Figure 3), which highlighted the differential response of enzyme activities to these physicochemical parameters between the two

sites. As soil enzymes are produced by the soil microbial community, changes to community composition could explain this differential response as microbes from more saline wetlands may produce enzymes that are more stable under higher conductivity. In Chapter 2, we demonstrate that, indeed, the fresh site (Chapter 2; Fresh Control) and salt site (Chapter 2; Meso Control) have distinct prokaryotic communities.

4.3 Sensitivity of Soil Enzymes Assays to Salinity

To our knowledge, this is the first paper to assess how wetland soil enzymes respond to varying conductivity levels. However, prior research has been conducted in upland soils, revealing enzyme-specific and time-specific effects (Saviozzi et al., 2011). For example, that study found protease activity was suppressed by increased conductivity for all sampling events (1, 20, and 40 days), whereas dehydrogenase activity was only suppressed on day 1, and activities recovered to control rates by day 40. This highlights the importance of considering temporal scale when assessing the sensitivity of enzyme activity to increased conductivity. The results from our third experiment should be considered a short-term (hours) response, and may not be representative of long-term changes to soil enzyme activities at elevated conductivities.

The enzymes from the salt site generally showed a positive relationship with increasing salinity, which can be explained by natural selection favoring enzyme production that reduces costs and promotes cellular benefits (Allison et al., 2011), and thus microbial community members at the salt site are likely selected for based on their and their enzyme's halotolerance. Enzymes isolated from halophiles display greater tolerance to increased conductivity compared to non-halophilic microbes (as discussed in Zahran (1997)). This selection can also be observed in thermophiles as their enzymes display greater tolerance to heat than enzymes isolated from mesophilic organisms (Beadle et al., 1999)

and in psychrophiles who have lower temperature optima than mesophilic organisms (Feller 2003, Coker et al., 2003).

Previous research in upland soils has found conductivities as low as 4 mS cm^{-1} (Saviozzi et al., 2011), our lowest conductivity manipulation, can suppress soil enzyme activities. When considering coastal soils, a recent study along a salinity gradient ($0.1 - 13.7 \text{ mS cm}^{-1}$) found that that enzyme activities were unaffected at conductivities below 2 mS cm^{-1} , but are suppressed at conductivities higher than 2 mS cm^{-1} (Dong et al., 2022). A study measuring soil enzyme activities across a smaller salinity gradient ($\sim 0 - 4 \text{ mS cm}^{-1}$) within the Chesapeake Bay watershed found a positive correlation with salinity and soil enzyme activities, and also found that the microbial community (abundance and composition) was tightly linked to soil enzyme activities (Morrissey et al., 2014). The assessment of soil enzyme activities across salinity gradients is informative when considering dynamics of organic matter mineralization; however these studies likely are not reflective of freshwater enzyme sensitivity to conductivity *per se*, as the microbial communities responsible for producing these enzymes differ in composition across these gradients (Morrissey et al., 2014, Chapter 2). As discussed above, members of the microbial communities at more saline sites may produce enzymes that are adapted to the conductivity of that site, and conclusions based on conductivity effects directly on enzyme activities may be due to the difference in enzyme structures mediated through the composition of the microbial community.

5. Conclusions

There are two main schools of thought in the literature about whether enzyme assay conditions should be optimized to determine maximum/peak reaction rates or adjusted to mimic *in situ* soil conditions. The first focuses on the optimization of assay conditions (pH, temperature, etc.) and the use of non-limiting substrate concentrations to determine maximum/peak reaction rates, which are then

interpreted as the *potential* of the soil to perform each given reaction (e.g., Nannipieri et al., 2018, Baldrian 2019, Dick 2011). The alternate approach focuses on replicating *in situ* soil conditions, thereby making the enzyme assays a more valuable proxy of microbial activity. Our study provides insights important to both approaches, and highlights the importance of slurry suspension choice as it can directly affect soil enzyme activities and thus alter the perceived site effect.

We demonstrated that site-specific porewater can be used as a suspension solution, which may be of interest to researchers attempting to mimic *in situ* conditions. Furthermore, we demonstrated that slurries created using porewater can result in different apparent site effects than when assayed using laboratory solutions. When performing extracellular enzyme assays using wetland soils, we propose that porewater is more representative than deionized water, and the use of porewater will not add an appreciable amount of extracellular enzymes to the soil slurry. Future studies of wetland enzymology should also consider using both *in-situ* (porewater) and optimal (laboratory solutions) conditions for each enzyme assay. This is also the first paper that assessed responses of wetland soil enzyme activities to conductivity, and demonstrated that enzyme activities in the salt soil were more affected by conductivity than enzyme activities in the fresh soil. This differential response of enzyme activity to changes in conductivity is likely an artifact of different selective forces acting upon the microbial communities from different ecosystems. Taken together, the results of these experiments have important implications for ecologists trying to decide whether to use protocols that mimic *in situ* soil conditions or instead focus on approaches that determine maximum potential reaction rates. Further, our use of porewater as a suspension solution could be of practical interest to researchers studying enzyme activity in saturated soils.

6. Tables and Figures

Table 1. Soil properties (mean \pm S.E., n=5 per site) for the two wetland soils. Corresponding p-values for each t-statistic are indicated as: (**) for $0.001 < p < 0.01$, and (***) for $p \leq 0.001$; all other $p > 0.05$.

Soil property	Fresh site	Salt site	p-value
Moisture (%)	73 \pm 1	67 \pm 1	0.004 **
pH	7.1 \pm 0.1	6.4 \pm 0.4	0.08
Redox (mV)	- 104 \pm 21	- 89 \pm 12	0.56
Conductivity (mS cm ⁻¹)	0.2 \pm 0.02	8.6 \pm 0.4	< 0.0001 ***
OM (%)	31 \pm 2	15 \pm 1	< 0.0001 ***
C:N	15.3 \pm 0.5	14.4 \pm 0.6	0.25

Table 2. Chemistry of the various porewater preparations for both sites (Fresh, Salt) considered in the first experiment.

Porewater preparation	pH		Conductivity (mS cm ⁻¹)		DOC (mg l ⁻¹)	
	Fresh	Salt	Fresh	Salt	Fresh	Salt
Porewater	8.1	8.3	0.5	26.1	8.3	32.1
+Filtered	8.8	8.3	0.6	21.2	8.6	34.5
+Autoclaved	8.1	8.8	0.3	27.9	69.1	32.2

Table 3. The pH and conductivity (mean \pm S.E., n=5) of each solution (“no soil”) as well as slurries prepared for the second and third experiments.

Solution Type	pH			Conductivity (mS cm ⁻¹)		
	No soil	Fresh soil	Salt soil	No soil	Fresh soil	Salt soil
Fresh site porewater	7.7	7.6 \pm 0.1	-	0.3	0.3 \pm 0.1	-
Salt site porewater	8.0	-	8.2 \pm 0.0	19.5	-	27.1 \pm 0.1
Deionized water	6.5	6.5 \pm 0.2	6.7 \pm 0.0	< 0.1	0.1 \pm 0.0	0.3 \pm 0.0
NaOAc buffer	5.6	5.6 \pm 0.0	5.5 \pm 0.1	4.2	4.2 \pm 0.0	4.4 \pm 0.1
PBS	7.2	6.9 \pm 0.0	7.0 \pm 0.0	19.9	17.3 \pm 0.1	17.6 \pm 0.1
Physiological saline	6.9	6.0 \pm 0.2	5.9 \pm 0.1	16.1	16.1 \pm 0.1	15.9 \pm 0.1
Conductivity 4	7.3	6.7 \pm 0.1	6.7 \pm 0.1	3.8	3.2 \pm 0.1	3.5 \pm 0.0
Conductivity 7	7.6	6.3 \pm 0.1	6.3 \pm 0.1	6.8	5.9 \pm 0.0	6.4 \pm 0.0
Conductivity 10	7.4	6.4 \pm 0.1	6.5 \pm 0.1	9.9	8.7 \pm 0.1	9.1 \pm 0.0
Conductivity 16	7.7	6.4 \pm 0.1	6.7 \pm 0.1	16.5	15.3 \pm 0.1	15.8 \pm 0.1

Table 4. Enzymes and substrates used for assays of soil enzyme activities.

Enzyme	Abbreviation	Target molecule	E.C. Number	Artificial substrate
β -1,4-glucosidase	BG	Cellulose	3.2.1.21	4-MUB- β -D-glycopyranoside
1,4- β -cellobiosidase	CHB	Cellulose	3.2.1.91	4-MUB- β -D-cellobioside
β -D-xylosidase	XYLO	Hemicellulose	3.2.1.37	4-MUB- β -D-xylopyranoside
Phenol oxidase	POX	Lignin	1.10.3.2	3,4-dihydroxy-L-phenylalanine
Leucyl aminopeptidase	LLAP	Polypeptides	3.4.11.1	L-Leucine-7-AMC
Alkaline phosphatase	PHOS	Phosphomonoesters	3.1.3.1	4-MUB-Phosphate
Arylsulfatase	SULF	Sulfatides	3.1.6.1	4-MUB-Sulfate Potassium Salt

Table 5. Ratio of activity in soil slurries relative to porewater alone (i.e., no soil added) for each porewater formulation from the first experiment.

Site	Enzyme	Porewater	+Filtered	+Autoclaving
Fresh	BG	0.2×10^4	5.1×10^4	6.8×10^5
	CHB	0.7×10^4	5.0×10^4	6.6×10^5
	XYLO	2.8×10^4	9.1×10^4	4.5×10^5
	POX	1.7×10^6	1.6×10^6	1.6×10^6
	LLAP	1.8×10^4	1.1×10^4	0.9×10^5
	PHOS	2.4×10^4	6.7×10^4	3.4×10^5
	SULF	15.4×10^4	19.7×10^4	2.4×10^5
Salt	BG	2.7×10^4	3.0×10^5	4.9×10^6
	CHB	2.9×10^4	0.9×10^5	1.3×10^6
	XYLO	4.8×10^4	4.8×10^5	1.7×10^6
	POX	2.3×10^6	2.2×10^6	2.5×10^6
	LLAP	7.0×10^4	4.3×10^5	1.7×10^6
	PHOS	5.7×10^4	9.4×10^5	0.7×10^6
	SULF	13.9×10^4	5.9×10^5	1.4×10^6

Table 6. Enzyme activity ($\text{pmol } \mu\text{l}^{-1} \text{ h}^{-1}$; means \pm S.E. with $n = 5$ each) for soil slurries prepared using each porewater formulation in the first experiment. Rates were compared using one-way ANOVA, and p-values for each F-statistic are reported. For each enzyme and each site, lowercase letters designate significant differences across porewater formulations determined via Tukey's HDS *post hoc* tests.

Site	Enzyme	Porewater	+Filtered	+Autoclaving	p-value
Fresh	BG	7.1 \pm 0.5 ^a	3.6 \pm 0.3 ^b	4.4 \pm 0.4 ^b	0.0002 ^{***}
	CHB	1.2 \pm 0.1 ^a	0.4 \pm 0.1 ^b	0.5 \pm 0.1 ^b	< 0.0001 ^{***}
	XYLO	1.8 \pm 0.2	1.1 \pm 0.1	1.5 \pm 0.3	0.08
	POX ($\times 10^3$)	2.1 \pm 0.1	2.0 \pm 0.1	2.0 \pm 0.0	0.30
	LLAP	8.0 \pm 0.4 ^a	5.2 \pm 0.4 ^b	5.5 \pm 1.0 ^b	< 0.0001 ^{***}
	PHOS	8.8 \pm 0.6 ^a	5.0 \pm 0.7 ^b	5.5 \pm 0.1 ^b	0.001 ^{***}
	SULF	1.7 \pm 0.1	1.4 \pm 0.1	1.5 \pm 0.1	0.09
Salt	BG	9.2 \pm 0.8 ^a	1.3 \pm 0.1 ^b	1.6 \pm 0.2 ^b	< 0.0001 ^{***}
	CHB	1.8 \pm 0.1 ^a	0.3 \pm 0.0 ^b	0.6 \pm 0.2 ^{ab}	0.01 ^{**}
	XYLO	1.0 \pm 0.1	0.8 \pm 0.1	1.0 \pm 0.2	0.23
	POX ($\times 10^3$)	2.9 \pm 0.1	2.7 \pm 0.1	3.0 \pm 0.1	0.29
	LLAP	5.6 \pm 0.3 ^a	4.1 \pm 0.2 ^b	4.8 \pm 0.3 ^{ab}	0.02 [*]
	PHOS	5.9 \pm 0.4	4.7 \pm 0.2	6.3 \pm 0.8	0.12
	SULF	1.7 \pm 0.1	1.5 \pm 0.0	2.0 \pm 0.3	0.18

Table 7. Effect of suspension solution conductivity on enzyme activity ($\mu\text{mol g-OM}^{-1} \text{ h}^{-1}$; means \pm S.E. with $n = 5$ each). Lowercase letters indicate significant effects of detected via ANOVA and Tukey's *post hoc* tests. Corresponding p-values for each F-statistic are indicated as: (*) for $0.01 < p < 0.05$, (**) for $0.001 < p < 0.01$, and (***) for $p \leq 0.001$; all other $p > 0.05$.

Site	Enzyme	DI H ₂ O	Conductivity 4	Conductivity 7	Conductivity 10	Conductivity 16	p-value
Fresh	BG	6.2 \pm 0.3	8.7 \pm 1.9	7.2 \pm 0.8	6.7 \pm 0.6	8.1 \pm 0.9	0.44
	CHB	0.8 \pm 0.1	1.1 \pm 0.2	1.3 \pm 0.2	0.9 \pm 0.1	1.5 \pm 0.2	0.56
	XYLO	1.9 \pm 0.1	1.9 \pm 0.2	2.2 \pm 0.2	1.8 \pm 0.2	2.4 \pm 0.3	0.17
	POX ($\times 10^3$)	1.4 \pm 0.1 ^b	1.9 \pm 0.1 ^a	1.8 \pm 0.1 ^a	1.8 \pm 0.1 ^a	1.5 \pm 0.1 ^b	< 0.0001 ^{***}
	LLAP	8.7 \pm 0.6	11.8 \pm 1.5	10.8 \pm 0.8	9.8 \pm 0.8	11.8 \pm 1.4	0.26
	PHOS	8.7 \pm 0.8	14.3 \pm 1.9	14.4 \pm 2.1	20.3 \pm 7.1	14.2 \pm 1.2	0.07
	SULF	2.6 \pm 0.1	2.5 \pm 0.2	2.7 \pm 0.2	2.2 \pm 0.1	3.1 \pm 0.4	0.12
Salt	BG	3.1 \pm 0.4 ^b	4.4 \pm 0.4 ^a	3.7 \pm 0.3 ^a	3.7 \pm 0.3 ^{ab}	5.5 \pm 0.8 ^a	0.03 [*]
	CHB	0.8 \pm 0.1	0.9 \pm 0.1	1.2 \pm 0.2	1.2 \pm 0.1	1.3 \pm 0.3	0.32
	XYLO	2.3 \pm 0.2	2.6 \pm 0.5	2.6 \pm 0.2	2.5 \pm 0.3	2.9 \pm 0.6	0.84
	POX ($\times 10^3$)	2.9 \pm 0.2 ^a	3.0 \pm 0.1 ^a	3.1 \pm 0.1 ^a	2.7 \pm 0.1 ^{ab}	2.5 \pm 0.1 ^b	0.02 [*]
	LLAP	8.9 \pm 1.1 ^b	19.2 \pm 2.7 ^a	13.7 \pm 1.4 ^a	15.0 \pm 1.2 ^{ab}	15.5 \pm 2.8 ^{ab}	0.03 [*]
	PHOS	16.5 \pm 1.5 ^b	24.6 \pm 2.7 ^a	28.3 \pm 3.8 ^a	30.3 \pm 1.1 ^a	28.6 \pm 2.1 ^a	0.005 ^{**}
	SULF	4.6 \pm 0.5	4.9 \pm 0.4	5.1 \pm 0.3	5.5 \pm 0.5	5.6 \pm 0.5	0.56

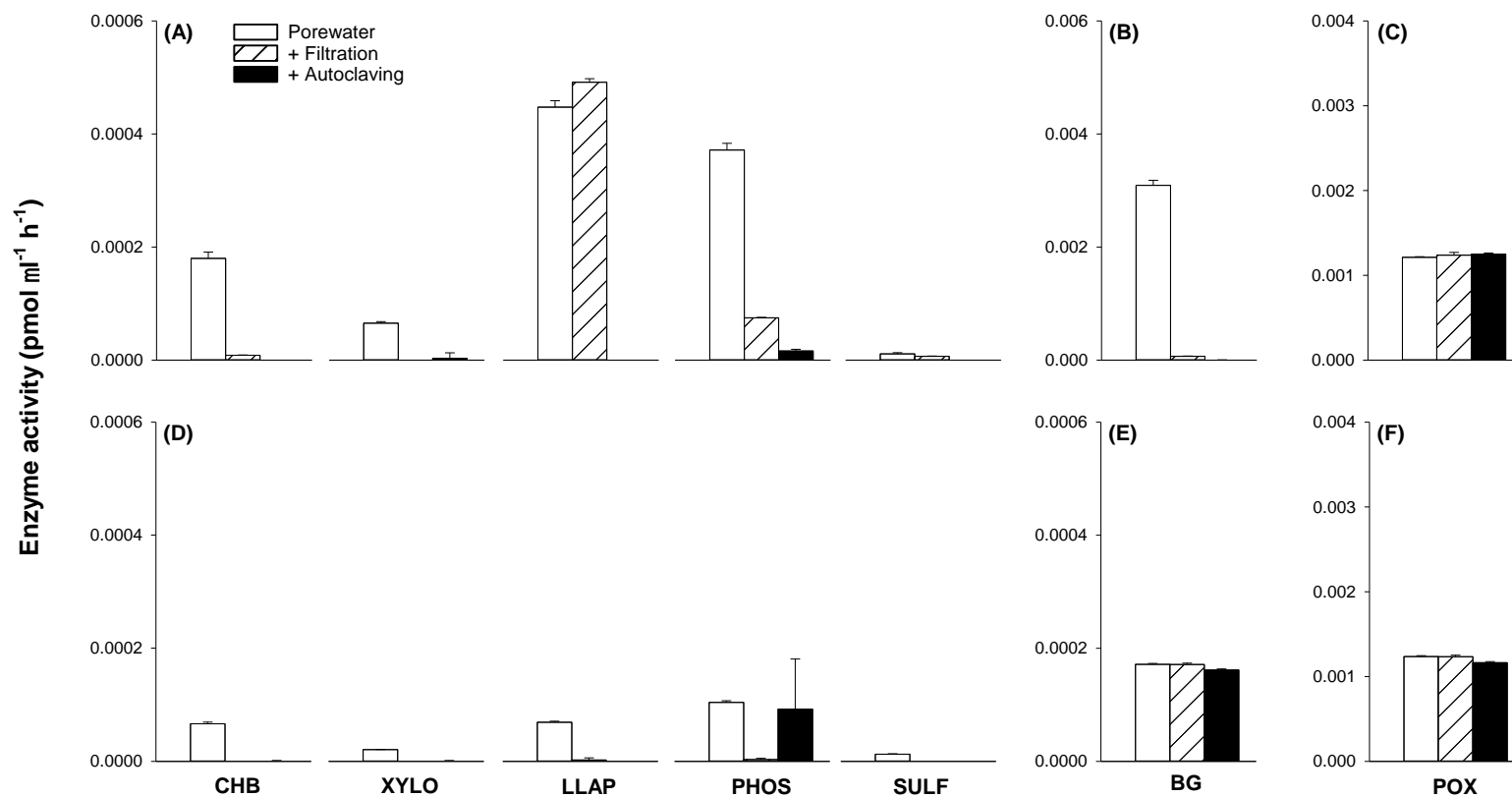


Figure 1. Enzyme activity ($\mu\text{mol l}^{-1} \text{h}^{-1}$; means \pm S.E. with $n=3$ for each bar) for the various porewater formulations (no soil) from the first experiment. The top panels (A, B, and C) display results for the fresh site, and the bottom panels (D, E, and F) display results for the salt site.

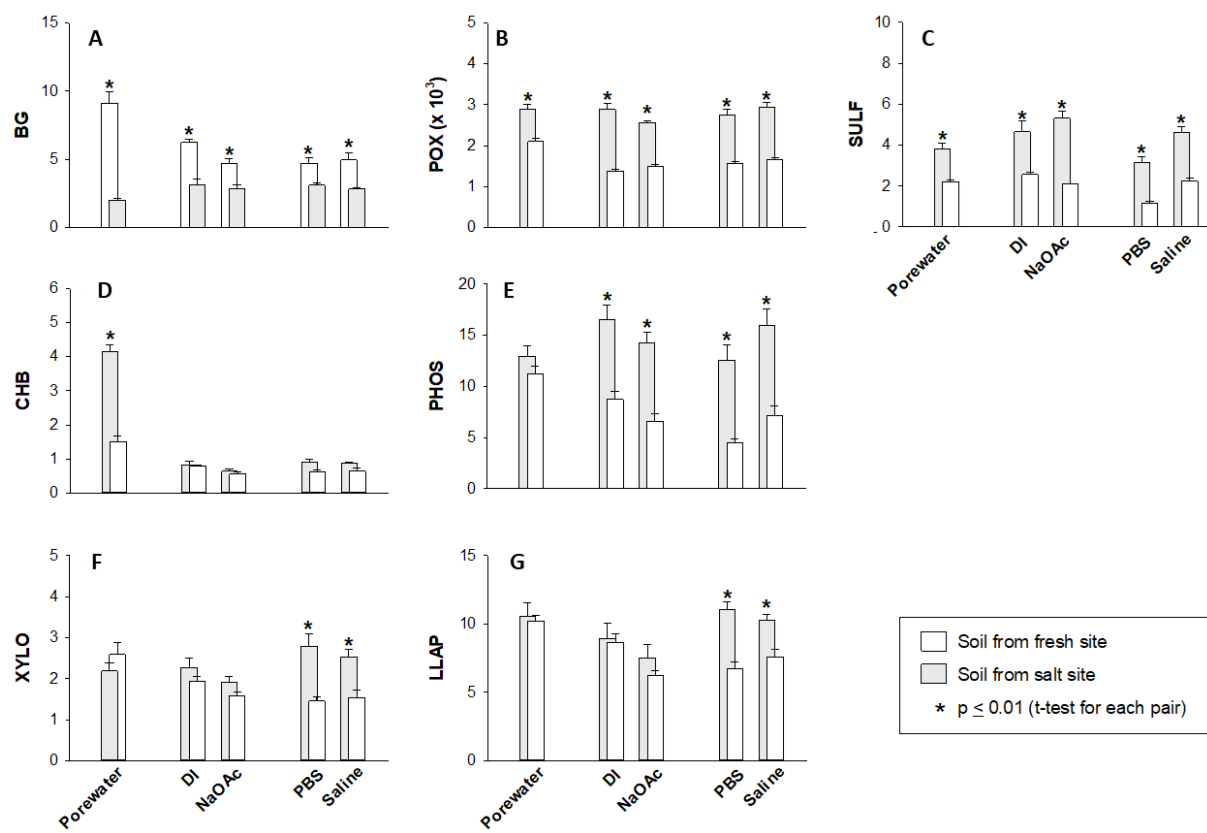


Figure 2. Soil enzyme activity (pmol g-OM⁻¹ h⁻¹; mean + S.E. with n=5 for each bar) measured in five different suspension solutions for the second experiment.

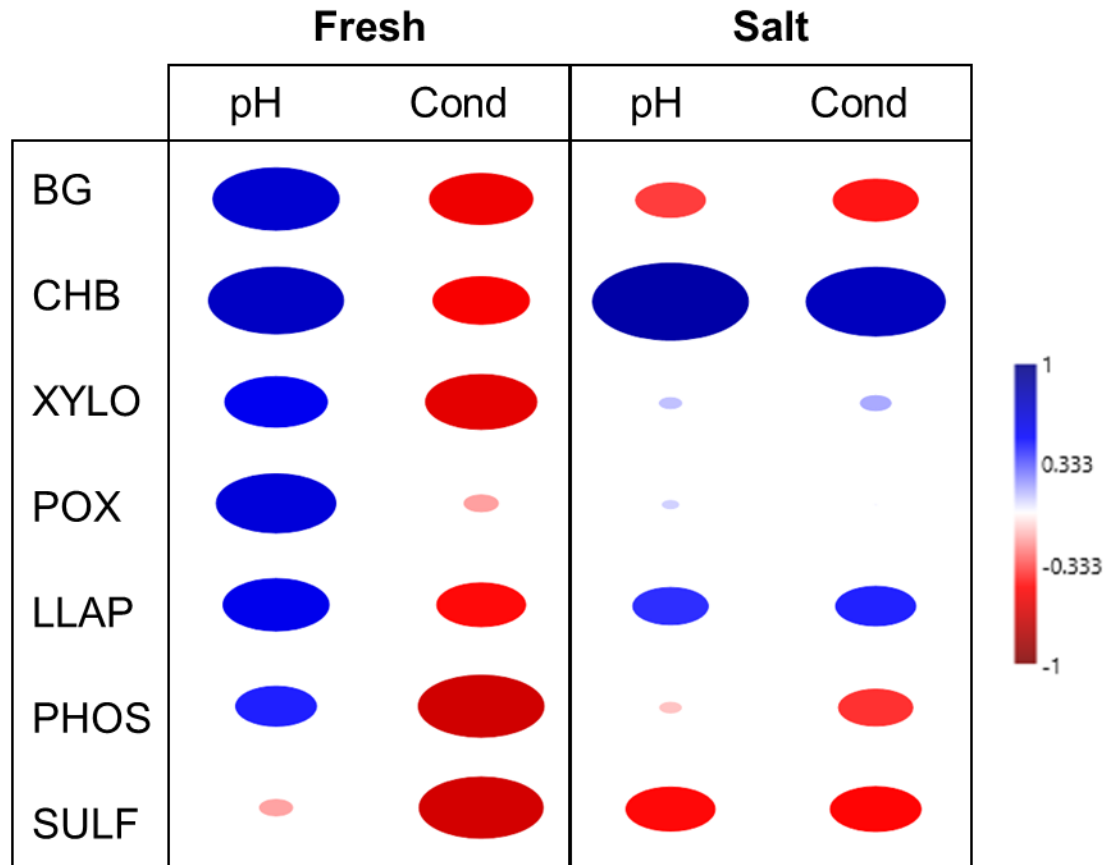


Figure 3. Correlation of enzyme activity with slurry pH and conductivity (“Cond”) for soils from the fresh site (left) and the salt site (right) for the second experiment. Blue and red colors correspond to positive and negative correlations, respectively. Ellipse size and color intensity indicate the strength of correlation with larger symbols and darker coloration having a larger absolute value of r .

CHAPTER 5: SYNTHESIS

Joseph C. Morina

In this dissertation, I examined the response of freshwater prokaryotic communities to salinization using multiple methods, timescales, and salinity levels, and found a consistent response: freshwater prokaryotic communities are relatively resistant to oligohaline levels of salinization. One of the greatest differences between the experimental designs of Chapter 2 and Chapter 3 was the presence and absence of prokaryotic community mixing, termed community coalescence. The mesh bags used in Chapter 2 allowed for host-site prokaryotes to immigrate into the transplanted soils, whereas the site water in Chapter 3 was mixed with artificial sea water that contained no brackish prokaryotes, thereby excluding immigration by nature of the experimental design. I see a substantial similarity when comparing the results of Chapter 2 fresh-to-oligohaline transplants (FO) and Chapter 3 salt treatment (Salt). The prokaryotic communities of these two treatments received approximately the same salinity exposure and for the same duration length (albeit longer in Chapter 3). Furthermore, enzymes from the freshwater soil utilized for the transplant experiment in Chapter 2 were not suppressed by increased salinity and, in some cases, were stimulated under oligohaline levels of salinity (Chapter 4).

To better contextualize and compare the results of these two studies, I combined the amplicon sequencing community data from Chapters 2 and 3, along with data from Dang et al. (2019) and data from ~90 samples collected over two years from six tidal wetlands along the salinity gradient of the Pamunkey River (including Cumberland Marsh and Taskinas Creek). After creating a dissimilarity matrix (Bray-Curtis), I ordinated the results using a Principal Coordinate Analysis (PCoA), and present the results in Figure 1. When comparing the results of the two soil transplant experiments (Chapter 2 and Dang et al. (2019)), I found that regardless of which freshwater wetland the soil was originally collected from (Taskinas Creek for Chapter 2, Cumberland Marsh for Dang et al. (2019)), exposure to mesohaline salinities in tandem with a source of mesohaline-adapted taxa restructures freshwater communities over time to become more similar and/or converge on the structure of mesohaline communities. While Dang et al. (2019) did not observe full convergence of the transplanted soil community to match the

mesohaline control within the one-year timeframe of their study, the amount of change is comparable to the amount observed during the first year of the mesohaline transplants from Chapter 2, suggesting that convergence would have been observed at a longer timescale. Figure 1 also illustrates that the structure of soil prokaryotic communities at Cumberland Marsh and Taskinas Creek are relatively stable over time, observed by the tight clustering of communities across multiple studies and years. When characterizing the impact of ecological disturbances on prokaryotic communities via community structure (Allison and Martiny 2008), generalized conclusions should only be made when the system in question is in a stable or steady state (Galand et al., 2016), suggesting our conclusion of prokaryotic responses to salinization are appropriate (i.e. end-member communities show tight clustering).

When considering the observed resistance of freshwater prokaryotes to oligohaline levels of salinity, physiological plasticity, dormancy, and community coalescence are all important biological features that may explain this observed response. Physiological plasticity could be a major factor explaining the response of freshwater communities to oligohaline levels of salinity. While small in number, taxa that showed a differential response to salinization in Chapter 3 are capable of multiple respiratory pathways, suggesting that freshwater prokaryotes that display metabolic flexibility may have competitive advantages over taxa with limited respiratory pathways. This is further supported by differentially abundant taxa identified in Chapter 2 as only eight families were more abundant in the FO soils than the fresh control soils, yet the oligohaline control community formed a distinct structure from that of the freshwater control. Taken together, this suggests that at least during the initial stages of salinization events wherein saline and freshwater communities mix, freshwater taxa are able to compete or coexist with oligohaline taxa. However, I cannot rule out that microbial dormancy may have a part to play, as our DNA-based approaches cannot differentiate between active and dormant community members.

In addition to the biological features of microbial communities, the differences I observed in community structure are likely also impacted by both the plant community and edaphic characteristics of the selected wetlands. For example, the response of microbial communities to disturbances can be mediated through plant communities (Finks et al., 2021), through a variety of mechanisms that include the introduction of oxygen into the rhizosphere, which in turn can stimulate aerobic respiration and/or detoxify reduced toxic compounds (e.g., sulfide). Furthermore, prokaryotic functional guilds such as denitrifiers show higher abundance in the rhizospheres of certain aquatic macrophytes (Morina et al., 2018), which could be a result of alterations to the physicochemical properties of the rhizosphere. Plant community composition can affect both the quality and quantity of soil OM, which can also shape microbial community compositional and functional responses (Sutton-Grier et al., 2011). The plant communities of the wetland sites chosen for Chapter 2 are representative of the plant communities along the freshwater to mesohaline salinity gradient of the Chesapeake Bay (Sharpe and Baldwin 2009), increasing the applicability of my findings to other efforts in the Chesapeake Bay Region. While I cannot isolate the direct or indirect effects of plant communities on the response of the prokaryotic community to salinization, in Chapter 2 and Chapter 3, I performed salinization in the field, thus incorporating plant effects into the microbial community response (at least in regards to community structure).

The response of microbial communities to increased salinity can also be mediated through edaphic characteristics such as organic matter content (as discussed in Szoboszlay et al. (2019)). I observed a clear link between prokaryotic community structure and the measured environmental variables in Chapter 2 (Supplemental Table 3); however, I could not find any correlation with community structure and edaphic characteristics in Chapter 3 (Table 5). This was likely due to the fact that treatment effects were minimal on soil and water chemistry in Chapter 3 relative to the unique soil characteristics observed at each wetland in Chapter 2. Thus the applicability of these findings may be limited in wetland soils with vastly different edaphic characteristics.

The findings of this dissertation highlight the value of profiling the prokaryotic communities responsible for the biogeochemical cycling of carbon and nitrogen. Furthermore, my results suggest that coastal freshwater wetland soils, from both tidal and non-tidal wetlands, are relatively resistant to oligohaline levels of salinity, and observed changes in community structure may require long temporal scales to manifest, even in the presence of site-adapted taxa. The communities of freshwater NO_3^- reducers showed sensitivity to salinization, especially mesohaline levels. In Chapter 2, communities of denitrifiers and DNRA-capable organisms changed in taxonomic composition when exposed to increased salinities, with changes occurring faster when exposed to mesohaline levels of salinity. The sensitivity of NO_3^- reducing communities to increased salinity observed in this study support previous findings that these guilds form unique communities across salinity gradients (Franklin et al., 2017, Dong et al., 2014) and in response to salinity manipulations (Wang et al., 2018, Neubauer et al., 2019). Rates of DNRA generally followed the paradigm of increasing importance under increased salinity and sulfide concentrations (Murphy et al., 2020, Herbert et al., 2015), in particular when exposed to mesohaline conditions (Giblin et al., 2010). When considering how microbial structure informed functional response, I observed that functional abundances of denitrifiers were linked to rates of denitrification for both qPCR-based and phylogenetic inferences (PICRUSt2), and for the DNRA pathway PICRUSt2-based functional profiles were linked to rates of DNRA. Both functions were correlated ($r > 0.6$) with PICRUSt2-based functional profiles, highlighting the usefulness of this new tool when considering predicted functional responses (Raes et al., 2021), and that metrics of prokaryotic community structure help our understanding of community functioning, especially in regards to NO_3^- reduction during salinization disturbance events.

The comprehensive review of global wetland salinization by Herbert et al. (2015) identified five main mechanisms by which coastal wetlands experience salinization; sea-level rise driven salinization, reduction of riverine freshwater inputs, alterations to subsurface freshwater flow, changes to coastal

geomorphology, and storm surges, all of which can differ in salinization intensity (i.e. salinity level) and duration of exposure. For instance, rates of sea-level rise display high spatial and temporal variability, and salinization via this mechanism will gradually increase salinity over long temporal scales (decades to centuries). Other mechanisms can result in rapid salinization (hours to days) with drastically elevated salinity levels such as storm surges, reduction of freshwater riverine inputs, and changes to coastal morphology. Furthermore, these mechanisms are not mutually exclusive and can act in tandem, thereby exacerbating salinization of coastal freshwater wetlands.

Taken together, the findings of this dissertation demonstrate that the prokaryotic communities of coastal freshwater wetland soils are relatively resistant to moderate increases in salinity over multi-year temporal scales, suggesting that mechanisms of salinization resulting in oligohaline levels of salinity will likely not result in the restructuring of these communities. However, I did observe that prokaryotic function can change when exposed to oligohaline levels of salinity, highlighting that these moderate levels of salinity may impart functional shifts without structural changes. On the other hand, mechanisms that result in long-term exposure to mesohaline levels of salinity will likely impart both structural and functional changes to prokaryotic communities. Furthermore, salinization events that result in the introduction of more saline-tolerant community members could decrease the temporal scales needed for structural changes to manifest in the prokaryotic communities of coastal wetland soils.

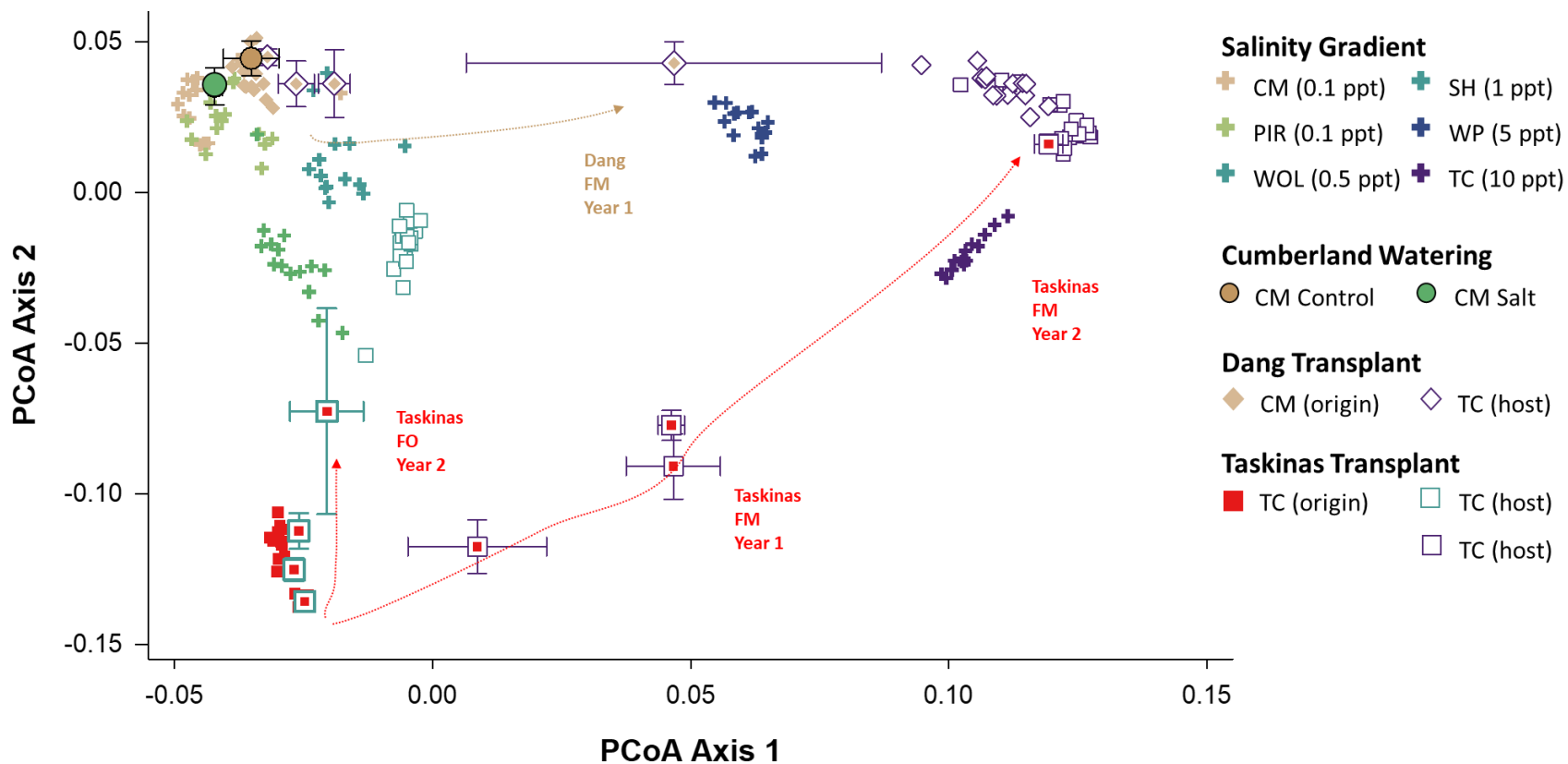


Figure 1. Principal coordinates analysis (PCoA) comparing salinization studies with salinity gradient communities within the Pamunkey River and York River Estuary. CM corresponds to Cumberland Marsh, and TC corresponds to Taskinas Creek. Transplant soils from Chapter 2 (Taskinas Transplant) and Dang et al. (2019) (Dang Transplant) are annotated with text and arrows showing changes in community structure over time. Communities from Chapter 3 (top left) only include samples from the third year.

REFERENCES

- Allison, S.D., Nielsen, C., Hughes, R.F., 2006. Elevated enzyme activities in soils under the invasive nitrogen-fixing tree *Falcataria moluccana*. *Soil Biology and Biochemistry* 38, 1537–1544. <https://doi.org/10.1016/j.soilbio.2005.11.008>
- Allison, S.D., Martiny, J.B.H., 2008. Resistance, resilience, and redundancy in microbial communities. *Proceedings of the National Academy of Sciences* 105, 11512–11519. <https://doi.org/10.1073/pnas.0801925105>
- Allison, S.D., Wallenstein, M.D., Bradford, M.A., 2010a. Soil-carbon response to warming dependent on microbial physiology. *Nature Geosci* 3, 336–340. <https://doi.org/10.1038/ngeo846>
- Allison, S.D., Weintraub, M.N., Gartner, T.B., Waldrop, M.P., 2010b. Evolutionary-Economic Principles as Regulators of Soil Enzyme Production and Ecosystem Function, in: Shukla, G., Varma, A. (Eds.), *Soil Enzymology*, Soil Biology. Springer Berlin Heidelberg, Berlin, Heidelberg, pp. 229–243. https://doi.org/10.1007/978-3-642-14225-3_12
- Anantharaman, K., Hausmann, B., Jungbluth, S.P., Kantor, R.S., Lavy, A., Warren, L.A., Rappé, M.S., Pester, M., Loy, A., Thomas, B.C., Banfield, J.F., 2018. Expanded diversity of microbial groups that shape the dissimilatory sulfur cycle. *ISME J* 12, 1715–1728. <https://doi.org/10.1038/s41396-018-0078-0>
- Ardón, M., Morse, J.L., Colman, B.P., Bernhardt, E.S., 2013. Drought-induced saltwater incursion leads to increased wetland nitrogen export. *Glob Change Biol* 19, 2976–2985. <https://doi.org/10.1111/gcb.12287>
- Ardón, M., Helton, A.M., Bernhardt, E.S., 2018. Salinity effects on greenhouse gas emissions from wetland soils are contingent upon hydrologic setting: a microcosm experiment. *Biogeochemistry* 140, 217–232. <https://doi.org/10.1007/s10533-018-0486-2>
- Arnosti, C., 2000. Substrate specificity in polysaccharide hydrolysis: Contrasts between bottom water and sediments. *Limnol. Oceanogr.* 45, 1112–1119. <https://doi.org/10.4319/lo.2000.45.5.1112>
- Arnosti, C., Bell, C., Moorhead, D.L., Sinsabaugh, R.L., Steen, A.D., Stromberger, M., Wallenstein, M., Weintraub, M.N., 2014. Extracellular enzymes in terrestrial, freshwater, and marine environments: perspectives on system variability and common research needs. *Biogeochemistry* 117, 5–21. <https://doi.org/10.1007/s10533-013-9906-5>
- Auguet, J.-C., Barberan, A., Casamayor, E.O., 2010. Global ecological patterns in uncultured Archaea. *ISME J* 4, 182–190. <https://doi.org/10.1038/ismej.2009.109>
- Babicki, S., Arndt, D., Marcu, A., Liang, Y., Grant, J.R., Maciejewski, A., Wishart, D.S., 2016. Heatmapper: web-enabled heat mapping for all. *Nucleic Acids Res* 44, W147–W153. <https://doi.org/10.1093/nar/gkw419>
- Bai, J., Luo, M., Yang, Y., Xiao, S., Zhai, Z., Huang, J., 2021. Iron-bound carbon increases along a freshwater–oligohaline gradient in a subtropical tidal wetland. *Soil Biology and Biochemistry* 154, 108128. <https://doi.org/10.1016/j.soilbio.2020.108128>
- Baldrian, P., 2019. The known and the unknown in soil microbial ecology. *FEMS Microbiology Ecology* 95. <https://doi.org/10.1093/femsec/fiz005>
- Baldwin, D.S., Rees, G.N., Mitchell, A.M., Watson, G., Williams, J., 2006. The short-term effects of salinization on anaerobic nutrient cycling and microbial community structure in sediment from a freshwater wetland. *Wetlands* 26, 455–464. [https://doi.org/10.1672/0277-5212\(2006\)26\[455:TSEOSO\]2.0.CO;2](https://doi.org/10.1672/0277-5212(2006)26[455:TSEOSO]2.0.CO;2)
- Bardgett, R.D., Caruso, T., 2020. Soil microbial community responses to climate extremes: resistance, resilience and transitions to alternative states. *Phil. Trans. R. Soc. B* 375, 20190112. <https://doi.org/10.1098/rstb.2019.0112>

- Beadle, B.M., Baase, W.A., Wilson, D.B., Gilkes, N.R., Shoichet, B.K., 1999. Comparing the Thermodynamic Stabilities of a Related Thermophilic and Mesophilic Enzyme. *Biochemistry* 38, 2570–2576. <https://doi.org/10.1021/bi9824902>
- Berga, M., Székely, A.J., Langenheder, S., 2012. Effects of Disturbance Intensity and Frequency on Bacterial Community Composition and Function. *PLoS ONE* 7, e36959. <https://doi.org/10.1371/journal.pone.0036959>
- Berga, M., Zha, Y., Székely, A.J., Langenheder, S., 2017. Functional and Compositional Stability of Bacterial Metacommunities in Response to Salinity Changes. *Front. Microbiol.* 8, 948. <https://doi.org/10.3389/fmicb.2017.00948>
- Bernard, R.J., Mortazavi, B., Kleinhuizen, A.A., 2015. Dissimilatory nitrate reduction to ammonium (DNRA) seasonally dominates NO_3^- reduction pathways in an anthropogenically impacted sub-tropical coastal lagoon. *Biogeochemistry* 125, 47–64. <https://doi.org/10.1007/s10533-015-0111-6>
- Berrier, D.J., Neubauer, S.C., Franklin, R.B., 2022. Cooperative microbial interactions mediate community biogeochemical responses to saltwater intrusion in wetland soils. *FEMS Microbiology Ecology* 98, fiac019. <https://doi.org/10.1093/femsec/fiac019>
- Bianchi, T.S., 2007. *Biogeochemistry of estuaries*. Oxford University Press, Oxford; New York.
- Bier, R.L., Bernhardt, E.S., Boot, C.M., Graham, E.B., Hall, E.K., Lennon, J.T., Nemergut, D.R., Osborne, B.B., Ruiz-González, C., Schimel, J.P., Waldrop, M.P., Wallenstein, M.D., 2015. Linking microbial community structure and microbial processes: an empirical and conceptual overview. *FEMS Microbiology Ecology* 91, fiv113. <https://doi.org/10.1093/femsec/fiv113>
- Bowen, H., Maul, J.E., Cavigelli, M.A., Yarwood, S., 2020. Denitrifier abundance and community composition linked to denitrification activity in an agricultural and wetland soil. *Applied Soil Ecology* 151, 103521. <https://doi.org/10.1016/j.apsoil.2020.103521>
- Bowen, J.L., Ward, B.B., Morrison, H.G., Hobbie, J.E., Valiela, I., Deegan, L.A., Sogin, M.L., 2011. Microbial community composition in sediments resists perturbation by nutrient enrichment. *ISME J* 5, 1540–1548. <https://doi.org/10.1038/ismej.2011.22>
- Brettar, I., Rheinheimer, G., 1991. Denitrification in the Central Baltic: evidence for H_2S -oxidation as motor of denitrification at the oxic-anoxic interface. *Mar. Ecol. Prog. Ser.* 77, 157–169. <https://doi.org/10.3354/meps077157>
- Bridgman, S.D., Cadillo-Quiroz, H., Keller, J.K., Zhuang, Q., 2013. Methane emissions from wetlands: biogeochemical, microbial, and modeling perspectives from local to global scales. *Glob Change Biol* 19, 1325–1346. <https://doi.org/10.1111/gcb.12131>
- Brunet, R.C., Garcia-Gil, L.J., 1996. Sulfide-induced dissimilatory nitrate reduction to ammonia in anaerobic freshwater sediments. *FEMS Microbiology Ecology* 21, 131–138. <https://doi.org/10.1111/j.1574-6941.1996.tb00340.x>
- Bünemann, E.K., Bongiorno, G., Bai, Z., Creamer, R.E., De Deyn, G., de Goede, R., Flesskens, L., Geissen, V., Kuiper, T.W., Mäder, P., Pulleman, M., Sukkel, W., van Groenigen, J.W., Brussaard, L., 2018. Soil quality – A critical review. *Soil Biology and Biochemistry* 120, 105–125. <https://doi.org/10.1016/j.soilbio.2018.01.030>
- Burgin, A.J., Hamilton, S.K., 2007. Have we overemphasized the role of denitrification in aquatic ecosystems? A review of nitrate removal pathways. *Frontiers in Ecology and the Environment* 5, 89–96. [https://doi.org/10.1890/1540-9295\(2007\)5\[89:HWOTRO\]2.0.CO;2](https://doi.org/10.1890/1540-9295(2007)5[89:HWOTRO]2.0.CO;2)
- Burns, R.G., DeForest, J.L., Marxsen, J., Sinsabaugh, R.L., Stromberger, M.E., Wallenstein, M.D., Weintraub, M.N., Zoppini, A., 2013. Soil enzymes in a changing environment: Current knowledge and future directions. *Soil Biology and Biochemistry* 58, 216–234. <https://doi.org/10.1016/j.soilbio.2012.11.009>

- Caldwell, B.A., 2005. Enzyme activities as a component of soil biodiversity: A review. *Pedobiologia* 49, 637–644. <https://doi.org/10.1016/j.pedobi.2005.06.003>
- Cannon, J., Sanford, R.A., Connor, L., Yang, W.H., Chee-Sanford, J., 2019. Optimization of PCR primers to detect phylogenetically diverse *nrfA* genes associated with nitrite ammonification. *Journal of Microbiological Methods* 160, 49–59. <https://doi.org/10.1016/j.mimet.2019.03.020>
- Caporaso, J.G., Lauber, C.L., Walters, W.A., Berg-Lyons, D., Lozupone, C.A., Turnbaugh, P.J., Fierer, N., Knight, R., 2011. Global patterns of *16S rRNA* diversity at a depth of millions of sequences per sample. *Proceedings of the National Academy of Sciences* 108, 4516–4522. <https://doi.org/10.1073/pnas.1000080107>
- Carini, P., Marsden, P.J., Leff, J.W., Morgan, E.E., Strickland, M.S., Fierer, N., 2017. Relic DNA is abundant in soil and obscures estimates of soil microbial diversity. *Nat Microbiol* 2, 16242. <https://doi.org/10.1038/nmicrobiol.2016.242>
- Castledine, M., Sierocinski, P., Padfield, D., Buckling, A., 2020. Community coalescence: an eco-evolutionary perspective. *Phil. Trans. R. Soc. B* 375, 20190252. <https://doi.org/10.1098/rstb.2019.0252>
- Castellano-Hinojosa, A., Strauss, S.L., 2021. Insights into the taxonomic and functional characterization of agricultural crop core rhizobiosomes and their potential microbial drivers. *Sci Rep* 11, 10068. <https://doi.org/10.1038/s41598-021-89569-7>
- Chambers, L.G., Reddy, K.R., Osborne, T.Z., 2011. Short-Term Response of Carbon Cycling to Salinity Pulses in a Freshwater Wetland. *Soil Science Society of America Journal* 75, 2000–2007. <https://doi.org/10.2136/sssaj2011.0026>
- Chambers, L.G., Davis, S.E., Troxler, T., Boyer, J.N., Downey-Wall, A., Scinto, L.J., 2013. Biogeochemical effects of simulated sea level rise on carbon loss in an Everglades mangrove peat soil. *Hydrobiologia* 726, 195–211. <https://doi.org/10.1007/s10750-013-1764-6>
- Chambers, L.G., Steinmuller, H.E., Breithaupt, J.L., 2019. Toward a mechanistic understanding of “peat collapse” and its potential contribution to coastal wetland loss. *Ecology* 100. <https://doi.org/10.1002/ecy.2720>
- Chen, H., Ma, K., Huang, Y., Fu, Q., Qiu, Y., Yao, Z., 2022. Significant response of microbial community to increased salinity across wetland ecosystems. *Geoderma* 415, 115778. <https://doi.org/10.1016/j.geoderma.2022.115778>
- Chen, Y., Chen, J., Luo, Y., 2019. Data-driven ENZYme (DENZY) model represents soil organic carbon dynamics in forests impacted by nitrogen deposition. *Soil Biology and Biochemistry* 138, 107575. <https://doi.org/10.1016/j.soilbio.2019.107575>
- Chen, Y.-J., Leung, P.M., Cook, P.L.M., Wong, W.W., Hutchinson, T., Eate, V., Kessler, A.J., Greening, C., 2021. Hydrodynamic disturbance controls microbial community assembly and biogeochemical processes in coastal sediments. *ISME J.* <https://doi.org/10.1038/s41396-021-01111-9>
- Cheung, M.K., Wong, C.K., Chu, K.H., Kwan, H.S., 2018. Community Structure, Dynamics and Interactions of Bacteria, Archaea and Fungi in Subtropical Coastal Wetland Sediments. *Sci Rep* 8, 14397. <https://doi.org/10.1038/s41598-018-32529-5>
- Chi, Z., Zhu, Y., Li, H., Wu, H., Yan, B., 2021. Unraveling bacterial community structure and function and their links with natural salinity gradient in the Yellow River Delta. *Science of The Total Environment* 773, 145673. <https://doi.org/10.1016/j.scitotenv.2021.145673>
- Cline, J.D., 1969. Spectrophotometric determination of hydrogen sulfide in natural waters. *Limnol. Oceanogr.* 14, 454–458. <https://doi.org/10.4319/lo.1969.14.3.0454>

- Coker, J.A., Sheridan, P.P., Loveland-Curtze, J., Gutshall, K.R., Auman, A.J., Brenchley, J.E., 2003. Biochemical Characterization of a β -Galactosidase with a Low Temperature Optimum Obtained from an Antarctic *Arthrobacter* Isolate. *J Bacteriol* 185, 5473–5482. <https://doi.org/10.1128/JB.185.18.5473-5482.2003>
- Corstanje, R., Reddy, K.R., Portier, K.M., 2007. Soil microbial ecophysiology of a wetland recovering from phosphorus eutrophication. *Wetlands* 27, 1046–1055. [https://doi.org/10.1672/0277-5212\(2007\)27\[1046:SMEOAW\]2.0.CO;2](https://doi.org/10.1672/0277-5212(2007)27[1046:SMEOAW]2.0.CO;2)
- Craft, C., 2007. Freshwater input structures soil properties, vertical accretion, and nutrient accumulation of Georgia and U.S. tidal marshes. *Limnol. Oceanogr.* 52, 1220–1230. <https://doi.org/10.4319/lo.2007.52.3.1220>
- Craft, C., Clough, J., Ehman, J., Joye, S., Park, R., Pennings, S., Guo, H., Machmuller, M., 2009. Forecasting the effects of accelerated sea-level rise on tidal marsh ecosystem services. *Frontiers in Ecology and the Environment* 7, 73–78. <https://doi.org/10.1890/070219>
- Crowe, S.A., Canfield, D.E., Mucci, A., Sundby, B., Maranger, R., 2012. Anammox, denitrification and fixed-nitrogen removal in sediments from the Lower St. Lawrence Estuary. *Biogeosciences* 9, 4309–4321. <https://doi.org/10.5194/bg-9-4309-2012>
- Dang, C., Morrissey, E.M., Neubauer, S.C., Franklin, R.B., 2019. Novel microbial community composition and carbon biogeochemistry emerge over time following saltwater intrusion in wetlands. *Glob Change Biol* 25, 549–561. <https://doi.org/10.1111/gcb.14486>
- DeForest, J.L., 2009. The influence of time, storage temperature, and substrate age on potential soil enzyme activity in acidic forest soils using MUB-linked substrates and l-DOPA. *Soil Biology and Biochemistry* 41, 1180–1186. <https://doi.org/10.1016/j.soilbio.2009.02.029>
- Delgado-Baquerizo, M., Reich, P.B., Trivedi, C., Eldridge, D.J., Abades, S., Alfaro, F.D., Bastida, F., Berhe, A.A., Cutler, N.A., Gallardo, A., García-Velázquez, L., Hart, S.C., Hayes, P.E., He, J.-Z., Hseu, Z.-Y., Hu, H.-W., Kirchmair, M., Neuhauser, S., Pérez, C.A., Reed, S.C., Santos, F., Sullivan, B.W., Trivedi, P., Wang, J.-T., Weber-Grullon, L., Williams, M.A., Singh, B.K., 2020. Multiple elements of soil biodiversity drive ecosystem functions across biomes. *Nat Ecol Evol* 4, 210–220. <https://doi.org/10.1038/s41559-019-1084-y>
- Dick, R.P., Dick, L.K., Deng, S., Li, X., Kandeler, E., Poll, C., Freeman, C., Jones, T.G., Weintraub, M.N., Esseili, K.A., Saxena, J., 2018. Cross-laboratory comparison of fluorimetric microplate and colorimetric bench-scale soil enzyme assays. *Soil Biology and Biochemistry* 121, 240–248. <https://doi.org/10.1016/j.soilbio.2017.12.020>
- Dick, W.A., 2015. Development of a Soil Enzyme Reaction Assay, in: Dick, R.P. (Ed.), *SSSA Book Series*. American Society of Agronomy, Crop Science Society of America, and Soil Science Society of America, Madison, WI, USA, pp. 71–84. <https://doi.org/10.2136/sssabookser9.c4>
- Dong, L.F., Smith, C.J., Paspasyrou, S., Stott, A., Osborn, A.M., Nedwell, D.B., 2009. Changes in Benthic Denitrification, Nitrate Ammonification, and Anammox Process Rates and Nitrate and Nitrite Reductase Gene Abundances along an Estuarine Nutrient Gradient (the Colne Estuary, United Kingdom). *Appl Environ Microbiol* 75, 3171–3179. <https://doi.org/10.1128/AEM.02511-08>
- Dong, L.F., Sobey, M.N., Smith, C.J., Rusmana, I., Phillips, W., Stott, A., Osborn, A.M., Nedwell, D.B., 2011. Dissimilatory reduction of nitrate to ammonium, not denitrification or anammox, dominates benthic nitrate reduction in tropical estuaries. *Limnol. Oceanogr.* 56, 279–291. <https://doi.org/10.4319/lo.2011.56.1.0279>
- Dong, Y., Chen, R., Petropoulos, E., Yu, B., Zhang, J., Lin, X., Gao, M., Feng, Y., 2022. Interactive effects of salinity and SOM on the coenzymatic activities across coastal soils subjected to a saline gradient. *Geoderma* 406, 115519. <https://doi.org/10.1016/j.geoderma.2021.115519>

- Douglas, G.M., Maffei, V.J., Zaneveld, J.R., Yurgel, S.N., Brown, J.R., Taylor, C.M., Huttenhower, C., Langille, M.G.I., 2020. PICRUSt2 for prediction of metagenome functions. *Nat Biotechnol* 38, 685–688. <https://doi.org/10.1038/s41587-020-0548-6>
- Drouillon, M., Merckx, R., 2005. Performance of para-nitrophenyl phosphate and 4-methylumbelliferyl phosphate as substrate analogues for phosphomonoesterase in soils with different organic matter content. *Soil Biology and Biochemistry* 37, 1527–1534. <https://doi.org/10.1016/j.soilbio.2005.01.008>
- Dunn, C., Jones, T.G., Girard, A., Freeman, C., 2014. Methodologies for Extracellular Enzyme Assays from Wetland Soils. *Wetlands* 34, 9–17. <https://doi.org/10.1007/s13157-013-0475-0>
- Emsens, W.-J., van Diggelen, R., Aggenbach, C.J.S., Cajthaml, T., Frouz, J., Klimkowska, A., Kotowski, W., Kozub, L., Liczner, Y., Seeber, E., Silvennoinen, H., Tanneberger, F., Vicena, J., Wilk, M., Verbruggen, E., 2020. Recovery of fen peatland microbiomes and predicted functional profiles after rewetting. *ISME J* 14, 1701–1712. <https://doi.org/10.1038/s41396-020-0639-x>
- Engström, P., Dalsgaard, T., Hulth, S., Aller, R.C., 2005. Anaerobic ammonium oxidation by nitrite (anammox): Implications for N₂ production in coastal marine sediments. *Geochimica et Cosmochimica Acta* 69, 2057–2065. <https://doi.org/10.1016/j.gca.2004.09.032>
- Falkowski, P.G., Fenchel, T., Delong, E.F., 2008. The Microbial Engines That Drive Earth's Biogeochemical Cycles. *Science* 320, 1034–1039. <https://doi.org/10.1126/science.1153213>
- Fear, J.M., Thompson, S.P., Gallo, T.E., Paerl, H.W., 2005. Denitrification rates measured along a salinity gradient in the eutrophic Neuse River estuary, North Carolina, USA. *Estuaries* 28, 608–619. <https://doi.org/10.1007/BF02696071>
- Feller, G., 2003. Molecular adaptations to cold in psychrophilic enzymes. *Cellular and Molecular Life Sciences (CMLS)* 60, 648–662. <https://doi.org/10.1007/s00018-003-2155-3>
- Fenner, N., Freeman, C., Reynolds, B., 2005. Observations of a seasonally shifting thermal optimum in peatland carbon-cycling processes; implications for the global carbon cycle and soil enzyme methodologies. *Soil Biology and Biochemistry* 37, 1814–1821. <https://doi.org/10.1016/j.soilbio.2005.02.032>
- Fierer, N., Jackson, J.A., Vilgalys, R., Jackson, R.B., 2005. Assessment of Soil Microbial Community Structure by Use of Taxon-Specific Quantitative PCR Assays. *Appl Environ Microbiol* 71, 4117–4120. <https://doi.org/10.1128/AEM.71.7.4117-4120.2005>
- Fierer, N., Jackson, R.B., 2006. The diversity and biogeography of soil bacterial communities. *Proc. Natl. Acad. Sci. U.S.A.* 103, 626–631. <https://doi.org/10.1073/pnas.0507535103>
- Fillery, I.R.P., Recous, S., 2001. Use of Enriched 15N Sources to study Soil N Transformations, in: Unkovich, M., Pate, J., McNeill, A., Gibbs, D.J. (Eds.), *Stable Isotope Techniques in the Study of Biological Processes and Functioning of Ecosystems*. Springer Netherlands, Dordrecht, pp. 167–194. https://doi.org/10.1007/978-94-015-9841-5_9
- Finks, S.S., Weihe, C., Kimball, S., Allison, S.D., Martiny, A.C., Treseder, K.K., Martiny, J.B.H., 2021. Microbial community response to a decade of simulated global changes depends on the plant community. *Elementa: Science of the Anthropocene* 9, 00124. <https://doi.org/10.1525/elementa.2021.00124>
- Francis, C.A., O'Mullan, G.D., Cornwell, J.C., Ward, B.B., 2013. Transitions in *nirS*-type denitrifier diversity, community composition, and biogeochemical activity along the Chesapeake Bay estuary. *Front. Microbiol.* 4. <https://doi.org/10.3389/fmicb.2013.00237>
- Frankenberger, W.T., Bingham, F.T., 1982. Influence of Salinity on Soil Enzyme Activities. *Soil Science Society of America Journal* 46, 1173–1177. <https://doi.org/10.2136/sssaj1982.03615995004600060011x>

- Franklin, R.B., Morrissey, E.M., Morina, J.C., 2017. Changes in abundance and community structure of nitrate-reducing bacteria along a salinity gradient in tidal wetlands. *Pedobiologia* 60, 21–26. <https://doi.org/10.1016/j.pedobi.2016.12.002>
- Frossard, A., Gerull, L., Mutz, M., Gessner, M.O., 2012. Disconnect of microbial structure and function: enzyme activities and bacterial communities in nascent stream corridors. *ISME J* 6, 680–691. <https://doi.org/10.1038/ismej.2011.134>
- Gaiero, J.R., Tosi, M., Bent, E., Boitt, G., Khosla, K., Turner, B.L., Richardson, A.E., Condrón, L.M., Dunfield, K.E., 2021. Soil microbial communities influencing organic phosphorus mineralization in a coastal dune chronosequence in New Zealand. *FEMS Microbiology Ecology* 97, fiab034. <https://doi.org/10.1093/femsec/fiab034>
- Gardner, W.S., McCarthy, M.J., 2009. Nitrogen dynamics at the sediment–water interface in shallow, sub-tropical Florida Bay: why denitrification efficiency may decrease with increased eutrophication. *Biogeochemistry* 95, 185–198. <https://doi.org/10.1007/s10533-009-9329-5>
- German, D.P., Weintraub, M.N., Grandy, A.S., Lauber, C.L., Rinkes, Z.L., Allison, S.D., 2011. Optimization of hydrolytic and oxidative enzyme methods for ecosystem studies. *Soil Biology and Biochemistry* 43, 1387–1397. <https://doi.org/10.1016/j.soilbio.2011.03.017>
- Giannopoulos, G., Lee, D.Y., Neubauer, S.C., Brown, B.L., Franklin, R.B., 2019. A simple and effective sampler to collect undisturbed cores from tidal marshes (preprint). *Ecology*. <https://doi.org/10.1101/515825>
- Giblin, A., Tobias, C., Song, B., Weston, N., Banta, G., Rivera-Monroy, V., 2013. The Importance of Dissimilatory Nitrate Reduction to Ammonium (DNRA) in the Nitrogen Cycle of Coastal Ecosystems. *oceanog* 26, 124–131. <https://doi.org/10.5670/oceanog.2013.54>
- Giblin, A.E., Weston, N.B., Banta, G.T., Tucker, J., Hopkinson, C.S., 2010. The Effects of Salinity on Nitrogen Losses from an Oligohaline Estuarine Sediment. *Estuaries and Coasts* 33, 1054–1068. <https://doi.org/10.1007/s12237-010-9280-7>
- Graham, E.B., Knelman, J.E., Schindlbacher, A., Siciliano, S., Breulmann, M., Yannarell, A., Beman, J.M., Abell, G., Philippot, L., Prosser, J., Foulquier, A., Yuste, J.C., Glanville, H.C., Jones, D.L., Angel, R., Salminen, J., Newton, R.J., Bürgmann, H., Ingram, L.J., Hamer, U., Siljanen, H.M.P., Peltoniemi, K., Potthast, K., Bañeras, L., Hartmann, M., Banerjee, S., Yu, R.-Q., Nogaro, G., Richter, A., Koranda, M., Castle, S.C., Goberna, M., Song, B., Chatterjee, A., Nunes, O.C., Lopes, A.R., Cao, Y., Kaisermann, A., Hallin, S., Strickland, M.S., Garcia-Pausas, J., Barba, J., Kang, H., Isobe, K., Papaspyrou, S., Pastorelli, R., Lagomarsino, A., Lindström, E.S., Basiliko, N., Nemergut, D.R., 2016. Microbes as Engines of Ecosystem Function: When Does Community Structure Enhance Predictions of Ecosystem Processes? *Front. Microbiol.* 7. <https://doi.org/10.3389/fmicb.2016.00214>
- Greenfield, L.M., Puissant, J., Jones, D.L., 2021. Synthesis of methods used to assess soil protease activity. *Soil Biology and Biochemistry* 158, 108277. <https://doi.org/10.1016/j.soilbio.2021.108277>
- Grieger, R., Capon, S.J., Hadwen, W.L., Mackey, B., 2020. Between a bog and a hard place: a global review of climate change effects on coastal freshwater wetlands. *Climatic Change* 163, 161–179. <https://doi.org/10.1007/s10584-020-02815-1>
- Grinsven, S., Sinninghe Damsté, J.S., Abdala Asbun, A., Engelmann, J.C., Harrison, J., Villanueva, L., 2020. Methane oxidation in anoxic lake water stimulated by nitrate and sulfate addition. *Environ Microbiol* 22, 766–782. <https://doi.org/10.1111/1462-2920.14886>
- Hammer, Ø., Harper, D.A., Ryan P.D., 2001. PAST: paleontological statistics software package for education and data analysis. *Palaeontol. Electron* 4, 9.
- Handa, I.T., Aerts, R., Berendse, F., Berg, M.P., Bruder, A., Butenschoen, O., Chauvet, E., Gessner, M.O., Jabiol, J., Makkonen, M., McKie, B.G., Malmqvist, B., Peeters, E.T.H.M., Scheu, S., Schmid, B., van Ruijven, J., Vos, V.C.A., Hättenschwiler, W., 2015. Microbial community structure and function in a temperate forest soil. *Soil Biology and Biochemistry* 88, 1–11. <https://doi.org/10.1016/j.soilbio.2015.07.017>

- S., 2014. Consequences of biodiversity loss for litter decomposition across biomes. *Nature* 509, 218–221. <https://doi.org/10.1038/nature13247>
- Hansen, K., Butzeck, C., Eschenbach, A., Gröngroft, A., Jensen, K., Pfeiffer, E.-M., 2017. Factors influencing the organic carbon pools in tidal marsh soils of the Elbe estuary (Germany). *J Soils Sediments* 17, 47–60. <https://doi.org/10.1007/s11368-016-1500-8>
- Hansen, A.T., Dolph, C.L., Foufoula-Georgiou, E., Finlay, J.C., 2018. Contribution of wetlands to nitrate removal at the watershed scale. *Nature Geosci* 11, 127–132. <https://doi.org/10.1038/s41561-017-0056-6>
- Hawkes, C.V., Keitt, T.H., 2015. Resilience vs. historical contingency in microbial responses to environmental change. *Ecol Lett* 18, 612–625. <https://doi.org/10.1111/ele.12451>
- Herbert, E.R., Boon, P., Burgin, A.J., Neubauer, S.C., Franklin, R.B., Ardón, M., Hopfensperger, K.N., Lamers, L.P.M., Gell, P., 2015. A global perspective on wetland salinization: ecological consequences of a growing threat to freshwater wetlands. *Ecosphere* 6, art206. <https://doi.org/10.1890/ES14-00534.1>
- Herbert, E.R., Schubauer-Berigan, J., Craft, C.B., 2018. Differential effects of chronic and acute simulated seawater intrusion on tidal freshwater marsh carbon cycling. *Biogeochemistry* 138, 137–154. <https://doi.org/10.1007/s10533-018-0436-z>
- Herbert, E.R., Schubauer-Berigan, J.P., Craft, C.B., 2020. Effects of 10 yr of nitrogen and phosphorus fertilization on carbon and nutrient cycling in a tidal freshwater marsh. *Limnol Oceanogr* 65, 1669–1687. <https://doi.org/10.1002/lno.11411>
- Herlemann, D.P., Labrenz, M., Jürgens, K., Bertilsson, S., Waniek, J.J., Andersson, A.F., 2011. Transitions in bacterial communities along the 2000 km salinity gradient of the Baltic Sea. *ISME J* 5, 1571–1579. <https://doi.org/10.1038/ismej.2011.41>
- Hintz, W.D., Fay, L., Relyea, R.A., 2022. Road salts, human safety, and the rising salinity of our fresh waters. *Frontiers in Ecol & Environ* 20, 22–30. <https://doi.org/10.1002/fee.2433>
- Hollister, E.B., Engledow, A.S., Hammett, A.J.M., Provin, T.L., Wilkinson, H.H., Gentry, T.J., 2010. Shifts in microbial community structure along an ecological gradient of hypersaline soils and sediments. *ISME J* 4, 829–838. <https://doi.org/10.1038/ismej.2010.3>
- Hou, L., Liu, M., Carini, S.A., Gardner, W.S., 2012. Transformation and fate of nitrate near the sediment–water interface of Copano Bay. *Continental Shelf Research* 35, 86–94. <https://doi.org/10.1016/j.csr.2012.01.004>
- Hu, Y., Hong, Y., Ye, J., Wu, J., Wang, Y., Ye, F., Chang, X., Long, A., 2021. Shift of DNRA bacterial community composition in sediment cores of the Pearl River Estuary and the impact of environmental factors. *Ecotoxicology* 30, 1689–1703. <https://doi.org/10.1007/s10646-020-02321-1>
- Huygens, D., Trimmer, M., Rütting, T., Müller, C., Heppell, C.M., Lansdown, K., Boeckx, P., 2015. Biogeochemical Nitrogen Cycling in Wetland Ecosystems: Nitrogen-15 Isotope Techniques, in: DeLaune, R.D., Reddy, K.R., Richardson, C.J., Megonigal, J.P. (Eds.), *SSSA Book Series*. American Society of Agronomy and Soil Science Society of America, Madison, WI, USA, pp. 553–591. <https://doi.org/10.2136/sssabookser10.c30>
- Jackson, C.R., Tyler, H.L., Millar, J.J., 2013. Determination of Microbial Extracellular Enzyme Activity in Waters, Soils, and Sediments using High Throughput Microplate Assays. *JoVE* 50399. <https://doi.org/10.3791/50399>
- Jackson, C.R., Vallaire, S.C., 2009. Effects of salinity and nutrients on microbial assemblages in Louisiana wetland sediments. *Wetlands* 29, 277–287. <https://doi.org/10.1672/08-86.1>

- Jian, S., Li, J., Chen, J., Wang, G., Mayes, M.A., Dzantor, K.E., Hui, D., Luo, Y., 2016. Soil extracellular enzyme activities, soil carbon and nitrogen storage under nitrogen fertilization: A meta-analysis. *Soil Biology and Biochemistry* 101, 32–43. <https://doi.org/10.1016/j.soilbio.2016.07.003>
- Jones, C.M., Hallin, S., 2010. Ecological and evolutionary factors underlying global and local assembly of denitrifier communities. *ISME J* 4, 633–641. <https://doi.org/10.1038/ismej.2009.152>
- Jordan, S.J., Stoffer, J., Nestlerode, J.A., 2011. Wetlands as Sinks for Reactive Nitrogen at Continental and Global Scales: A Meta-Analysis. *Ecosystems* 14, 144–155. <https://doi.org/10.1007/s10021-010-9400-z>
- Joye, S.B., Hollibaugh, J.T., 1995. Influence of Sulfide Inhibition of Nitrification on Nitrogen Regeneration in Sediments. *Science* 270, 623–625. <https://doi.org/10.1126/science.270.5236.623>
- Kamimura, Y., Hayano, K., 2000. Properties of protease extracted from tea-field soil. *Biology and Fertility of Soils* 30, 351–355. <https://doi.org/10.1007/s003740050015>
- Kelley, K., 2007. Methods for the Behavioral, Educational, and Social Sciences: An R package. *Behavior Research Methods* 39, 979–984. <https://doi.org/10.3758/BF03192993>
- Kim, K., Samaddar, S., Chatterjee, P., Krishnamoorthy, R., Jeon, S., Sa, T., 2019. Structural and functional responses of microbial community with respect to salinity levels in a coastal reclamation land. *Applied Soil Ecology* 137, 96–105. <https://doi.org/10.1016/j.apsoil.2019.02.011>
- Koop-Jakobsen, K., Giblin, A.E., 2009. Anammox in Tidal Marsh Sediments: The Role of Salinity, Nitrogen Loading, and Marsh Vegetation. *Estuaries and Coasts* 32, 238–245. <https://doi.org/10.1007/s12237-008-9131-y>
- Kou, Y., Liu, Y., Li, J., Li, C., Tu, B., Yao, M., Li, X., 2021. Patterns and Drivers of *nirK*-Type and *nirS*-Type Denitrifier Community Assembly along an Elevation Gradient. *mSystems* e00667-21. <https://doi.org/10.1128/mSystems.00667-21>
- Kremer, R.J., 1994. Determination of soil phosphatase activity using a microplate method. *Communications in Soil Science and Plant Analysis* 25, 319–325. <https://doi.org/10.1080/00103629409369039>
- Lal, R., 2008. Carbon sequestration. *Phil. Trans. R. Soc. B* 363, 815–830. <https://doi.org/10.1098/rstb.2007.2185>
- Langille, M.G.I., Zaneveld, J., Caporaso, J.G., McDonald, D., Knights, D., Reyes, J.A., Clemente, J.C., Burkepile, D.E., Vega Thurber, R.L., Knight, R., Beiko, R.G., Huttenhower, C., 2013. Predictive functional profiling of microbial communities using 16S rRNA marker gene sequences. *Nat Biotechnol* 31, 814–821. <https://doi.org/10.1038/nbt.2676>
- Larsen, L. G., S. Moseman, A. Santoro, K. Hopfensperger, and A. Burgin. 2010. A complex-systems approach to predicting effects of sea level rise and nitrogen loading on nitrogen cycling in coastal wetland. *Eco-DAS VIII*: 67–92.
- Larson, J.L., Zak, D.R., Sinsabaugh, R.L., 2002. Extracellular Enzyme Activity Beneath Temperate Trees Growing Under Elevated Carbon Dioxide and Ozone. *Soil Sci. Soc. Am. J.* 66, 1848–1856. <https://doi.org/10.2136/sssaj2002.1848>
- Lauber, C.L., Hamady, M., Knight, R., Fierer, N., 2009. Pyrosequencing-Based Assessment of Soil pH as a Predictor of Soil Bacterial Community Structure at the Continental Scale. *Appl Environ Microbiol* 75, 5111–5120. <https://doi.org/10.1128/AEM.00335-09>
- Lee, D.Y., De Meo, O.A., Thomas, R.B., Tillett, A.L., Neubauer, S.C., 2016. Design and Construction of an Automated Irrigation System for Simulating Saltwater Intrusion in a Tidal Freshwater Wetland. *Wetlands* 36, 889–898. <https://doi.org/10.1007/s13157-016-0801-4>

- Lehman, R.M., O'Connell, S.P., 2002. Comparison of Extracellular Enzyme Activities and Community Composition of Attached and Free-Living Bacteria in Porous Medium Columns. *Appl Environ Microbiol* 68, 1569–1575. <https://doi.org/10.1128/AEM.68.4.1569-1575.2002>
- Li, X., Wang, A., Wan, W., Luo, X., Zheng, L., He, G., Huang, D., Chen, W., Huang, Q., 2021. High Salinity Inhibits Soil Bacterial Community Mediating Nitrogen Cycling. *Appl Environ Microbiol* 87, e01366-21. <https://doi.org/10.1128/AEM.01366-21>
- Li, X., Gao, D., Hou, L., Liu, M., 2019. Salinity stress changed the biogeochemical controls on CH₄ and N₂O emissions of estuarine and intertidal sediments. *Science of The Total Environment* 652, 593–601. <https://doi.org/10.1016/j.scitotenv.2018.10.294>
- Liu, H., Lennartz, B., 2019. Short Term Effects of Salinization on Compound Release from Drained and Restored Coastal Wetlands. *Water* 11, 1549. <https://doi.org/10.3390/w11081549>
- Love, M.I., Huber, W., Anders, S., 2014. Moderated estimation of fold change and dispersion for RNA-seq data with DESeq2. *Genome Biology* 15, 550. <https://doi.org/10.1186/s13059-014-0550-8>
- Lowley, D.R., Dwyer, D.F., Klug, M.J., 1982. Kinetic Analysis of Competition Between Sulfate Reducers and Methanogens for Hydrogen in Sediments. *Appl Environ Microbiol* 43, 1373–1379. <https://doi.org/10.1128/aem.43.6.1373-1379.1982>
- Lozupone, C.A., Knight, R., 2007. Global patterns in bacterial diversity. *Proc. Natl. Acad. Sci. U.S.A.* 104, 11436–11440. <https://doi.org/10.1073/pnas.0611525104>
- Luo, M., Huang, J.-F., Zhu, W.-F., Tong, C., 2019. Impacts of increasing salinity and inundation on rates and pathways of organic carbon mineralization in tidal wetlands: a review. *Hydrobiologia* 827, 31–49. <https://doi.org/10.1007/s10750-017-3416-8>
- Magalhães, C.M., Joye, S.B., Moreira, R.M., Wiebe, W.J., Bordalo, A.A., 2005. Effect of salinity and inorganic nitrogen concentrations on nitrification and denitrification rates in intertidal sediments and rocky biofilms of the Douro River estuary, Portugal. *Water Research* 39, 1783–1794. <https://doi.org/10.1016/j.watres.2005.03.008>
- Marks, B.M., Chambers, L., White, J.R., 2016. Effect of Fluctuating Salinity on Potential Denitrification in Coastal Wetland Soil and Sediments. *Soil Science Society of America Journal* 80, 516–526. <https://doi.org/10.2136/sssaj2015.07.0265>
- Martin, R.M., Moseman-Valtierra, S., 2015. Greenhouse Gas Fluxes Vary Between Phragmites Australis and Native Vegetation Zones in Coastal Wetlands Along a Salinity Gradient. *Wetlands* 35, 1021–1031. <https://doi.org/10.1007/s13157-015-0690-y>
- Marton, J.M., Herbert, E.R., Craft, C.B., 2012. Effects of Salinity on Denitrification and Greenhouse Gas Production from Laboratory-incubated Tidal Forest Soils. *Wetlands* 32, 347–357. <https://doi.org/10.1007/s13157-012-0270-3>
- Marx, M.-C., Wood, M., Jarvis, S.C., 2001. A microplate fluorimetric assay for the study of enzyme diversity in soils. *Soil Biology and Biochemistry* 33, 1633–1640. [https://doi.org/10.1016/S0038-0717\(01\)00079-7](https://doi.org/10.1016/S0038-0717(01)00079-7)
- McBeth, J.M., Fleming, E.J., Emerson, D., 2013. The transition from freshwater to marine iron-oxidizing bacterial lineages along a salinity gradient on the Sheepscot River, Maine, USA: Estuarine iron mat communities. *Environmental Microbiology Reports* 5, 453–463. <https://doi.org/10.1111/1758-2229.12033>
- McClagherty, C.A., Linkins, A.E., 1990. Temperature responses of enzymes in two forest soils. *Soil Biology and Biochemistry* 22, 29–33. [https://doi.org/10.1016/0038-0717\(90\)90056-6](https://doi.org/10.1016/0038-0717(90)90056-6)

- McDonald, D., Price, M.N., Goodrich, J., Nawrocki, E.P., DeSantis, T.Z., Probst, A., Andersen, G.L., Knight, R., Hugenholtz, P., 2012. An improved Greengenes taxonomy with explicit ranks for ecological and evolutionary analyses of bacteria and archaea. *ISME J* 6, 610–618. <https://doi.org/10.1038/ismej.2011.139>
- McMurdie, P.J., Holmes, S., 2013. phyloseq: An R Package for Reproducible Interactive Analysis and Graphics of Microbiome Census Data. *PLoS ONE* 8, e61217. <https://doi.org/10.1371/journal.pone.0061217>
- Mitra, S., Wassmann, R., Vlek, P.L., 2005. An appraisal of global wetland area and its organic carbon stock. *Curr Sci* 88, 25–35.
- Mitsch, W.J., Gosselink, J.G., 2015. *Wetlands*, Fifth edition. ed. John Wiley and Sons, Inc, Hoboken, NJ.
- Mobilian, C., Wisnoski, N.I., Lennon, J.T., Alber, M., Widney, S., Craft, C.B., 2020. Differential effects of press vs. pulse seawater intrusion on microbial communities of a tidal freshwater marsh. *Limnol Oceanogr* 65, 10171. <https://doi.org/10.1002/lol2.10171>
- Molnar, N., Welsh, D.T., Marchand, C., Deborde, J., Meziane, T., 2013. Impacts of shrimp farm effluent on water quality, benthic metabolism and N-dynamics in a mangrove forest (New Caledonia). *Estuarine, Coastal and Shelf Science* 117, 12–21. <https://doi.org/10.1016/j.ecss.2012.07.012>
- Moorhead, D.L., Sinsabaugh, R.L., 2006. A theoretical model of litter decay and microbial interaction. *Ecological Monographs* 76, 151–174. [https://doi.org/10.1890/0012-9615\(2006\)076\[0151:ATMOLD\]2.0.CO;2](https://doi.org/10.1890/0012-9615(2006)076[0151:ATMOLD]2.0.CO;2)
- Morina, J.C., Morrissey, E.M., Franklin, R.B., 2018. Vegetation Effects on Bacteria and Denitrifier Abundance in the Soils of Two Tidal Freshwater Wetlands in Virginia. *Applied and Environmental Soil Science* 2018, 1–10. <https://doi.org/10.1155/2018/4727258>
- Morrissey, E.M., Franklin, R.B., 2015. Evolutionary history influences the salinity preference of bacterial taxa in wetland soils. *Front. Microbiol.* 6. <https://doi.org/10.3389/fmicb.2015.01013>
- Morrissey, E.M., Gillespie, J.L., Morina, J.C., Franklin, R.B., 2014. Salinity affects microbial activity and soil organic matter content in tidal wetlands. *Glob Change Biol* 20, 1351–1362. <https://doi.org/10.1111/gcb.12431>
- Mosier, A.C., Francis, C.A., 2008. Relative abundance and diversity of ammonia-oxidizing archaea and bacteria in the San Francisco Bay estuary. *Environmental Microbiology* 10, 3002–3016. <https://doi.org/10.1111/j.1462-2920.2008.01764.x>
- Murphy, A.E., Bulseco, A.N., Ackerman, R., Vineis, J.H., Bowen, J.L., 2020. Sulphide addition favours respiratory ammonification (DNRA) over complete denitrification and alters the active microbial community in salt marsh sediments. *Environ Microbiol* 22, 2124–2139. <https://doi.org/10.1111/1462-2920.14969>
- Naeher, S., Huguet, A., Roose-Amsaleg, C.L., Laverman, A.M., Fosse, C., Lehmann, M.F., Derenne, S., Zopfi, J., 2015. Molecular and geochemical constraints on anaerobic ammonium oxidation (anammox) in a riparian zone of the Seine Estuary (France). *Biogeochemistry* 123, 237–250. <https://doi.org/10.1007/s10533-014-0066-z>
- Nannipieri, P., Trasar-Cepeda, C., Dick, R.P., 2018. Soil enzyme activity: a brief history and biochemistry as a basis for appropriate interpretations and meta-analysis. *Biol Fertil Soils* 54, 11–19. <https://doi.org/10.1007/s00374-017-1245-6>
- Nelson, T.M., Streten, C., Gibb, K.S., Chariton, A.A., 2015. Saltwater intrusion history shapes the response of bacterial communities upon rehydration. *Science of The Total Environment* 502, 143–148. <https://doi.org/10.1016/j.scitotenv.2014.08.109>
- Neubauer, S.C., 2013. Ecosystem Responses of a Tidal Freshwater Marsh Experiencing Saltwater Intrusion and Altered Hydrology. *Estuaries and Coasts* 36, 491–507. <https://doi.org/10.1007/s12237-011-9455-x>

- Neubauer, S.C., Franklin, R.B., Berrier, D.J., 2013. Saltwater intrusion into tidal freshwater marshes alters the biogeochemical processing of organic carbon. *Biogeosciences* 10, 8171–8183. <https://doi.org/10.5194/bg-10-8171-2013>
- Neubauer, S.C., Piehler, M.F., Smyth, A.R., Franklin, R.B., 2019. Saltwater Intrusion Modifies Microbial Community Structure and Decreases Denitrification in Tidal Freshwater Marshes. *Ecosystems* 22, 912–928. <https://doi.org/10.1007/s10021-018-0312-7>
- Noe, G.B., Krauss, K.W., Lockaby, B.G., Conner, W.H., Hupp, C.R., 2013. The effect of increasing salinity and forest mortality on soil nitrogen and phosphorus mineralization in tidal freshwater forested wetlands. *Biogeochemistry* 114, 225–244. <https://doi.org/10.1007/s10533-012-9805-1>
- Oksanen, J., F. G. Blanchet, R. Kindt, P. Legendre, P. R. Minchin, R. B. O’Hara, G. L. Simpson, P. Solymons, M. Henry, H. Stevens, & H. Wagner, 2015. *vegan: Community Ecology Package*. 254.
- Olander, L.P., Vitousek, P.M., 2000. Regulation of soil phosphatase and chitinase activity by N and P availability. *Biogeochemistry* 49, 175–191. <https://doi.org/10.1023/A:1006316117817>
- Oremland, R.S., Polcin, S., 1982. Methanogenesis and Sulfate Reduction: Competitive and Noncompetitive Substrates in Estuarine Sediments. *Appl Environ Microbiol* 44, 1270–1276. <https://doi.org/10.1128/aem.44.6.1270-1276.1982>
- Orland, C., Emilson, E.J.S., Basiliko, N., Mykytczuk, N.C.S., Gunn, J.M., Tanentzap, A.J., 2019. Microbiome functioning depends on individual and interactive effects of the environment and community structure. *ISME J* 13, 1–11. <https://doi.org/10.1038/s41396-018-0230-x>
- Orlygsson, J., Kristjansson, J.K., 2014. The Family Hydrogenophilaceae, in: Rosenberg, E., DeLong, E.F., Lory, S., Stackebrandt, E., Thompson, F. (Eds.), *The Prokaryotes*. Springer Berlin Heidelberg, Berlin, Heidelberg, pp. 859–868. https://doi.org/10.1007/978-3-642-30197-1_244
- Osborne, R.I., Bernot, M.J., Findlay, S.E.G., 2015. Changes in Nitrogen Cycling Processes Along a Salinity Gradient in Tidal Wetlands of the Hudson River, New York, USA. *Wetlands* 35, 323–334. <https://doi.org/10.1007/s13157-014-0620-4>
- Otte, M.L., Morris, J.T., 1994. Dimethylsulphoniopropionate (DMSP) in *Spartina alterniflora* Loisel. *Aquatic Botany* 48, 239–259. [https://doi.org/10.1016/0304-3770\(94\)90018-3](https://doi.org/10.1016/0304-3770(94)90018-3)
- Pandey, C.B., Kumar, U., Kaviraj, M., Minick, K.J., Mishra, A.K., Singh, J.S., 2020. DNRA: A short-circuit in biological N-cycling to conserve nitrogen in terrestrial ecosystems. *Science of The Total Environment* 738, 139710. <https://doi.org/10.1016/j.scitotenv.2020.139710>
- Peacock, M., Jones, T.G., Airey, B., Johncock, A., Evans, C.D., Lebron, I., Fenner, N., Freeman, C., 2015. The effect of peatland drainage and rewetting (ditch blocking) on extracellular enzyme activities and water chemistry. *Soil Use Manage* 31, 67–76. <https://doi.org/10.1111/sum.12138>
- Peng, J., Wegner, C.-E., Liesack, W., 2017. Short-Term Exposure of Paddy Soil Microbial Communities to Salt Stress Triggers Different Transcriptional Responses of Key Taxonomic Groups. *Front. Microbiol.* 8. <https://doi.org/10.3389/fmicb.2017.00400>
- Penton, C.R., Newman, S., 2007. Enzyme activity responses to nutrient loading in subtropical wetlands. *Biogeochemistry* 84, 83–98. <https://doi.org/10.1007/s10533-007-9106-2>
- Pereyra, L.P., Hiibel, S.R., Prieto Riquelme, M.V., Reardon, K.F., Pruden, A., 2010. Detection and Quantification of Functional Genes of Cellulose- Degrading, Fermentative, and Sulfate-Reducing Bacteria and Methanogenic Archaea. *Appl Environ Microbiol* 76, 2192–2202. <https://doi.org/10.1128/AEM.01285-09>

- Philippot, L., Griffiths, B.S., Langenheder, S., 2021. Microbial Community Resilience across Ecosystems and Multiple Disturbances. *Microbiol Mol Biol Rev* 85, e00026-20. <https://doi.org/10.1128/MMBR.00026-20>
- Phillips, L.E., Leonard, T.J., 1976. Extracellular and Intracellular Phenoloxidase Activity during Growth and Development in *Schizophyllum*. *Mycologia* 68, 268. <https://doi.org/10.2307/3758998>
- Podell, S., Emerson, J.B., Jones, C.M., Ugalde, J.A., Welch, S., Heidelberg, K.B., Banfield, J.F., Allen, E.E., 2014. Seasonal fluctuations in ionic concentrations drive microbial succession in a hypersaline lake community. *ISME J* 8, 979–990. <https://doi.org/10.1038/ismej.2013.221>
- Prosser, J.A., Speir, T.W., Stott, D.E., 2015. Soil Oxidoreductases and FDA Hydrolysis, in: Dick, R.P. (Ed.), *SSSA Book Series*. American Society of Agronomy, Crop Science Society of America, and Soil Science Society of America, Madison, WI, USA, pp. 103–124. <https://doi.org/10.2136/sssabookser9.c6>
- Qi, M., Qian, W., Chen, Z., Tong, C., Li, X., 2021. Disproportionate variations in denitrification and anaerobic ammonium oxidation across freshwater-oligohaline wetlands in Min River Estuary, Southeast China. *Environ Sci Pollut Res*. <https://doi.org/10.1007/s11356-021-16152-y>
- Quast, C., Pruesse, E., Yilmaz, P., Gerken, J., Schweer, T., Yarza, P., Peplies, J., Glöckner, F.O., 2012. The SILVA ribosomal RNA gene database project: improved data processing and web-based tools. *Nucleic Acids Research* 41, D590–D596. <https://doi.org/10.1093/nar/gks1219>
- Raes, E.J., Karsh, K., Sow, S.L.S., Ostrowski, M., Brown, M.V., van de Kamp, J., Franco-Santos, R.M., Bodrossy, L., Waite, A.M., 2021. Metabolic pathways inferred from a bacterial marker gene illuminate ecological changes across South Pacific frontal boundaries. *Nat Commun* 12, 2213. <https://doi.org/10.1038/s41467-021-22409-4>
- Ramirez, K.S., Leff, J.W., Barberán, A., Bates, S.T., Betley, J., Crowther, T.W., Kelly, E.F., Oldfield, E.E., Shaw, E.A., Steenbock, C., Bradford, M.A., Wall, D.H., Fierer, N., 2014. Biogeographic patterns in below-ground diversity in New York City's Central Park are similar to those observed globally. *Proc. R. Soc. B* 281, 20141988. <https://doi.org/10.1098/rspb.2014.1988>
- Ren, C., Zhao, F., Shi, Z., Chen, J., Han, X., Yang, G., Feng, Y., Ren, G., 2017. Differential responses of soil microbial biomass and carbon-degrading enzyme activities to altered precipitation. *Soil Biology and Biochemistry* 115, 1–10. <https://doi.org/10.1016/j.soilbio.2017.08.002>
- Rietl, A.J., Overlander, M.E., Nyman, A.J., Jackson, C.R., 2016. Microbial Community Composition and Extracellular Enzyme Activities Associated with *Juncus roemerianus* and *Spartina alterniflora* Vegetated Sediments in Louisiana Saltmarshes. *Microb Ecol* 71, 290–303. <https://doi.org/10.1007/s00248-015-0651-2>
- Risgaard-Petersen, N., Nielsen, L.P., Rysgaard, S., Dalsgaard, T., Meyer, R.L., 2003. Application of the isotope pairing technique in sediments where anammox and denitrification coexist: Anammox and isotope pairing. *Limnol. Oceanogr. Methods* 1, 63–73. <https://doi.org/10.4319/lom.2003.1.63>
- Rocca, J.D., Simonin, M., Bernhardt, E.S., Washburne, A.D., Wright, J.P., 2020. Rare microbial taxa emerge when communities collide: freshwater and marine microbiome responses to experimental mixing. *Ecology* 101. <https://doi.org/10.1002/ecy.2956>
- Rognes, T., Flouri, T., Nichols, B., Quince, C., Mahé, F., 2016. VSEARCH: a versatile open source tool for metagenomics. *PeerJ* 4, e2584. <https://doi.org/10.7717/peerj.2584>
- Romanowicz, K.J., Kane, E.S., Potvin, L.R., Daniels, A.L., Kolka, R.K., Lilleskov, E.A., 2015. Understanding drivers of peatland extracellular enzyme activity in the PEATcosm experiment: mixed evidence for enzymic latch hypothesis. *Plant Soil* 397, 371–386. <https://doi.org/10.1007/s11104-015-2746-4>

- Rysgaard, Søren, Thastum, P., Dalsgaard, T., Christensen, P.B., Sloth, N.P., Rysgaard, Søren, 1999. Effects of Salinity on NH₄⁺ Adsorption Capacity, Nitrification, and Denitrification in Danish Estuarine Sediments. *Estuaries* 22, 21. <https://doi.org/10.2307/1352923>
- Saiya-Cork, K.R., Sinsabaugh, R.L., Zak, D.R., 2002. The effects of long term nitrogen deposition on extracellular enzyme activity in an *Acer saccharum* forest soil. *Soil Biology and Biochemistry* 34, 1309–1315. [https://doi.org/10.1016/S0038-0717\(02\)00074-3](https://doi.org/10.1016/S0038-0717(02)00074-3)
- Santoro, A.E., 2010. Microbial nitrogen cycling at the saltwater–freshwater interface. *Hydrogeol J* 18, 187–202. <https://doi.org/10.1007/s10040-009-0526-z>
- Saviozzi, A., Cardelli, R., Di Puccio, R., 2011. Impact of Salinity on Soil Biological Activities: A Laboratory Experiment. *Communications in Soil Science and Plant Analysis* 42, 358–367. <https://doi.org/10.1080/00103624.2011.542226>
- Schimel, J., 2003. The implications of exoenzyme activity on microbial carbon and nitrogen limitation in soil: a theoretical model. *Soil Biology and Biochemistry* 35, 549–563. [https://doi.org/10.1016/S0038-0717\(03\)00015-4](https://doi.org/10.1016/S0038-0717(03)00015-4)
- Schloss, P.D., Westcott, S.L., Ryabin, T., Hall, J.R., Hartmann, M., Hollister, E.B., Lesniewski, R.A., Oakley, B.B., Parks, D.H., Robinson, C.J., Sahl, J.W., Stres, B., Thallinger, G.G., Van Horn, D.J., Weber, C.F., 2009. Introducing mothur: Open-Source, Platform-Independent, Community-Supported Software for Describing and Comparing Microbial Communities. *Appl Environ Microbiol* 75, 7537–7541. <https://doi.org/10.1128/AEM.01541-09>
- Scott, J.T., McCarthy, M.J., Gardner, W.S., Doyle, R.D., 2008. Denitrification, dissimilatory nitrate reduction to ammonium, and nitrogen fixation along a nitrate concentration gradient in a created freshwater wetland. *Biogeochemistry* 87, 99–111. <https://doi.org/10.1007/s10533-007-9171-6>
- Segata, N., Izard, J., Waldron, L., Gevers, D., Miropolsky, L., Garrett, W.S., Huttenhower, C., 2011. Metagenomic biomarker discovery and explanation. *Genome Biol* 12, R60. <https://doi.org/10.1186/gb-2011-12-6-r60>
- Seitzinger, S., Harrison, J.A., Böhlke, J.K., Bouwman, A.F., Lowrance, R., Peterson, B., Tobias, C., Drecht, G.V., 2006. DENITRIFICATION ACROSS LANDSCAPES AND WATERSCAPES: A SYNTHESIS. *Ecological Applications* 16, 2064–2090. [https://doi.org/10.1890/1051-0761\(2006\)016\[2064:DALAWA\]2.0.CO;2](https://doi.org/10.1890/1051-0761(2006)016[2064:DALAWA]2.0.CO;2)
- Senga, Y., Mochida, K., Fukumori, R., Okamoto, N., Seike, Y., 2006. N₂O accumulation in estuarine and coastal sediments: The influence of H₂S on dissimilatory nitrate reduction. *Estuarine, Coastal and Shelf Science* 67, 231–238. <https://doi.org/10.1016/j.ecss.2005.11.021>
- Servais, S., Kominoski, J.S., Charles, S.P., Gaiser, E.E., Mazzei, V., Troxler, T.G., Wilson, B.J., 2019. Saltwater intrusion and soil carbon loss: Testing effects of salinity and phosphorus loading on microbial functions in experimental freshwater wetlands. *Geoderma* 337, 1291–1300. <https://doi.org/10.1016/j.geoderma.2018.11.013>
- Servais, S., Kominoski, J.S., Coronado-Molina, C., Bauman, L., Davis, S.E., Gaiser, E.E., Kelly, S., Madden, C., Mazzei, V., Rudnik, D., Santamaria, F., Sklar, F.H., Stachelek, J., Troxler, T.G., Wilson, B.J., 2020. Effects of Saltwater Pulses on Soil Microbial Enzymes and Organic Matter Breakdown in Freshwater and Brackish Coastal Wetlands. *Estuaries and Coasts* 43, 814–830. <https://doi.org/10.1007/s12237-020-00708-1>
- Sgouridis, F., Heppell, C.M., Wharton, G., Lansdown, K., Trimmer, M., 2011. Denitrification and dissimilatory nitrate reduction to ammonium (DNRA) in a temperate re-connected floodplain. *Water Research* 45, 4909–4922. <https://doi.org/10.1016/j.watres.2011.06.037>
- Shade, A., Peter, H., Allison, S.D., Baho, D.L., Berga, M., Bürgmann, H., Huber, D.H., Langenheder, S., Lennon, J.T., Martiny, J.B.H., Matulich, K.L., Schmidt, T.M., Handelsman, J., 2012. Fundamentals of Microbial Community Resistance and Resilience. *Front. Microbio.* 3. <https://doi.org/10.3389/fmicb.2012.00417>

- Sharpe, P.J., Baldwin, A.H., 2009b. Patterns of wetland plant species richness across estuarine gradients of Chesapeake Bay. *Wetlands* 29, 225–235. <https://doi.org/10.1672/08-111.1>
- Simachew, A., Lanzén, A., Gessesse, A., Øvreås, L., 2016. Prokaryotic Community Diversity Along an Increasing Salt Gradient in a Soda Ash Concentration Pond. *Microb Ecol* 71, 326–338. <https://doi.org/10.1007/s00248-015-0675-7>
- Sinsabaugh, R.L., Findlay, S., 1995. Microbial production, enzyme activity, and carbon turnover in surface sediments of the Hudson River estuary. *Microb Ecol* 30. <https://doi.org/10.1007/BF00172569>
- Sinsabaugh, R.L., Reynolds, H., Long, T.M., 2000. Rapid assay for amidohydrolase (urease) activity in environmental samples. *Soil Biology and Biochemistry* 32, 2095–2097. [https://doi.org/10.1016/S0038-0717\(00\)00102-4](https://doi.org/10.1016/S0038-0717(00)00102-4)
- Smith, C.J., Dong, L.F., Wilson, J., Stott, A., Osborn, A.M., Nedwell, D.B., 2015. Seasonal variation in denitrification and dissimilatory nitrate reduction to ammonia process rates and corresponding key functional genes along an estuarine nitrate gradient. *Front. Microbiol.* 6. <https://doi.org/10.3389/fmicb.2015.00542>
- Song, B., Lisa, J.A., Tobias, C.R., 2014. Linking DNRA community structure and activity in a shallow lagoonal estuarine system. *Front. Microbiol.* 5. <https://doi.org/10.3389/fmicb.2014.00460>
- Steinberg, L.M., Regan, J.M., 2009. *mcrA*-Targeted Real-Time Quantitative PCR Method To Examine Methanogen Communities. *Appl Environ Microbiol* 75, 4435–4442. <https://doi.org/10.1128/AEM.02858-08>
- Steinmuller, H.E., Chambers, L.G., 2018. Can Saltwater Intrusion Accelerate Nutrient Export from Freshwater Wetland Soils? An Experimental Approach. *Soil Sci. Soc. Am. j.* 82, 283–292. <https://doi.org/10.2136/sssaj2017.05.0162>
- Sun, Z., Li, G., Zhang, C., Wang, Z., Lin, Q., Zhao, X., 2020. Contrasting resilience of soil microbial biomass, microbial diversity and ammonification enzymes under three applied soil fumigants. *Journal of Integrative Agriculture* 19, 2561–2570. [https://doi.org/10.1016/S2095-3119\(20\)63201-4](https://doi.org/10.1016/S2095-3119(20)63201-4)
- Sutton-Grier, Ariana.E., Keller, J.K., Koch, R., Gilmour, C., Megonigal, J.P., 2011. Electron donors and acceptors influence anaerobic soil organic matter mineralization in tidal marshes. *Soil Biology and Biochemistry* 43, 1576–1583. <https://doi.org/10.1016/j.soilbio.2011.04.008>
- Szoboszlai, M., Näther, A., Liu, B., Carrillo, A., Castellanos, T., Smalla, K., Jia, Z., Tebbe, C.C., 2019. Contrasting microbial community responses to salinization and straw amendment in a semiarid bare soil and its wheat rhizosphere. *Sci Rep* 9, 9795. <https://doi.org/10.1038/s41598-019-46070-6>
- Tabatabai, M.A., 2018. Soil Enzymes, in: Weaver, R.W., Angle, S., Bottomley, P., Bezdicek, D., Smith, S., Tabatabai, A., Wollum, A. (Eds.), *SSSA Book Series. Soil Science Society of America, Madison, WI, USA*, pp. 775–833. <https://doi.org/10.2136/sssabookser5.2.c37>
- Taylor, J.P., Wilson, B., Mills, M.S., Burns, R.G., 2002. Comparison of microbial numbers and enzymatic activities in surface soils and subsoils using various techniques. *Soil Biology and Biochemistry* 34, 387–401. [https://doi.org/10.1016/S0038-0717\(01\)00199-7](https://doi.org/10.1016/S0038-0717(01)00199-7)
- Throbäck, I.N., Enwall, K., Jarvis, A., Hallin, S., 2004. Reassessing PCR primers targeting *nirS*, *nirK* and *nosZ* genes for community surveys of denitrifying bacteria with DGGE. *FEMS Microbiology Ecology* 49, 401–417. <https://doi.org/10.1016/j.femsec.2004.04.011>
- Tobias, C., Anderson, I., Canuel, E., Macko, S., 2001. Nitrogen cycling through a fringing marsh-aquifer ecotone. *Mar. Ecol. Prog. Ser.* 210, 25–39. <https://doi.org/10.3354/meps210025>
- Trasar-Cepeda, C., Leirós, M.C., Gil-Sotres, F., 2008. Hydrolytic enzyme activities in agricultural and forest soils. Some implications for their use as indicators of soil quality. *Soil Biology and Biochemistry* 40, 2146–2155. <https://doi.org/10.1016/j.soilbio.2008.03.015>

- Tully, K., Gedan, K., Epanchin-Niell, R., Strong, A., Bernhardt, E.S., BenDor, T., Mitchell, M., Kominoski, J., Jordan, T.E., Neubauer, S.C., Weston, N.B., 2019. The Invisible Flood: The Chemistry, Ecology, and Social Implications of Coastal Saltwater Intrusion. *BioScience* 69, 368–378. <https://doi.org/10.1093/biosci/biz027>
- Turner, B.L., 2010. Variation in pH Optima of Hydrolytic Enzyme Activities in Tropical Rain Forest Soils. *Appl Environ Microbiol* 76, 6485–6493. <https://doi.org/10.1128/AEM.00560-10>
- Ury, E.A., Wright, J.P., Ardón, M., Bernhardt, E.S., 2022. Saltwater intrusion in context: soil factors regulate impacts of salinity on soil carbon cycling. *Biogeochemistry* 157, 215–226. <https://doi.org/10.1007/s10533-021-00869-6>
- Van de Broek, M., Temmerman, S., Merckx, R., Govers, G., 2016. Controls on soil organic carbon stocks in tidal marshes along an estuarine salinity gradient. *Biogeosciences* 13, 6611–6624. <https://doi.org/10.5194/bg-13-6611-2016>
- van den Berg, E.M., Boleij, M., Kuenen, J.G., Kleerebezem, R., van Loosdrecht, M.C.M., 2016. DNRA and Denitrification Coexist over a Broad Range of Acetate/N-NO₃⁻ Ratios, in a Chemostat Enrichment Culture. *Front. Microbiol.* 7. <https://doi.org/10.3389/fmicb.2016.01842>
- van Dijk, G., Lamers, L.P.M., Loeb, R., Westendorp, P.-J., Kuiperij, R., van Kleef, H.H., Klinge, M., Smolders, A.J.P., 2019. Salinization lowers nutrient availability in formerly brackish freshwater wetlands; unexpected results from a long-term field experiment. *Biogeochemistry* 143, 67–83. <https://doi.org/10.1007/s10533-019-00549-6>
- Waite, D.W., Vanwonterghem, I., Rinke, C., Parks, D.H., Zhang, Y., Takai, K., Sievert, S.M., Simon, J., Campbell, B.J., Hanson, T.E., Woyke, T., Klotz, M.G., Hugenholtz, P., 2017. Comparative Genomic Analysis of the Class Epsilonproteobacteria and Proposed Reclassification to Epsilonbacteraeota (phyl. nov.). *Front. Microbiol.* 8, 682. <https://doi.org/10.3389/fmicb.2017.00682>
- Waite, D.W., Chuvochina, M., Pelikan, C., Parks, D.H., Yilmaz, P., Wagner, M., Loy, A., Naganuma, T., Nakai, R., Whitman, W.B., Hahn, M.W., Kuever, J., Hugenholtz, P.Y.R., 2020. Proposal to reclassify the proteobacterial classes Deltaproteobacteria and Oligoflexia, and the phylum Thermodesulfobacteria into four phyla reflecting major functional capabilities. *International Journal of Systematic and Evolutionary Microbiology* 70, 5972–6016. <https://doi.org/10.1099/ijsem.0.004213>
- Wallenius, K., Rita, H., Mikkonen, A., Lappi, K., Lindström, K., Hartikainen, H., Raateland, A., Niemi, R.M., 2011. Effects of land use on the level, variation and spatial structure of soil enzyme activities and bacterial communities. *Soil Biology and Biochemistry* 43, 1464–1473. <https://doi.org/10.1016/j.soilbio.2011.03.018>
- Wallenstein, M.D., Burns, R.G., 2015. Ecology of Extracellular Enzyme Activities and Organic Matter Degradation in Soil: A Complex Community-Driven Process, in: Dick, R.P. (Ed.), *SSSA Book Series*. American Society of Agronomy, Crop Science Society of America, and Soil Science Society of America, Madison, WI, USA, pp. 35–55. <https://doi.org/10.2136/sssabookser9.c2>
- Wang, G., Post, W.M., Mayes, M.A., 2013. Development of microbial-enzyme-mediated decomposition model parameters through steady-state and dynamic analyses. *Ecological Applications* 23, 255–272. <https://doi.org/10.1890/12-0681.1>
- Wang, H., 2016. Determining the Spatial Variability of Wetland Soil Bulk Density, Organic Matter, and the Conversion Factor between Organic Matter and Organic Carbon across Coastal Louisiana, U.S.A. *Journal of Coastal Research* 33, 507. <https://doi.org/10.2112/JCOASTRES-D-16-00014.1>
- Wang, H., Gilbert, J.A., Zhu, Y., Yang, X., 2018. Salinity is a key factor driving the nitrogen cycling in the mangrove sediment. *Science of The Total Environment* 631–632, 1342–1349. <https://doi.org/10.1016/j.scitotenv.2018.03.102>
- Wang, S., Zhu, G., Peng, Y., Jetten, M.S.M., Yin, C., 2012. Anammox Bacterial Abundance, Activity, and Contribution in Riparian Sediments of the Pearl River Estuary. *Environ. Sci. Technol.* 46, 8834–8842. <https://doi.org/10.1021/es3017446>

- Wei, W., Isobe, K., Nishizawa, T., Zhu, L., Shiratori, Y., Ohte, N., Koba, K., Otsuka, S., Senoo, K., 2015. Higher diversity and abundance of denitrifying microorganisms in environments than considered previously. *ISME J* 9, 1954–1965. <https://doi.org/10.1038/ismej.2015.9>
- Welsh, A., Chee-Sanford, J.C., Connor, L.M., Löffler, F.E., Sanford, R.A., 2014. Refined *nrfA* Phylogeny Improves PCR-Based *nrfA* Gene Detection. *Appl. Environ. Microbiol.* 80, 2110–2119. <https://doi.org/10.1128/AEM.03443-13>
- Wen, Y., Bernhardt, E.S., Deng, W., Liu, W., Yan, J., Baruch, E.M., Bergemann, C.M., 2019. Salt effects on carbon mineralization in southeastern coastal wetland soils of the United States. *Geoderma* 339, 31–39. <https://doi.org/10.1016/j.geoderma.2018.12.035>
- Wenk, C.B., Zopfi, J., Gardner, W.S., McCarthy, M.J., Niemann, H., Veronesi, M., Lehmann, M.F., 2014. Partitioning between benthic and pelagic nitrate reduction in the Lake Lugano south basin. *Limnol. Oceanogr.* 59, 1421–1433. <https://doi.org/10.4319/lo.2014.59.4.1421>
- Westcott, S.L., Schloss, P.D., 2017. OptiClust, an Improved Method for Assigning Amplicon-Based Sequence Data to Operational Taxonomic Units. *mSphere* 2. <https://doi.org/10.1128/mSphereDirect.00073-17>
- Weston, N.B., Dixon, R.E., Joye, S.B., 2006. Ramifications of increased salinity in tidal freshwater sediments: Geochemistry and microbial pathways of organic matter mineralization. *J. Geophys. Res.* 111, G01009. <https://doi.org/10.1029/2005JG000071>
- Weston, N.B., Giblin, A.E., Banta, G.T., Hopkinson, C.S., Tucker, J., 2010. The Effects of Varying Salinity on Ammonium Exchange in Estuarine Sediments of the Parker River, Massachusetts. *Estuaries and Coasts* 33, 985–1003. <https://doi.org/10.1007/s12237-010-9282-5>
- Weston, N.B., Vile, M.A., Neubauer, S.C., Velinsky, D.J., 2011. Accelerated microbial organic matter mineralization following salt-water intrusion into tidal freshwater marsh soils. *Biogeochemistry* 102, 135–151. <https://doi.org/10.1007/s10533-010-9427-4>
- Widney, S.E., Smith, D., Herbert, E.R., Schubauer-Berigan, J.P., Li, F., Pennings, S.C., Craft, C.B., 2019. Chronic but not acute saltwater intrusion leads to large release of inorganic N in a tidal freshwater marsh. *Science of The Total Environment* 695, 133779. <https://doi.org/10.1016/j.scitotenv.2019.133779>
- Wieder, W.R., Bonan, G.B., Allison, S.D., 2013. Global soil carbon projections are improved by modelling microbial processes. *Nature Clim Change* 3, 909–912. <https://doi.org/10.1038/nclimate1951>
- Więski, K., Guo, H., Craft, C.B., Pennings, S.C., 2010. Ecosystem Functions of Tidal Fresh, Brackish, and Salt Marshes on the Georgia Coast. *Estuaries and Coasts* 33, 161–169. <https://doi.org/10.1007/s12237-009-9230-4>
- Wilson, B.J., Servais, S., Mazzei, V., Kominoski, J.S., Hu, M., Davis, S.E., Gaiser, E., Sklar, F., Bauman, L., Kelly, S., Madden, C., Richards, J., Rudnick, D., Stachelek, J., Troxler, T.G., 2018. Salinity pulses interact with seasonal dry-down to increase ecosystem carbon loss in marshes of the Florida Everglades. *Ecol Appl* 28, 2092–2108. <https://doi.org/10.1002/eap.1798>
- Wirth, S.J., Wolf, G.A., 1992. Micro-plate colourimetric assay for Endo -acting cellulase, xylanase, chitinase, 1,3- β -glucanase and amylase extracted from forest soil horizons. *Soil Biology and Biochemistry* 24, 511–519. [https://doi.org/10.1016/0038-0717\(92\)90074-8](https://doi.org/10.1016/0038-0717(92)90074-8)
- Wood, J.L., Tang, C., Franks, A.E., 2018. Competitive Traits Are More Important than Stress-Tolerance Traits in a Cadmium-Contaminated Rhizosphere: A Role for Trait Theory in Microbial Ecology. *Frontiers in Microbiology* 9, 121. <https://doi.org/10.3389/fmicb.2018.00121>
- Xiao, W., Chen, X., Jing, X., Zhu, B., 2018. A meta-analysis of soil extracellular enzyme activities in response to global change. *Soil Biology and Biochemistry* 123, 21–32. <https://doi.org/10.1016/j.soilbio.2018.05.001>

- Xie, K., Deng, Y., Zhang, S., Zhang, W., Liu, J., Xie, Y., Zhang, X., Huang, H., 2017. Prokaryotic Community Distribution along an Ecological Gradient of Salinity in Surface and Subsurface Saline Soils. *Sci Rep* 7, 13332. <https://doi.org/10.1038/s41598-017-13608-5>
- Xu, Z., Yu, G., Zhang, X., Ge, J., He, N., Wang, Q., Wang, D., 2015. The variations in soil microbial communities, enzyme activities and their relationships with soil organic matter decomposition along the northern slope of Changbai Mountain. *Applied Soil Ecology* 86, 19–29. <https://doi.org/10.1016/j.apsoil.2014.09.015>
- Yang, J., Ma, L., Jiang, H., Wu, G., Dong, H., 2016. Salinity shapes microbial diversity and community structure in surface sediments of the Qinghai-Tibetan Lakes. *Sci Rep* 6, 25078. <https://doi.org/10.1038/srep25078>
- Yang, W.H., Traut, B.H., Silver, W.L., 2015. Microbially mediated nitrogen retention and loss in a salt marsh soil. *Ecosphere* 6, 1–15. <https://doi.org/10.1890/ES14-00179.1>
- Yoon, S., Cruz-García, C., Sanford, R., Ritalahti, K.M., Löffler, F.E., 2015. Denitrification versus respiratory ammonification: environmental controls of two competing dissimilatory $\text{NO}_3^-/\text{NO}_2^-$ reduction pathways in *Shewanella loihica* strain PV-4. *ISME J* 9, 1093–1104. <https://doi.org/10.1038/ismej.2014.201>
- Zahrán, H.H., 1997. Diversity, adaptation and activity of the bacterial flora in saline environments. *Biology and Fertility of Soils* 25, 211–223. <https://doi.org/10.1007/s003740050306>
- Zantua, M.I., Bremner, J.M., 1975. Comparison of methods of assaying urease activity in soils. *Soil Biology and Biochemistry* 7, 291–295. [https://doi.org/10.1016/0038-0717\(75\)90069-3](https://doi.org/10.1016/0038-0717(75)90069-3)
- Zhang, G., Bai, J., Tebbe, C.C., Zhao, Q., Jia, J., Wang, W., Wang, X., Yu, L., 2021. Salinity controls soil microbial community structure and function in coastal estuarine wetlands. *Environ Microbiol* 23, 1020–1037. <https://doi.org/10.1111/1462-2920.15281>
- Zhao, Q., Bai, J., Gao, Y., Zhao, H., Zhang, G., Cui, B., 2020. Shifts in the soil bacterial community along a salinity gradient in the Yellow River Delta. *Land Degrad Dev* 31, 2255–2267. <https://doi.org/10.1002/ldr.3594>
- Zheng, Y., Hou, L., Liu, M., Liu, Z., Li, X., Lin, X., Yin, G., Gao, J., Yu, C., Wang, R., Jiang, X., 2016. Tidal pumping facilitates dissimilatory nitrate reduction in intertidal marshes. *Sci Rep* 6, 21338. <https://doi.org/10.1038/srep21338>
- Zhou, M., Butterbach-Bahl, K., Vereecken, H., Brüggemann, N., 2017. A meta-analysis of soil salinization effects on nitrogen pools, cycles and fluxes in coastal ecosystems. *Glob Change Biol* 23, 1338–1352. <https://doi.org/10.1111/gcb.13430>
- Zhou, Z., Ge, L., Huang, Y., Liu, Y., Wang, S., 2021. Coupled relationships among anammox, denitrification, and dissimilatory nitrate reduction to ammonium along salinity gradients in a Chinese estuarine wetland. *Journal of Environmental Sciences* 106, 39–46. <https://doi.org/10.1016/j.jes.2021.01.015>

VITA

Joseph C. Morina II was born February 5th 1991 in Virginia Beach, Virginia. He graduated from First Colonial High School in 2009. He received a Bachelor of Science in Biology from Virginia Commonwealth University in 2013. He worked as a field and laboratory technician before entering into the Master of Science Program at VCU. In 2016, he transferred into the Integrative Life Sciences Doctoral Program. During his time in graduate school, he received multiple awards and grants including the Virginia Sea Grant Graduate Research Fellowship, VCU Rice Rivers Center Student Research Award, Virginia Water Resources Research Center Student Grant, VCU Department of Biology “Outstanding PhD student in Ecology” Award, and The Virginia Association of Wetland Professionals Student Scholarship. During his graduate studies, he traveled to Japan and Germany to join an international research group, which resulted in multiple collaborations and publications.